

Dr. 1942

**LA-8526-MS**

Informal Report

124  
11/5/40

**Notes on Beam Dynamics in Linear Accelerators**

**MASTER**

University of California



**LOS ALAMOS SCIENTIFIC LABORATORY**

Post Office Box 1663 Los Alamos, New Mexico 87545

LA-8526-MS  
Informal Report  
UC-28  
Issued: September 1980

# Notes on Beam Dynamics in Linear Accelerators

R. L. Gluckstern\*

## DISCLAIMER

This book was prepared as an account of work sponsored by an agency of the United States Government. Neither the United States Government nor any agency thereof, nor any of their employees, makes any warranty, express or implied, or assumes any legal liability or responsibility for the accuracy, completeness, or usefulness of any information, apparatus, product, or process disclosed, or represents that its use would not infringe privately owned rights. Reference herein to any specific commercial product, process, or service by trade name, trademark, manufacturer, or otherwise does not necessarily constitute or imply its endorsement, recommendation, or favoring by the United States Government or any agency thereof. The views and opinions of authors expressed herein do not necessarily state or reflect those of the United States Government or any agency thereof.

\*Consultant. University of Maryland, College Park, MD 20742.



ep  
continued

## Foreword

During the period 1975-1980, Dr. R. L. Gluckstern maintained an active practice in the field of accelerator physics through consulting with a number of groups, while at the same time he was Vice-Chancellor for Academic Affairs and Provost at the University of Massachusetts, Amherst (1970-1975) and Chancellor of the University of Maryland (1975-Present). The Accelerator Systems Development Group (MP-9) at LAMPF has been fortunate to have his advice during the development of the LAMPF proton linear accelerator to its design goals. During the first few years of this period, extensive modeling studies were being conducted to develop tuning procedures and optimum tunes for the machine. In particular, we were looking at the longitudinal dynamics of the 201.25 MHz drift-tube linac to explain discrepancies between observed and predicted performance, using many measurements of tank field characteristics obtained during the 1975 "Great Shutdown" and measurements with beam. The notes include analyses of the effect of frequency perturbations on field distributions in uncompensated low-beta Alvarez tanks, and the acceptance characteristics of such tanks as functions of field tilt and injection energy, comments about the radial dependencies of longitudinal acceptance, the measurement of axial field distributions in long tanks, and the influence of an unpowered but resonant tank on a coasting beam. The effects of multipole aberrations in magnetic systems were also studied.

During the same time, the potential need for an accelerator system capable of producing pions for cancer therapy, but optimized for a hospital environment, led to the Pion Generator for Medical Irradiation (PIGMI) project. The possibility of achieving higher accelerating gradients using modern technology made feasible the consideration of the alternating-phase-focusing concept, where longitudinal acceleration and transverse focusing are both achieved using the rf field without the need for focusing magnets. Analyses were made of the longitudinal, transverse, and coupled motions.

Soon after the Accelerator Technology (AT) Division was formed, the potential of a new type of low-velocity accelerator structure invented in the USSR was realized. This structure, called the radio-frequency quadrupole (RFQ), provides a spacially-uniform, time-varying, strong-focusing quadrupole field at the rf frequency. This field is perturbed geometrically to produce a longitudinal component which can be carefully tailored to bunch and accelerate a particle beam. Between 1978 and 1980, the theory, computer beam dynamics, and mechanical realization of this concept was developed, and in early 1980, a proof-of-principle test was completed. This structure is a major breakthrough in accelerator technology, and will find wide application. Gluckstern enthusiastically joined in the program, and a series of notes in this compilation contributed substantially to our understanding as the development program progressed, beginning with the analysis of a point-charge model.

Another note discusses the general properties of the longitudinal and transverse beam dynamics, including coupling and space-charge effects, and another the relation of frequency and field distribution parameters from the structure analysis code SUPERFISH to the RFQ beam dynamics parameters. Exploitation of the outstanding characteristics of the RFQ as a beam buncher required a detailed understanding of how to vary the RFQ longitudinal fields in an approximately adiabatic manner in order to obtain good longitudinal bunching without introducing excessive coupling to the transverse phase space. In two important notes, Gluckstern covers longitudinal and radial effects in the initial bunching region of the RFQ. In order to match the beam transversely into the time-varying focusing field, the quadrupole field is tapered at the input end, over a short distance, from a low value up to the final level. An analysis shows that the resulting acceptance is indeed almost independent of incoming particle phase. Finally, the tolerance of the RFQ to misalignment errors is explored. As predicted from this study and because of the way the RFQ is built, we found on the proof-of-principle test that the RFQ is very forgiving of errors in manufacture or tuning.

Throughout this entire period, the high-average-intensity of LAMPF, the subsequent Fusion-Materials-Irradiation Test (FMIT) facility

linac project of AT-Division, and other high-intensity applications caused an increasing need to understand and control the factors which contribute to degradation in the transverse or longitudinal emittance of the accelerated beam. We need to control the beam quality to prevent excessive beam losses along the machine that would cause maintenance problems due to radioactivity buildup, and to achieve requirements on the final beam quality. Bob Gluckstern was a pioneer in this field, producing a series of seminal papers at the accelerator conferences of the late 1960's and early 1970's. Our interest, and that of others in the accelerator community, has been renewed and intensified in the past couple of years, and Gluckstern has returned to the fray. The analysis of emittance behavior is extremely complicated and has not yet yielded very complete or convenient guidelines. In a series of notes presented at the beginning of this compilation, Gluckstern catalogs the contributing factors to emittance dilution, and treats some aspects in detail. A need for improved simulation studies and more accurate experimental measurements prompted work on the characterization of multidimensional phase-space distributions and on errors in emittance measurements.

The notes are arranged in approximately reverse chronological order, beginning with the currently important topics of emittance growth, phase-space distributions, emittance measurement errors, and then the RFQ accelerator structure. Next comes a series on longitudinal and transverse dynamics from the LAMPF work, to which is added a later note on the permanent magnet developments of Halbach. Finally, there are three notes on alternating-phase-focusing.

It was our great pleasure and privilege to work with Dr. Gluckstern during this period, and we look forward to more adventures in accelerator technology.

Robert A. Jameson

## TABLE OF CONTENTS

	Page
1. Emittance Growth - I	2
2. Emittance Growth - II	9
3. Estimating the Frequencies of Collective Motion in a K-V Beam	19
4. Adiabatic Behavior of Bunched Beam	22
5. Stability of Two- and Three-Dimensional Particle Distributions	25
6. Image Charge Calculations Near a Cylindrical Boundary	32
-----	
7. Six-Dimensional Phase Space Distributions	36
8. Projections of Multidimensional Phase-Space Distributions	42
9. Slit Width Effect	48
-----	
10. Aspects of the 4-Vane Structure	53
11. Discussion of Beam Dynamics in a Kapchinsky-Teplyakov- like Structure	70
12. Relation of Structure to Beam Dynamics Parameters in a 4-Vane Structure	77
13. Beam Dynamics in the 4-Vane Structure (with emphasis on Jacobians)	80
14. Tapered Matching in the Radio-Frequency-Quadrupole (RFQ)	95
15. Misalignments in the RFQ	99
16. Bunching Region of an RFQ	102
17. Radial Effects During Initial Bunching	107
-----	
18. Measurement of Axial Field Distributions in a Long Tank	112
19. Comments on $r, \dot{r}$ Phase Space	118
20. Dependence of Tank Gradient on Incoming Beam Energy and Tank Tilt	121

	Page
21. Field Distribution at Low Beta	125
22. Beam Coasting Through Resonant Tanks	129
23. Effect of Frequency Errors on Tank Flattening	131
24. Distributed Effect of Localized Frequency Errors	135
25. Effect of Multipole Aberrations	138
26. Effect of Magnetic Multipole	142
27. Permanent Magnet Calculation	144
<hr/>	
28. Phase Rocking	150
29. Alternating Phase Focusing (APF)	154
30. Estimate of x-z Coupling in APF	161

NOTES ON BEAM DYNAMICS IN LINEAR ACCELERATORS

by

R. L. Gluckstern

ABSTRACT

A collection of notes is presented, on various aspects of beam dynamics in linear accelerators, which were produced by the author during five years (1975-1980) of consultation for the LASL Accelerator Technology (AT) Division and Medium-Energy Physics (MP) Division.



EMITTANCE GROWTH - II. Introduction

There is still no definitive model for predicting emittance growth in beams. Clearly, many different effects can contribute, including

1. non linear particle motion
2. couplings between component oscillations
3. misalignments, steering errors and other "noise"
4. mismatches in phase space
5. beam instabilities, resonances, and particle-particle interactions

In the present note, we comment on some of the features of emittance growth in the above context, in the hope that particular computational models can be built to help interpret observed growth.

II. No Space Charge; One Dimension

- A. Motion governed by a simple harmonic oscillator is clearly periodic, and points in phase space rotate at constant angular velocity provided the velocity axis is scaled by the angular frequency of the oscillator. If the initial phase space distribution is matched to the "circular" trajectories, the beam will have a constant cross section which will not grow. If the beam is not matched, its distribution in phase space will change as pattern rotates, and beam envelope oscillations will be observed at multiples of the particle rotation frequency, depending on the symmetry of the initial distribution.
- B. Perturbations to all particles which are independent of the particle position and velocity (like steering errors, magnet position misalignments) will generate rigid body motion of the original phase space distribution in that space. Although the beam may exceed aperture limitations, there is still no growth in the phase space area occupied by the beam.
- C. Adiabatic variation of the oscillator parameters (mass and spring constant) does not affect the conclusions reached above about constant emittance and coherent response to misalignments. However, the scale of the axis in the phase space plot will change adiabatically.

ically, as will the rotation rate.

- D. If our one dimensional oscillator has non-linear behavior, the situation may change. In this case the trajectories will not be circular. Nevertheless, a beam initially matched to the phase space trajectory will not grow, although different parts of the distribution will "rotate" at different rates.
- E. If the phase space distribution is not matched to the trajectory, streaming or filamentation will occur because the "rotation" rate will depend on the amplitude of the oscillation. The beam will then appear to fill the entire area within the externally tangent trajectory on a time scale determined by the difference between the rotation frequencies for a particle at the external tangent point and a particle at the internal tangent point.
- F. If misalignments are present in the non-linear oscillator, even a matched beam will grow, since coherent oscillations will force some particles to larger and smaller oscillation amplitudes. In this case, the difference frequency will be determined by the "coherent" oscillation amplitude generated by the misalignments. Non-linear orbit perturbations due to magnet multipoles will similarly cause mismatch and subsequent beam growth.

### III. No Space Charge; Several Dimension:

- A. Motion governed by uncoupled simple harmonic oscillators will appear to behave in each dimension as if the others did not exist. Beam profiles in real space will appear to change though, within fixed maxima in each coordinate, if the frequencies of rotation in different directions are different. If the frequencies are the same (such as with axial symmetry) the beam profiles will correspondingly remain fixed. Uncoupled misalignments will similarly not introduce any behaviors different from those for a single oscillator. Also uncoupled nonlinearities will behave as before.
- B. The presence of a coupling term (derivable from a Hamiltonian) will cause the two coupled oscillators to exchange energy at a rate determined by the coupling strength but by an amount which depends on the initial state of each oscillator and how "resonant" the coupling term is in the Hamiltonian. If the coupling dies out, there will be a

permanent change in the oscillation of each oscillator which can appear as an emittance growth in each phase space since all relative phases are present between the initial oscillations.

To illustrate, let us calculate the effect on the transverse motion due to coupling with the longitudinal motion given by

$$x' + k_t^2 x = \epsilon k_t^2 z x. \quad (1)$$

To lowest order in  $\epsilon$  we shall take the uncoupled solution for  $z$ , namely

$$z \cong z_0 \sin(k_\ell s + \phi_\ell). \quad (2)$$

A phase amplitude calculation (equivalent to using a Green's function) leads to a change in amplitude of the  $x$  oscillation (radial variable in the phase space plot) given by

$$\frac{\Delta A}{A} = k_t \frac{z_0}{4} \int_0^\infty ds \epsilon(s) \left[ \sin\left((2k_t - k_\ell)s + 2\phi_t - \phi_\ell\right) + \sin\left((2k_t + k_\ell)s + 2\phi_t + \phi_\ell\right) \right].$$

If we assume that  $\epsilon(s)$  decreases slowly to zero as  $s \rightarrow \infty$ , we obtain

$$\frac{\Delta A(\infty)}{A} \cong \frac{k_t z_0 \epsilon(0)}{4} \left[ \frac{\cos(2\phi_t - \phi_\ell)}{2k_t - k_\ell} + \frac{\cos(2\phi_t + \phi_\ell)}{2k_t + k_\ell} \right]. \quad (3)$$

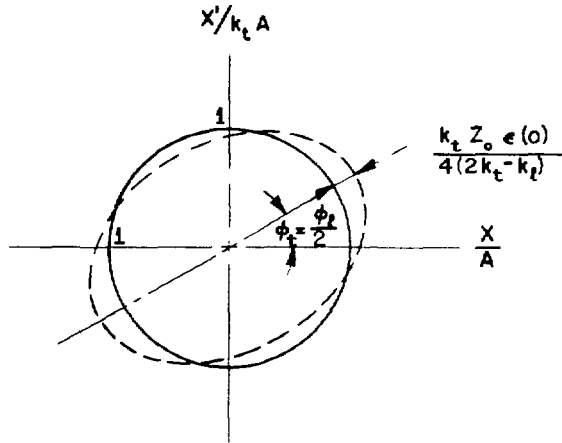
Let us further assume that  $2k_t - k_\ell$  is much smaller than  $2k_t + k_\ell$ , in which case the first term in the bracket dominates.

The result is an elliptical distortion of amplitude

$$\frac{\Delta A(\infty)}{A} = \frac{k_t z_0 \epsilon(0)}{4(2k_t - k_\ell)} \quad (4)$$

at an orientation given by

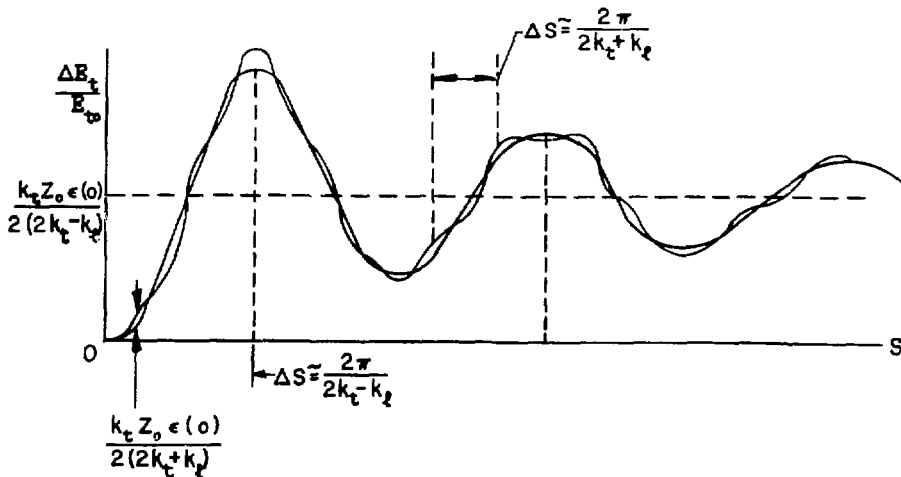
$$\phi_t = \frac{\phi_\ell}{2}, \frac{\phi_\ell}{2} + \pi. \quad (5)$$



If all initial values of  $\phi_\ell$  are present for each particle in the transverse phase space  $(A, \phi_t)$ , the transverse emittance will appear to grow by

$$\frac{\Delta E_t}{E_t} \cong \frac{k_t z_0 \epsilon(0)}{2(2k_t - k_\ell)}. \quad (6)$$

One further observation is significant: The apparent growth of emittance will overshoot (6) by a factor of about 2 and will oscillate with frequency  $2k_t - k_\ell$  before settling down. A smaller oscillation of frequency  $2k_t + k_\ell$  will also be present, so the emittance will have the general form



Although we have treated only the lowest order non-linear coupling, the general case will be quite similar if the coupling term in (1) is replaced by

$$\varepsilon k_t^{2 \times m-1} z^n \quad . \quad (7)$$

In particular

$$\frac{\Delta E_t(\infty)}{E_t} \approx \frac{4c(0)k_t z_0^n A^{m-2}}{2^{m+n} (mk_t - nk_\ell)} \quad , \quad (8)$$

where we have assumed the dominance of the frequency difference  $mk_t - nk_\ell$ .

- C. The presence of further non-linearities adds to the complications of matching the phase space in several coordinates at one time. Obviously (3) corresponds to a skewing of the multidimensional phase space shape resulting in apparent growth of the projected areas. Misalignments will also be converted to emittance growth by way of increasing the values of  $z_0$  and  $A$  in (8).
- D. Clearly, exact resonance of the form  $mk_t = nk_\ell$  will lead to emittance growth limited only by the development of amplitudes sufficiently large that  $k_t$  and  $k_\ell$  will be moved off resonance by couplings and/or linearities. If the parameters  $k_t$  and  $k_\ell$  cross a resonance during their adiabatic change, a further contribution to the growth will take place proportional to  $\varepsilon$  evaluated in the vicinity of the resonance. Since there may be many non-linear coupling terms present at one time, one can expect high order resonances to provide continuing small contributions to emittance growth during traversal of the accelerator. The factor  $2^{-(m+n)}$  in (8) suggests that high order resonances provide diminishing contributions.
- E. We have thus far ignored the strong focusing character of the transverse oscillations. This should not alter the conclusions, unless one operates near the stability limit, in which case the periodic focusing variation nearly resonates with the transverse oscillations. Formulas for emittance growth will however contain the Courant-Snyder parameter

$\beta_{c.s.}$  in some factors, a feature which is consistent with the smoothed approximation which makes use of the relation

$$k_t = \overline{\beta_{c.s.}^{-1}}.$$

- F. Special mention needs to be made of coupling between the two transverse dimensions from magnetic multipoles, quadrupole fringing, magnet rotation misalignment, etc. Because the two transverse frequencies are the same, it can readily be shown that although each oscillation is perturbed by the coupling, the quantity  $x_{\max}^2 + y_{\max}^2$  remains unchanged. Thus, a beam with different emittance in the two transverse directions will tend to enlarge until it is "circular", while a "circular" beam (equal transverse emittances) will not grow in the presence of couplings between the two transverse directions.
- G. Our discussion of couplings can be generalized to the situation where all three frequencies are unequal, in which case resonance can occur when a linear combination of the three frequencies (with integer coefficients) vanishes.

#### IV. Space Charge

- A. The simplest space charge model for which calculations are possible is the two dimensional KV distribution which provides linear, uncoupled space charge forces and a self consistent equilibrium phase space distribution. In this ideal case, all earlier considerations should apply, and emittance growths should not be greatly different from the no charge case.
- B. Because computational models can only handle a finite number of charged particles, there will be density fluctuations, leading to the presence of non-linearities in the space charge density, which are irregular. Furthermore, all six dimensional phase space distributions have non-linear, coupled space charge forces, as do all four dimensional distributions other than KV. In fact, non-linear external forces will even perturb a KV distribution so that non-linear space charge forces develop. As a result, we expect coupling terms of all kinds in the presence of space charge, with coefficients which go up linearly (or even faster if the space charge causes growth of the non-linearities) with the average current.

- C. The parameters which seem to govern the behavior and growth of beams with space charge are the ratios of the space charge defocusing force to the external focusing force in both the longitudinal and transverse directions. Instabilities develop as either of these parameters approaches 1. Designs which have these parameters in the range from 0.5 to 0.8 appear to require emittances which are matched in size in all three directions, and which lead to rapid emittance growth which settles down at a factor of between 1.5 and 2. If one examines the variation of emittance with axial distance, it may be possible to identify which non-linear terms are important.
- D. Another feature of some of the numerical computations is that the presence of bunching forces occasionally leads to localized regions in which the space charge defocussing exceeds the external focussing. Localized instabilities then develop in such a way that the beam contains turbulent eddies. Some form of turbulent diffusion may then need to be included in any definitive analysis.
- E. Particle-particle collisions will cause scattering of occasional particles outside the stable region of the beam. However, because of the large number of particles in a beam bunch, these effects are insignificant in accelerators. Nevertheless, since computations contain only a finite number of particles, it is not uncommon for such computations to exhibit artificial "collisional" growth. It is essential that this effect be removed from computational models in order to obtain a realistic simulation of an actual beam.

EMITTANCE GROWTH - IISummary

The following paper reviews the usual known mechanisms which can contribute to emittance growth. These include mismatching, coupling, misalignment, non-linearities, space charge, all of which have the capability of leading to apparent emittance growth either singly or in combination.

Special attention is given in Section (11) to the case of fluctuating space charge density along the axis. In particular, if this density fluctuation varies with longitudinal phase, an emittance growth can be calculated directly.

It would be useful at this point to study the axial charge density and its variation with longitudinal position. If this should be of sufficient magnitude to account for computed growth, it may open the way to further study and control of emittance growth via a relatively simple parameter.



The linearized uncoupled equation for particle motion is of the form

$$x'' + k_t^2 x = 0 \quad . \quad (1)$$

A distribution of particles occupying a circle in the  $(x, x'/k_t)$  phase space will travel in circles at rotational frequency  $k_t/2\pi$  and the phase space boundary will not change in time. Such an initial distribution (occupying a circle) is called matched to the focusing system.

Several complications can now be introduced. They will be discussed one at a time.

(1) Suppose the beam is mismatched, that is, centered at the phase space origin but in the shape of an ellipse. This ellipse will rotate as a rigid body at frequency  $(k_t/2\pi)$  and the phase space area will be preserved. However, the beam envelope will appear to be pulsating and space charge forces will vary with double the rotation frequency.

(2) If the beam is misaligned, the initial distribution will be off-center in phase space. Once again phase space area will be preserved, but there can be both a coherent oscillation and a "breathing" oscillation.

(3) If the restoring force is non-linear particles further away from the phase space origin will rotate more slowly. A perfectly matched beam (requires a figure different from a circle) will once again be preserved. However, a mismatched or off-center beam will filament in time, ultimately occupying the entire matched boundary which contains the initial beam. In this case, the emittance appears to grow by an amount which is of the order of the mismatch, or of the order of the ratio of the coherent oscillation amplitude to the matched beam size. The time of growth will be determined by the difference in rotation frequency between the matched trajectory externally tangent to the phase space beam distribution and the one tangent internally.

(4) Let us now introduce couplings in the form

$$x'' + k_t^2 x = \epsilon(s) \quad . \quad (2)$$

The lowest order coupling to the longitudinal motion is of the form

$$\epsilon(s) \cong \frac{k_\ell^2}{2} \frac{x(\phi - \phi_s)}{|\phi_s|} \quad (3)$$

corresponding to the variation in r-f defocussing due to the oscillating phase of the accelerating field.

A phase-amplitude analysis of (2) and (3) in the case of slow variation of parameters (coupling decreases with energy) leads to the conclusion that an initially matched circle in the  $(x, x/k_t)$  space will be distorted to an ellipse, with relative amplitude distortion

$$\frac{\Delta A^{(\infty)}}{A} \approx \frac{k_\ell^2}{8|2k_t - k_\ell|k_t} \frac{(\phi - \phi_s)}{|\phi_s|} \equiv \delta \quad (4)$$

and with orientation depending on the initial phase of the longitudinal motion. In arriving at (4) we consider the primary contribution to come from the difference frequency  $2k_t - k_\ell$  rather than from the sum frequency  $2k_t + k_\ell$ . Furthermore the maximum distortion will be reached when

$$|2k_t - k_\ell|s = \pi \quad (5)$$

and will have a value approximately double that in (4).

Since all phases of longitudinal motion are presumed to be present, all orientations of the distorted ellipse will be present at once, and the beam will appear to grow in emittance by a relative amount which is twice that given in (4).

(5) Higher order couplings of the form

$$\epsilon(t) = \frac{k_\ell^2}{2} x \left\{ \frac{(\phi - \phi_s)^2}{2}, \frac{(\phi - \phi_s)^3}{6|\phi_s|}, \frac{(\phi - \phi_s)^4}{24}, \frac{(\phi - \phi_s)^5}{120|\phi_s|} \dots \right\}$$

are also present, but contribute decreasing amounts to the growth, unless a particular resonance of the form

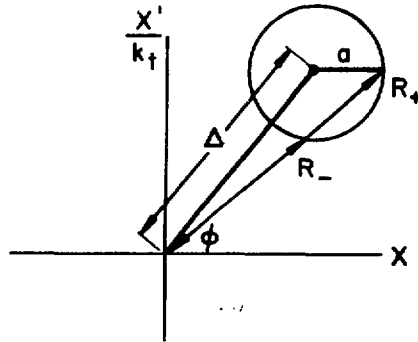
$$2k_t - nk_g \cong 0$$

should dominate over a significant portion of the accelerator.

(6) An important point to mention at this time is that the rms emittance of the beam will not change in lowest order in the coupling, but will instead vary as the square of (4). The reason for this is that the coupling leads to an increase in amplitude for some particles and a decrease in amplitude for some others. Clearly the 100% emittance contour will grow as indicated in (4) and the 90% contour somewhat less than that given by (4). The test of each application must be considered separately.

(7) The effect of misalignments and steering errors can also be discussed at this point. In such a case, the term  $\epsilon(s)$  in (2) represents an external driving term which is the same for all particles, and therefore leads to a coherent oscillation of the beam as a whole. This will not correspond to an emittance growth unless there are non-linearities which lead to filamentation as discussed in Section (3).

If there are misalignments and coupling present at the same time, without non-linearities (or in a time too short for their effect to be felt) there may be appreciable growth. Consider a beam displaced as shown. The coupling will distort the circles such that



$$R_+ \rightarrow R_+(1 + \delta)$$

$$R_- \rightarrow R_-(1 - \delta)$$

where  $\delta$  is given in (4). The increase in area (emittance) can be shown to be

$$\frac{\Delta W}{W} = \left\{ \begin{array}{ll} 2\delta & \text{for } \Delta < a \\ 2\delta + \frac{4\delta}{\pi} \left( \frac{\sqrt{\Delta^2 - a^2}}{a} - \tan^{-1} \frac{\sqrt{\Delta^2 - a^2}}{a} \right) & \text{for } \Delta > a \\ 2\delta + \frac{4\delta\Delta}{\pi a} & \text{for } \Delta \gg a \end{array} \right\} .$$

If the "misalignments" are quadrupole rotation errors or other similar errors where the driving term depends on the oscillating displacements, the  $\epsilon(s)$  term will contain  $x(s)$ ,  $y(s)$ ,  $\phi(s)$ . For a systematic variation in  $\epsilon(s)$  the description will be that of the coupled systems discussed in the next Section. For  $\epsilon(s)$  which behaves in a random fashion the description will be that discussed in Section (11).

(8) Let us consider both oscillations which enter into the coupling, in the form

$$\left. \begin{aligned} x'' + k_1^2 x &= \epsilon n x^{n-1} y^m \\ y'' + k_2^2 y &= \epsilon m x^n y^{m-1} \end{aligned} \right\} \quad (6)$$

derivable from the  $\epsilon x^n y^m$  term in the Hamiltonian. It can be shown that a resonance of the form

$$n k_1 - m k_2 = 0 \quad (7)$$

leads to the possibility of significant energy exchange between the two oscillations. It can be shown further that the energies of the oscillations (equivalent to the emittance within the phase space trajectory) satisfy the relationship

$$\frac{W_x}{n} + \frac{W_y}{m} = \text{const} \quad (8)$$

The conclusion from (8) is that the presence of terms which can resonate causes an exchange of energy for various particles. Because all oscillation phases are present, the smaller emittance will appear to grow until it is approximately the same size as the larger one. It is this phenomenon which has been interpreted by some as a thermal connection between oscillation modes leading to an equipartition of energy (emittance). Computation results appear to be consistent with such growths. Moreover, a beam matched in all coordinates will have approximately equal emittances in these coordinates. This is again confirmed in the computations.

(9) It is of course important to know if such coupling terms are present. This is indeed the case for the external fields where couplings are due to

- (a) The non-linear dependence of the longitudinal restoring force on phase;
- (b) The radial dependence of the transit time factor;
- (c) Multipole components in the quadrupole magnets;
- (d) Fringing fields of the quadrupoles
- (e) The higher order difference between  $v_z$  and

$$v = \sqrt{v_z^2 + v_x^2 + v_y^2} .$$

It is, of course, true that all space charge distributions other than the two-dimensional K-V one will lead to non-linear and coupled terms in the equations of motion. It is of course difficult to estimate the magnitude (and fluctuation) of such terms, but an order of magnitude estimate might be obtained by assuming Gaussian shaped distributions.

(10) The primary effects of space charge distributions is to decrease the small oscillation frequency in each direction by a factor  $(1 - \mu)^{1/2}$ , where  $\mu$  is the ratio of the space charge gradient to the external focussing gradient near the beam center. In addition, the non-linear terms clearly make the oscillation frequencies amplitude dependent.

Calculations done by several groups indicate that high current beams are limited by the values of  $\mu_t$  and  $\mu_l$  in the range of 1/2 to 2/3. This corresponds to  $(1 - \mu)^{1/2} \sim .7$  to  $.6$  -- that is, depression of the phase advance by 30% to 40% compared to the zero space charge value.

In the analysis mentioned in Section (2) it is important to recognize that the coherent oscillation frequency will be that of the zero space charge beam. In treating the longitudinal-transverse coupling in Section (4), it should be mentioned that the  $k_t$  and the  $k_l$  in the denominator of (4) are to be multiplied by  $(1 - \mu_t)^{1/2}$  and  $(1 - \mu_l)^{1/2}$  respectively, while the  $k_l^2$  in the numerator, which has its origin in the accelerating field strength, remains unchanged. The result is an increase in (4) by a factor  $\sim (1 - \mu)^{-1}$  of 2 or 3. In the case  $k_t = k_l$ ,  $(\phi - \phi_s)_{\max} \approx |\phi_s|$ ,  $\mu = 2/3$  one has

$$\frac{\Delta W}{W} \cong 2 \frac{\Delta A}{A} \sim \frac{3}{4} ,$$

suggesting that the emittance will grow by its own order of magnitude. For such a large value of  $\Delta W/W$ , even the rms emittance will grow appreciably.

(11) Let us now consider (2) with a driving term which corresponds to a space charge density which fluctuates along the axis. In this case (2) can be written as

$$x'' + k_t^2 x = x \epsilon(s) , \quad (9)$$

where  $\epsilon(s)$  is the fluctuating density component only ( $\epsilon(s)$  average to 0 over  $s$ ). Equation (9) can be solved approximately by a phase amplitude method. Setting

$$x = A \sin (k_t s + \phi) \quad x' = k_t A \cos (k_t s + \phi)$$

one obtains

$$\frac{A'}{A} = \frac{k_t \epsilon(s)}{2} \sin (2k_t s + 2\phi) . \quad (10)$$

To lowest order in  $\epsilon$ ,  $\phi$  is constant and (10) can be integrated to obtain

$$\begin{aligned} \frac{\Delta A}{A} &= k_t \frac{\cos 2\phi}{2} \int_0^\infty ds \sin 2k_t s \epsilon(s) \\ &+ k_t \frac{\sin 2\phi}{2} \int_0^\infty ds \cos 2k_t s \epsilon(s) \\ &\equiv R \sin 2\phi + I \cos 2\phi . \end{aligned} \quad (11)$$

Once again the result is a distortion of magnitude

$$\frac{\Delta A_{\max}}{A} = \sqrt{R^2 + I^2} = \frac{k_t}{2} \left| \int_0^{\infty} ds \varepsilon(s) e^{i2k_t s} \right| . \quad (12)$$

This will be turned into an apparent emittance growth if nonlinearities have time to filament the distortion, or if  $\varepsilon(s)$  depends on another parameter (e.g., the longitudinal phase of the particle oscillation) and therefore leads to R and I having a range of values.

From (12), the most serious situation is clearly one in which  $\varepsilon(s)$  contains a strong component of frequency  $2k_t$ . This is, in fact, the case for a mismatched beam, in which case the space charge density will fluctuate with the frequency  $2k_t$ . If the mismatch also depends on longitudinal position within the bunch, all the necessary ingredients are present to lead to emittance growth. At this point the computations require selecting a particular model for  $\varepsilon(s)$  and proceeding accordingly.

Let us imagine that  $\varepsilon(s)$  has a component which varies with longitudinal position, such that  $\varepsilon(s)$  is given by

$$\varepsilon(s) = \varepsilon_0(s) + \varepsilon_1(s)(\phi - \phi_s) .$$

Writing

$$\phi - \phi_s = \psi_{\max} \cos(k_\ell s + \phi_\ell) ,$$

we can extend (10) to

$$\frac{\Delta A'}{A} \approx \psi_{\max} \frac{k_t}{4} \varepsilon_1(s) \sin\left((2k_t - k_\ell)s + 2\phi - \phi_\ell\right) ,$$

where we have kept only the  $2k_t - k_\ell$  term. We can now rewrite (12) as

$$\frac{\Delta A}{A} = R_1 \sin(2\phi - \phi_\ell) + I_1 \cos(2\phi - \phi_\ell) ,$$

where

$$\frac{\Delta A_{\max}}{A} = \sqrt{R_1^2 + I_1^2} = \frac{k_t}{4} \psi_{\max} \left| \int_0^{\infty} ds \epsilon(s) e^{i(2k_t - k_\ell)s} \right| .$$

In this case, since all value of  $\phi_\ell$  are present, the apparent emittance will grow directly by  $\frac{2\Delta A_{\max}}{A}$  .

As a final calculation, let us take a model where  $\epsilon(s)$  has random fluctuations of the form

$$\begin{aligned} \epsilon(s) &= \epsilon_j & jT - T < s < jT \\ & & j &= 1, 2, 3, \dots \end{aligned}$$

where all the  $\epsilon_j$  are uncorrelated. Then  $(2k_t$  is replaced by  $2k_t - k_\ell$  if longitudinal variation is included)

$$\int_0^{\infty} ds \epsilon(s) e^{2ik_t s} = \sum_{j=1}^{J_{\max}} \epsilon_j \left( \int_{-\frac{T}{2}}^{\frac{T}{2}} ds e^{2ik_t s} \right) e^{-2i(j - \frac{1}{2})Tk_t} .$$

The average over the  $\epsilon_j$  leads to

$$\overline{\left| \int ds \epsilon(s) e^{2ik_t s} \right|^2} \cong \frac{1}{\epsilon^2} T^2 \frac{\sin^2 k_t T}{(k_t T)^2} J_{\max} .$$

Since  $s_{\max} = J_{\max} T$ , one can write

$$\overline{\left| \frac{\Delta A}{A} \right|^2} \cong \frac{1}{\epsilon^2} \frac{\sin^2 k_t T}{k_t T} k_t s_{\max}$$



or

$$\frac{\Delta W}{W} \cong 2 \left( \frac{\Delta A}{A} \right)_{\text{rms}} = 2\epsilon_{\text{rms}} \frac{|\sin k_t T|}{(k_t T)^{1/2}} \sqrt{k_t s_{\text{max}}} .$$

Thus the emittance will grow by an amount proportional to  $(k_t s_{\text{max}})^{1/2}$  where  $\frac{k_t s_{\text{max}}}{2\pi}$  is the number of transverse oscillations that have taken place. The function  $\frac{\sin x}{\sqrt{x}}$  has a broad maximum of about 1.55 at  $x = 1.15$  and varies from 1.41 to 1.55 to 1.41 as  $x$  goes from  $\pi/4$  to 1.15 to  $\pi/2$  .

ESTIMATING THE FREQUENCIES OF COLLECTIVE MOTION

IN A K-V BEAM

The basic equations of motion in a K-V beam are

$$x'' + k_1^2 x = \frac{Ix}{a(a+b)} \quad (1)$$

$$y'' + k_2^2 y = \frac{Iy}{b(a+b)} \quad (2)$$

where  $I$  is proportional to the beam current, and  $2a, 2b$  are the elliptical beam widths (in  $x$  and  $y$ ).

The corresponding envelope equations are

$$a'' + k_1^2 a = \frac{I}{a+b} + \frac{\epsilon_1^2}{a^3} \quad (3)$$

$$b'' + k_2^2 b = \frac{I}{a+b} + \frac{\epsilon_2^2}{b^3} \quad (4)$$

where  $\epsilon_1$  and  $\epsilon_2$  are proportional to the  $x$  and  $y$  beam emittances.

The general procedure is to put  $a'' = b'' = 0$  in (3) and (4) and to solve for the matched beam sizes  $a_0$  and  $b_0$ . The small oscillation frequency is then obtained by expanding  $a$  and  $b$  around  $a_0$  and  $b_0$ . We shall do the simple analysis for a round equilibrium beam by setting

$$\left. \begin{aligned} k_1 &= k_2 = k \\ \epsilon_1 &= \epsilon_2 = \epsilon \end{aligned} \right\} \quad (5)$$

$$\left. \begin{aligned} a'' + k^2 a &= \frac{I}{a+b} + \frac{\epsilon^2}{a^3} \\ b'' + k^2 b &= \frac{I}{a+b} + \frac{\epsilon^2}{b^3} \end{aligned} \right\} \quad (6)$$

Clearly  $k^2 a_0^2 = \frac{I}{2} + \frac{\epsilon^2}{a_0^2}$   $a_0 = b_0$  . (7)

Setting

$$a = a_0 + u \quad u \ll a_0$$

$$b = b_0 + v \quad v \ll b_0$$

one finds

$$u'' + k^2 u = -\frac{Iu}{4a_0^2} - \frac{I}{4a_0^2} v - \frac{3\epsilon^2}{a_0^4} u \quad (8)$$

$$v'' + k^2 v = -\frac{Iv}{4a_0^2} - \frac{Iu}{4a_0^2} - \frac{3\epsilon^2}{a_0^4} v \quad (9)$$

Using (7) we can eliminate  $\epsilon$  from (8) and (9), obtaining

$$u'' + u \left( 4k^2 - \frac{3}{2} \frac{I}{a_0^2} \right) = -\frac{I}{4a_0^2} (u + v) \quad (10)$$

$$v'' + v \left( 4k^2 - \frac{3}{2} \frac{I}{a_0^2} \right) = -\frac{I}{4a_0^2} (u + v) \quad (11)$$

We can now return to (1) and (2) and recognize that

$$\mu = \frac{I}{2a_0^2 k^2} \quad (12)$$

is the ratio of the space charge defocusing force to the external focusing force, and that the tune depression factor is

$$\frac{\sigma}{\sigma_0} = (1 - \mu)^{1/2} \quad (13)$$

In terms of  $\mu$ , one can write (10) and (11) as

$$u'' + k^2 u(4 - 3\mu) = -k^2 \frac{\mu}{2} (u + v) \quad (14)$$

$$v'' + k^2 v(4 - 3\mu) = -k^2 \frac{\mu}{2} (u + v) \quad (15)$$

Setting  $\xi = u + v$ ,  $\eta = u - v$ , we have

$$\xi'' + k^2 \xi(4 - 2\mu) = 0 \quad (16)$$

$$\eta'' + k^2 \eta(4 - 3\mu) = 0 \quad (17)$$

from which we get the oscillation frequencies

$$k_a = k\sqrt{4 - 2\mu} \quad \text{breathing} \quad - \quad x \text{ and } y \quad 180^\circ \text{ out of phase}$$

$$k_b = k\sqrt{4 - 3\mu} \quad \text{breathing} \quad - \quad x \text{ and } y \quad \text{in phase}.$$

These are the small oscillation modes set up by a K-V beam with slightly mismatched parameters a and b.

$\frac{\sigma}{\sigma_0}$	$\mu$	$\frac{k_a}{k}$	$\frac{k_b}{k}$
1.0	.00	2.00	2.00
.9	.19	1.90	1.85
.8	.36	1.81	1.71
.7	.51	1.73	1.57
.6	.64	1.65	1.44
.5	.75	1.58	1.32
.4	.84	1.52	1.22
.3	.96	1.44	1.06
.2	.96	1.44	1.06
.1	.99	1.42	1.01
.0	1.00	1.41	1.00

$$\frac{k_a^2}{k^2} = 2 + \frac{2\sigma^2}{\sigma_0^2}$$

$$\frac{k_b^2}{k^2} = 1 + \frac{3\sigma^2}{\sigma_0^2}$$

$$\mu = 1 - \frac{\sigma^2}{\sigma_0^2}$$

For non-K-V beams, the frequencies will be similar.

ADIABATIC BEHAVIOR OF BUNCHED BEAM

The approximate equations of motion (linear and uncoupled) for a three dimensional beam with ellipsoidal space charge (semi-axes a, a, b) are

$$\frac{d}{ds} \left( \beta^3 \frac{d\phi}{ds} \right) = - \frac{2\pi eET}{\lambda Mc^2} \sin |\phi_s| \psi (1 - \mu_\ell) \quad (1)$$

$$\delta\gamma = - \frac{\beta^3 \lambda}{2\pi} \frac{d\phi}{ds} \quad k_\ell^2 = \frac{2\pi eET}{\lambda \beta^3 Mc^2} \sin |\phi_s| \quad (2)$$

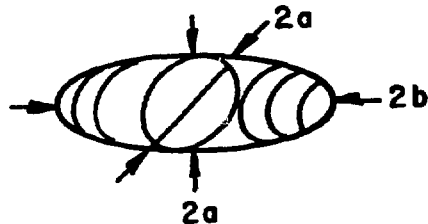
$$\frac{1}{\beta} \frac{d}{ds} \left( \beta \frac{dx}{ds} \right) = - k_t^2 x (1 - \mu_t) \quad , \quad (3)$$

where  $k_t^2$  takes into account the r.f. defocussing as well as the primary (smoothed) quadrupole focusing. Here

$$\mu_\ell = \frac{15}{\pi} \text{ ohms} \frac{I \lambda^2}{ab^2} \frac{\beta}{ET \sin |\phi_s|} = 30 \text{ ohms} \frac{eI}{Mc^2} \frac{\lambda}{ab^2} \frac{1}{\beta^2 k_\ell^2} \quad (4)$$

$$\mu_t = 45 \text{ ohms} \frac{eI}{Mc^2} \frac{\lambda}{ab^2} \frac{1}{\beta^2 k_t^2} \quad , \quad (5)$$

where we have assumed that the ellipsoidal space charge function  $f\left(\frac{b}{a}\right) \approx \frac{a}{3b} \ll 1$ .



The adiabatic variation of  $E$ ,  $|\phi_s|$ ,  $\beta$ ,  $k_t$  will cause the dimensions of the bunch,  $a$ , and  $b$  to vary, according to the relations.

### Longitudinal

$$\hat{\psi} \equiv (\phi - \phi_s)_{\max} \sim \frac{1}{\left[\beta^6 k_\ell^2 (1 - \mu_\ell)\right]^{1/4}} G_\ell \quad (6)$$

$$\hat{\delta Y} = \frac{\beta^3 \lambda}{2\pi} k_\ell (1 - \mu)^{1/4} \sim \left[\beta^6 k_\ell^2 (1 - \mu_\ell)\right]^{1/4} G_\ell \quad (7)$$

$$b = \frac{\beta \lambda}{2\pi} \hat{\psi} \sim \left[\beta^2 k_\ell^2 (1 - \mu_\ell)\right]^{-1/4} G_\ell \quad (8)$$

Note that the phase space area does not vary adiabatically. Also, we have included a growth factor  $G_\ell$  for the longitudinal motion which takes into account the effect of couplings and non-linearities, corresponding to observed emittance growths.

### Transverse

$$\hat{x} \equiv a \sim \left[\beta^2 k_t^2 (1 - \mu_t)\right]^{-1/4} G_t \quad (9)$$

$$\hat{\beta x'} \equiv \frac{\hat{p}_x}{Mc} \sim \left[\beta^2 k_t^2 (1 - \mu_t)\right]^{1/4} G_t \quad (10)$$

The phase space areas occupied by the beam then vary as

$$W_\ell \sim G_\ell^2, \quad W_t \sim G_t^2 \quad (11)$$

We can use (8) and (9) in (4) or (5) to give us the values of  $\mu_t$  and  $\mu_\ell$  as the parameters change. As a result of studies of the oscillation modes of charged particle bunches, one should avoid the regions near  $\mu_t = 1$ ,  $\mu_\ell = 1$ . As a guide, one should choose parameters in such a way that  $\mu_t$  and  $\mu_\ell$  vary smoothly and do not exceed 0.5 or 0.6.

The variation of  $\mu_t$  and  $\mu_\ell$  with the parameters can be obtained by using (8) and (9) in (4) and (5), leading to

$$\mu_\ell \sim (\beta k_t)^{+1/2} (1 - \mu_t)^{+1/4} (\beta k_\ell)^{-1} (1 - \mu_\ell)^{+1/2} G_t^{-1} G_\ell^{-2} \quad (12)$$

$$\mu_t \sim (\beta k_t)^{-1} (1 - \mu_t)^{+1/2} (\beta k_\ell)^{+1/2} (1 - \mu_\ell)^{+1/4} G_t^{-2} G_\ell^{-1} \quad (13)$$

Smooth variation of  $\mu_\ell$  and  $\mu_t$  therefore corresponds to smooth variation of  $\beta k_t$  and  $\beta k_\ell$  independently. The former ( $\beta k_t$ ) corresponds to constant transverse phase advance per period. The latter ( $\beta k_\ell$ ) also corresponds to constant longitudinal phase advance per cell, and is related to the accelerating parameters by (2) such that

$$\beta^2 k_\ell^2 = \frac{2\pi e}{\lambda M c^2} \left( \frac{ET \sin|\phi_s|}{\beta} \right) .$$

The product  $ET \sin|\phi_s|$  should therefore be approximately proportional to  $\beta$ .

It would be useful to monitor the values of  $\mu_t$  and  $\mu_\ell$  during computational runs, as a guide to reasonable matching in the presence of space charge.

STABILITY OF TWO-AND THREE- DIMENSIONAL PARTICLE  
DISTRIBUTIONS

In a high current accelerator, the tolerance on beam loss can be severe. In order to estimate or predict the beam loss, it is important to explore the low density (halo or tail) regions of the phase space distribution. In addition, since the actual charge distribution will not be completely stable, these low density regions can regenerate even if beam apertures and scrapers are used. The purpose of this note is to discuss the stability of various phase space distributions, with a view to finding the "most stable", and preparing the incoming beam optimally.

It is well known that the Kapchinsky - Vladimirovsky distribution leads to uniform two dimensional charge density, linear forces, and a stationary distribution. A study of the mode spectrum for oscillation about the stationary KV distribution\* shows that for most values of the parameter  $\mu$ , defined by

$$\mu = \frac{\text{space charge defocusing gradient at } r=0}{\text{external focusing gradient (at } r=0)}$$

all frequencies are real and the KV distribution will be stable ( $0 < \mu < \text{about } .9$ ).

Numerical calculations starting with a KV distribution nevertheless show a gradual rounding and departure from the KV distribution with time. This is attributed to the particle - particle space charge interaction in the computational model used, which introduces a collision-like term, whereas the KV model represents a continuous fluid without collisions.

Since there are also collision terms in a real beam, it is reasonable to expect a KV distribution (which seems not to occur in nature) to change with time. In fact, all distributions should eventually tend to the statistically stable one, namely the Boltzmann distribution. This one should be stable in

\*R. L. Gluckstern, Proc. of the NAL Linac Conference 1970, p. 811;  
(see also subsequent analysis by F. Sacherer, CERN)



time, and is probably the most desirable for injection (will probably minimize diffusion type effects).

It should be interesting to perform the following numerical calculations (in the absence of acceleration, and with linear external forces).

- 1) Start with a KV distribution (a reasonable  $\mu$  might be 1/2) in 2 dimensions ( $x, x', y, y'$ ) and watch it evolve in time, using a model with  $N$  line charges or currents.
  - a) Calculate space charge by calculating each pair interaction.
  - b) Calculate space charge assuming azimuthal symmetry.
  - c) See if the distribution settles down, and if so, how long it took to do so.
  - d) Repeat a) and/or b) and c) for twice as large an  $N$ , or  $4x$  or  $10x$ ---. (Keep total current the same). Does it tend to the same final distribution? If so, does the rate depend on  $N$ ? (The cutoff will have to be handled carefully).
  - e) Repeat for  $\mu = .2, \mu = .98$ .
- 2) Repeat 1) for another initial distribution (for example,  $n = 1$  in the analytic forms described in Gluckstern, Chasman, and Crandall, Proc. NAL Linac Conf. 1970, p. 823).
- 3) Start with a Boltzmann distribution in 2 dimensions and repeat 1).
- 4) Use a Boltzmann distribution in 3 dimensions ( $z, z', x, x', y, y'$ ) with spherical symmetry to make the analysis simple. See what changes take place in going from 2 to 3 dimensions.

Analytic expressions needed

1) KV Distribution

$$f(W) = \delta(W_0 - W)$$

$$W = \frac{x'^2}{2} + \frac{y'^2}{2} + \left(\frac{1-\mu}{2}\right)(x^2 + y^2) ; \quad W_0 = \frac{1-\mu}{2} a^2$$

a) Initial distribution

$$\left[ \frac{d(\phi)}{2\pi} \right] \left[ \frac{d(\alpha)}{2\pi} \right] \left[ \frac{d\left(\frac{r^2}{a^2}\right)}{2} \right] \left[ \frac{d\left(\frac{\sigma^2}{a^2(1-\mu)}\right)}{2} \right] \times \delta\left(\frac{1-\mu}{2} a^2 - \frac{1-\mu}{2} r^2 - \sigma^2\right)$$

$x = r \cos\phi$   
 $y = r \sin\phi$   
 $x' = \sigma \cos\alpha$   
 $y' = \sigma \sin\alpha$

Each of the bracketed quantities is to be selected randomly on the interval 0 to 1, and the delta function interpreted as a narrow strip.

An alternative formulation which avoids the delta function comes about by writing

$$\begin{aligned} r &= a \cos\psi \\ \sigma &= a \sqrt{1-\mu} \sin\psi \end{aligned} \quad 0 \leq \psi \leq \frac{\pi}{2}$$

leading to

$$\left[ \frac{d(\phi)}{2\pi} \right] \left[ \frac{d(\alpha)}{2\pi} \right] \left[ \frac{d(\cos 2\psi)}{2} \right] \quad \text{starting distribution.}$$

b) Individual motion equation ( $n_j$  is the number with radius  $r_j$ )

$$x_i'' + k^2 x_i = k^2 \mu \frac{x_i}{r_i^2} \left[ \frac{\sum_{r_j < r_i} n_j}{N} \right] a^2 .$$

This assumes azimuthal symmetry. For pair interactions make the replacement

$$\frac{x_i}{r_i^2} \left[ \frac{\sum_{r_j < r_i} n_j}{N} \right] \longrightarrow \frac{1}{N} \sum_{j \neq i} \left( \frac{x_i - x_j}{r_{ij}^2} \right) .$$

It turns out to be convenient to go to the dimensionless variables

$$x = Xa$$

$$s = ks$$

in which case

$$\frac{d^2 X_i}{ds^2} + X_i = \mu \frac{X_i}{R_i^2} \frac{\sum_{R_j < R_i} n_j}{N}$$

$$X_i = \cos\psi \cos\phi$$

$$Y_i = \cos\psi \sin\phi$$

$$\frac{dX_i}{ds} = \sqrt{1 - \mu} \sin\psi \cos\alpha$$

$$\frac{dY_i}{ds} = \sqrt{1 - \mu} \sin\psi \sin\alpha .$$

- 2) n = 1 distribution (Proc. NAL Conference, P. 825) (Uniform distribution within hypersphere)

$$\frac{1}{R} \frac{d}{dR} \left( R \frac{dg}{dR} \right) = -1 + \mu g$$

$g = 0$  defines the outer boundary  $R_o$

$$g(R^2) = \frac{1}{\mu} - \frac{1-\mu}{\mu} I_0(\sqrt{\mu} R)$$

$$J(R^2) = \int_0^{R^2} dR^2 \left[ \frac{1}{\mu} - \frac{1-\mu}{\mu} I_0(\sqrt{\mu} R) \right], \quad J_o \equiv J(R_o^2)$$

$$J_o = \frac{R_o^2}{\mu} - \frac{2(1-\mu)}{\mu^{3/2}} R_o I_1(\sqrt{\mu} R_o) \quad dJ = g dR^2$$

- a) The individual particle motion is given by

$$\frac{d^2 X_i}{dS^2} + X_i = \mu J_o \frac{X_i}{R_i^2} \frac{\sum_{R_j < R_i} n_j}{N}$$

Here  $X_i$  is not the same as in 1). The initial distribution is chosen according to

$$\left[ \frac{d(\phi)}{2\pi} \right] \left[ \frac{d(\alpha)}{2\pi} \right] \left[ \frac{d(J)}{J_o} \right] \left[ \frac{d(R'^2)}{4g} \right]$$

- 3) Two dimensional Boltzmann distribution

- a) Must first solve numerically for the function  $g$

$$\frac{d}{dR^2} \left( R^2 \frac{dg}{dR^2} \right) = \frac{1-\mu}{4} e^{-g}$$

$$e \left( -\frac{Mv^2}{2RT} - \frac{e\phi}{kT} \right)$$

$$g(0) = 0$$

$$\frac{dg}{dR^2} = \frac{1-\mu}{4}$$

b) Let

$$H(R^2) = \int_0^{R^2} dR^2 e^{-g} \quad dH = e^{-g} dR^2$$

$$H_0 = H(\infty) = \int_0^{\infty} dR^2 e^{-g}$$

Individual particle motion is governed by

$$\frac{d^2 X_i}{dS^2} + X_i = \mu P_0 \frac{X_i}{R_i^2} \frac{\sum_{R_j < R_i} n_j}{N} .$$

c) Initial distribution

$$\left[ \frac{d(\phi)}{2\pi} \right] \left[ \frac{d(\alpha)}{2\pi} \right] \left[ d \left( e^{-\frac{R_i^2}{4}} \right) \right] \left[ \frac{d(H)}{H_0} \right]$$

4) Three dimensional Boltzmann distribution

$$\frac{1}{R^2} \frac{d}{dR} \left( r^2 \frac{dg}{dr} \right) = 1 - \mu e^{-g}$$

The distribution requires spherical coordinates, and the individual motion equation requires the change

$$\frac{X_i}{R_i^2} \longrightarrow \frac{X}{R^3} .$$

This analysis can be carried out along the same lines as that in 3) and will be done later.

5) Plotting variable

It is most useful to plot the distribution as a function of the energy variable  $W$ , as the distribution progresses apart from constants, it appears to be expressible as

$$W = \frac{1}{2} \left( \frac{dX}{dS} \right)^2 + \frac{1}{2} \left( \frac{dY}{dS} \right)^2 + \frac{R^2}{2} - \mu \begin{pmatrix} 1 \\ J_0 \\ H_0 \end{pmatrix} \left\{ \frac{\sum_{R_j < R} \ln \frac{R}{R_j} n_j}{N} \right\} .$$

This should be checked numerically.

IMAGE CHARGE CALCULATIONS NEAR A CYLINDRICAL BOUNDARY

A. The potential for a line charge in a cylinder can be solved by using a single line charge. But for a point charge in a cylinder, one has to use some type of expansion (usually called a Green's Function Method.)

Suppose we have a point charge  $Q$  located at  $z = 0$ ,  $r = a$ ,  $\theta = 0$  in a cylindrical pipe of radius  $R$ . One can write for a general solution of the Poisson (Laplace except at  $z = 0$ ,  $x = a$ ,  $y = 0$ ) equation which vanishes at  $r = R$ , and at  $z = \pm\infty$

$$\phi(r, \theta, z) = \sum_{n=1}^{\infty} \sum_{m=-\infty}^{\infty} A_{mn} e^{im\theta} J_m\left(\frac{p_{nm}r}{R}\right) e^{-\frac{p_{nm}}{R}|z|} \quad (1)$$

$$\text{where } J_m(p_{nm}) = 0 \quad .$$

$$\text{Writing } \nabla^2 \phi = -4\pi Q \delta(z) \delta(x-a) \delta(y) \quad (2)$$

it is possible to integrate (2), with  $\phi$  replaced by (1), across the discontinuity, unfolding the orthonormal set in  $r, \theta$  to obtain

$$A_{mn} = \frac{2Q}{R} \frac{J_m\left(\frac{p_{nm}a}{R}\right)}{P_{nm} J_{m+1}^2(p_{nm})} \quad . \quad (3)$$

One therefore obtains

$$\phi(r, \theta, z) = \sum_{n=1}^{\infty} \sum_{m=0}^{\infty} \frac{4Q}{R^2} \frac{J_m\left(\frac{p_{nm}a}{R}\right) J_m\left(\frac{p_{nm}r}{R}\right)}{P_{nm} J_{m+1}^2(p_{nm})} \cos m\theta e^{-\frac{p_{nm}}{R}|z|} \quad , \quad (4)$$

where  $2_m = 2$  for  $m = 0$ , and 1 for  $m \neq 0$ .

## B. Convergence

The series in (4) and the fields which can be derived from it are convergent only from the  $e^{-\frac{p_{nm}|z|}{R}}$ , where  $p_{nm}$  is given asymptotically by

$$p_{nm} \cong (2n + 1) \frac{\pi}{2} + \left(m + \frac{1}{2}\right) \frac{\pi}{2} \quad \text{large } m, n. \quad (5)$$

Thus (4) can be used only when  $|z|$  is large enough to get useful convergence. In principle, the radial force due to the image alone, evaluated at the charge, is obtained by setting  $r = a$ ,  $\theta = 0$  in (4) and evaluating the sum for ever decreasing values of  $|z|$  (slower and slower convergence). Another form of calculation is needed near or at  $z = 0$ .

C. An alternate series to (1) is

$$\theta(r, \theta, z) = \int_0^\infty dk \sum_{n=0}^\infty A_n(k) \cos n\theta \begin{cases} \frac{I_n(kr)}{I_n(ka)} & , \quad 0 \leq r < a \\ \frac{F_n(kr)}{F_n(ka)} & , \quad r < a \leq R \end{cases} \quad (6)$$

where

$$F_n(kr) = K_n(k_n) - \frac{K_n(kR)}{I_n(kR)} I_n(kr) \quad (7)$$

Using (2), one can eventually find

$$\phi = \frac{4Q}{\pi} \int_0^\infty dk \cos kz \sum_{n=0}^\infty \frac{\cos n\theta}{2^n} \left[ - \frac{I_n(ka)K_n(kR)I_n(kr)}{I_n(kR)} + \begin{cases} \frac{I_n(kr)K_n(ka)}{0 \leq r < a} \\ \frac{I_n(ka)K_n(kr)}{a < r \leq R} \end{cases} \right] \quad (8)$$



Since the first term in [ ] vanishes for  $R \rightarrow \infty$ , and the second term is independent of  $R$ , the first term is the image potential and the second is the self potential in free space. Thus

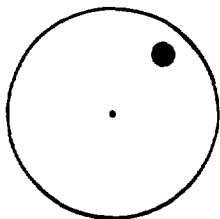
$$\phi_{\text{image}} = -\frac{4Q}{\pi} \int_0^{\infty} dk \cos kz \sum_{n=0}^{\infty} \frac{\cos n\theta}{2^n} \frac{I_n(ka)K_n(kR)I_n(kr)}{I_n(kR)} \quad (9)$$

#### D. Convergence

This expression has no singularities for  $0 < r < a$  and therefore converges well, except if both  $r$  and  $a$  are near  $R$ , in which case there is an effective point charge image at  $r = 2R - a$ ,  $\theta = 0$ ,  $z = 0$ .

#### E. Approximations

The existing PARMILA program calculated the centroid of the actual charge distribution. It is then possible to use (9) to calculate the image fields from such a charge placed at the centroid. However, an approximate method is desirable in order to make the calculations fast.



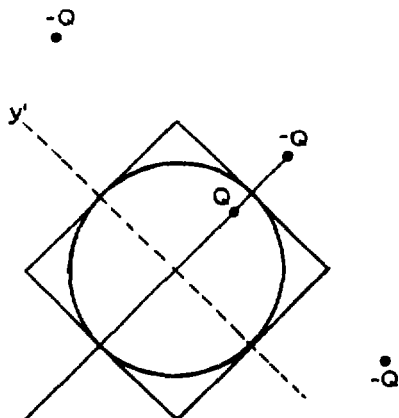
The proposed approximation is to replace the cylinder by a square, oriented along the radial line to the centroid, and use the 4 primary

images, located at

$$\begin{pmatrix} x' \\ y' \end{pmatrix} = \begin{pmatrix} \textcircled{1} \\ \textcircled{2} \end{pmatrix}, \begin{pmatrix} \textcircled{2} \\ \textcircled{3} \end{pmatrix}, \begin{pmatrix} \textcircled{3} \\ \textcircled{4} \end{pmatrix}, \begin{pmatrix} \textcircled{4} \\ \textcircled{1} \end{pmatrix}$$

Actually, if  $a$  is near  $R$ , one should probably not use images 3 and 4, or one should add the next 4 (with charge  $+Q$ ) at

$$\begin{pmatrix} \textcircled{5} \\ \textcircled{6} \end{pmatrix}, \begin{pmatrix} \textcircled{6} \\ \textcircled{7} \end{pmatrix}, \begin{pmatrix} \textcircled{7} \\ \textcircled{8} \end{pmatrix}, \begin{pmatrix} \textcircled{8} \\ \textcircled{5} \end{pmatrix}$$



Another possible variation is to use a square of the same area as the circle, which should give more correct fields near  $r = 0$ , but less correct fields near  $r = a$ .

---

F. Suggested procedure:

- (1) Use a square  $2R \times 2R$
- (2) Try centroid locations at  $x' = 0, \frac{R}{4}, \frac{2R}{4}, \frac{3R}{4}$ , and  $z' = z = 0, \pm\frac{R}{4}, \pm\frac{R}{2}, \pm R, \pm 2R$ . Calculate the fields  $E_x, E_z$  from 2 image charges, and for 4 image charges
- (3) Repeat (2) using (9)
- (4) Repeat (2) for a smaller square if (3) and (2) are not sufficiently close to one another.

When the comparisons are made, it will probably be a simple matter to improve the procedure as necessary.

SIX-DIMENSIONAL PHASE SPACE DISTRIBUTIONS

I. INTRODUCTION

Numerical calculations are being carried out for particle distributions and the corresponding phase space projections and emittances in the presence of space charge forces and non-linear longitudinal external forces (from an accelerating bucket). The result is an asymmetric distribution in the longitudinal displacement, which makes fitting to an ellipsoid problematical. The purpose of this note is to develop a realistic parametrization of the distribution to help in the fitting and analysis of the computations.

We shall assume axial symmetry in our 6-D phase space distribution which is taken to be of the form

$$f(x,x',y,y',z,z') = \text{const} \left[ 1 - \frac{r^2}{a^2} - \frac{z^2}{b^2} - \epsilon \frac{z^3}{b^3} - \delta \frac{r^2}{a^2} \frac{z}{b} - \frac{x'^2 + y'^2}{c^2} - \frac{z'^2}{d^2} \right]^m . \quad (1)$$

The distribution is then determined by the shape parameter  $m$ , by the scale parameters  $a, b, c, d$ , and by the dimensionless asymmetry parameters  $\epsilon, \delta$ .

II. PROJECTIONS

A. The projection onto the spatial coordinates is obtained by integrating (1) over  $x', y', z'$ . The process is simple and leads to the real space charge density

$$\rho(r,z) = \text{const} \left[ 1 - \frac{r^2}{a^2} - \frac{z^2}{b^2} - \epsilon \frac{z^3}{b^3} - \delta \frac{r^2}{a^2} \frac{z}{b} \right]^{m+\frac{3}{2}} . \quad (2)$$

At this point it is important to point out that  $z = 0$  has been defined to be the position of maximum density. It is also clear that there is an  $r$  dependent asymmetry in the longitudinal direction governed by both  $\epsilon$  and  $\delta$ .

B. The projection onto the  $z, z'$  plane is equally straightforward, and is

$$G(z,z') = \text{const} \frac{\left[ 1 - \frac{z^2}{b^2} - \epsilon \frac{z^3}{b^3} - \frac{z'^2}{d^2} \right]^{m+2}}{1 + \delta \frac{z}{b}} . \quad (3)$$

C. The projection onto the  $x, x'$  plane can similarly be derived and is

$$H(x, x') = \text{const} \int \frac{dz}{b} \frac{\left[ 1 - \frac{x^2}{a^2} - \frac{z^2}{b^2} - \frac{\epsilon z^3}{b^3} - \delta \frac{x^2}{a^2} \frac{z}{b} - \frac{x'^2}{c^2} \right]^{m+\frac{3}{2}}}{\left[ 1 + \delta \frac{z}{b} \right]^{1/2}} \quad (4)$$

Unfortunately, the integral can be carried out in terms of simple functions only for special values of  $m$ . However, the outer borders in the  $x, x'$  distribution correspond to small values of  $\frac{z}{b}$ , in which case the distribution is approximately

$$H(x, x') \cong \text{const} \left[ 1 - \frac{x^2}{a^2} - \frac{x'^2}{c^2} \right]^{m+2} \quad (5)$$

[Corrections to (5) are of order  $\delta^2$  near the border  $\frac{x^2}{a^2} + \frac{x'^2}{c^2} \approx 1$  and of order  $\delta$  and  $\epsilon$  near  $(x, x') \cong (0, 0)$ .]

### III. NUMERICAL CALCULATION OF PARAMETERS

#### A. Parameter $m$

The value of  $m$  governs the shape of the distribution and can be most easily obtained by examining the even moments of  $r$  and  $z$ , which will be independent of  $\epsilon, \delta$  to second order. Using

$$\int_0^1 dt t^{\alpha-1} (1-t)^{\beta-1} = \frac{\Gamma(\alpha)\Gamma(\beta)}{\Gamma(\alpha+\beta)} \quad (6)$$

one finds

$$\overline{\left(\frac{x}{a}\right)^{2i} \left(\frac{y}{a}\right)^{2j} \left(\frac{z}{b}\right)^{2k}} \cong \frac{\Gamma\left(i + \frac{1}{2}\right)}{\Gamma\left(\frac{1}{2}\right)} \cdot \frac{\Gamma\left(j + \frac{1}{2}\right)}{\Gamma\left(\frac{1}{2}\right)} \cdot \frac{\Gamma\left(k + \frac{1}{2}\right)}{\Gamma\left(\frac{1}{2}\right)} \cdot \frac{\Gamma(m+4)}{\Gamma(m+4+i+j+k)} \quad (7)$$

Specifically

$$\begin{aligned}
\overline{x^2} = \overline{y^2} &= \frac{a^2}{2(m+4)} \quad , \quad \overline{z^2} = \frac{b^2}{2(m+4)} \\
\overline{x^4} = \overline{y^4} &= \frac{3a^4}{4(m+5)(m+4)} \quad , \quad \overline{z^4} = \frac{3b^4}{4(m+5)(m+4)} \\
\overline{x^2 y^2} &= \frac{a^4}{4(m+5)(m+4)} \quad , \quad \overline{x^2 z^2} = \overline{y^2 z^2} = \frac{a^2 b^2}{4(m+5)(m+4)} \\
\overline{r^2} &= \frac{a^2}{m+4} \quad , \quad \overline{r^4} = \frac{a^4}{(m+5)(m+4)} \\
\overline{r^2 z^2} &= \frac{a^2 b^2}{2(m+5)(m+4)}
\end{aligned} \quad \left. \vphantom{\begin{aligned} \overline{x^2} = \overline{y^2} \\ \overline{x^4} = \overline{y^4} \\ \overline{x^2 y^2} \\ \overline{r^2} \\ \overline{r^2 z^2} \end{aligned}} \right\} \quad (8)$$

The value of  $m$  can be inferred from (8) by using combinations like

$$\begin{aligned}
\frac{\overline{r^4}}{(\overline{r^2})^2} &= \left( \frac{m+4}{m+5} \right) \quad , \quad \frac{\overline{z^4}}{(\overline{z^2})^2} = \frac{3(m+4)}{(m+5)} \\
\frac{\overline{r^2 z^2}}{\overline{r^2} \overline{z^2}} &= \left( \frac{m+4}{m+5} \right)
\end{aligned} \quad \left. \vphantom{\begin{aligned} \frac{\overline{r^4}}{(\overline{r^2})^2} \\ \frac{\overline{r^2 z^2}}{\overline{r^2} \overline{z^2}} \end{aligned}} \right\} \quad (9)$$

This permits testing the consistency of the form of the distribution (1).

B. Scale Parameters a, b, c, d

Once  $m$  is set, the scale parameters  $a$  and  $b$  can be determined from (8).

For example

$$a^2 = 2(m+4) \overline{x^2} = (m+4) \overline{r^2} \quad , \quad b^2 = 2(m+4) \overline{z^2} \quad . \quad (10)$$

Similarly  $c^2$  and  $d^2$  are obtained from

$$c^2 = 2(m+4) \overline{x'^2} \quad , \quad d^2 = 2(m+4) \overline{z'^2} \quad . \quad (11)$$

C. Asymmetry Parameters  $\epsilon, \delta$

In order to determine  $\epsilon, \delta$ , we must take odd moments of the distribution in (2). The average of

$$\overline{x^{2i} y^{2j} z^{2k+1}}$$

then requires expansion of (2) to terms linear in  $\epsilon$  and  $\delta$ , i.e.

$$\left(1 - \frac{r^2}{a^2} - \frac{z^2}{b^2}\right)^{m+\frac{3}{2}} - \left(m + \frac{3}{2}\right) \left(\frac{\epsilon z^3}{b^3} + \delta \frac{r^2 z}{a^2 b}\right) \left(1 - \frac{r^2}{a^2} - \frac{z^2}{b^2}\right)^{m+\frac{1}{2}} + \dots$$

As a result, it can be shown that

$$\begin{aligned} \overline{\left(\frac{x}{a}\right)^{2i} \left(\frac{y}{a}\right)^{2j} \left(\frac{z}{b}\right)^{2k+1}} &= - \frac{\Gamma(m+4)}{\Gamma(m+5+i+j+k)} \cdot \frac{\Gamma\left(i + \frac{1}{2}\right)}{\Gamma\left(\frac{1}{2}\right)} \cdot \frac{\Gamma\left(j + \frac{1}{2}\right)}{\Gamma\left(\frac{1}{2}\right)} \cdot \frac{\Gamma\left(k + \frac{3}{2}\right)}{\Gamma\left(\frac{1}{2}\right)} \cdot \\ &\quad \left[ \epsilon \left(k + \frac{3}{2}\right) + \delta(i+j+1) \right] \end{aligned} \quad (12)$$

Specifically

$$\left. \begin{aligned} \overline{\frac{z}{b}} &= - \frac{1}{2} \frac{\left(\frac{3}{2}\epsilon + \delta\right)}{(m+4)} \\ \overline{\frac{z^3}{b^3}} &= - \frac{3}{4} \frac{\left(\frac{5}{2}\epsilon + \delta\right)}{(m+5)(m+4)} \\ \overline{\frac{x^2 z}{a^2 b}} = \overline{\frac{y^2 z}{a^2 b}} = \frac{1}{2} \overline{\frac{r^2 z}{a^2 b}} &= - \frac{1}{4} \frac{\left(\frac{3}{2}\epsilon + 2\delta\right)}{(m+5)(m+4)} \end{aligned} \right\} \cdot \quad (13)$$

Clearly the three observables  $\overline{z}$ ,  $\overline{z^3}$  and  $\overline{zr^2}$  in (13) can be used to calculate  $\epsilon$  and  $\delta$ , and to check the consistency of the form of the distribution once again.

#### IV. EMITTANCE

A. x, x' Emittance. Once the parameters a, c are determined, it is possible to obtain a measure of the x, x' emittance by evaluating the area and number of particles contained within the curve

$$H(x, x') = P H(0, 0) \quad (14)$$

where P is a number between 0 and 1. If the shape of the curve is given by (5), one finds for the emittance

$$E^x = \pi a c \left[ 1 - \frac{1}{P^{m+2}} \right] \quad (15)$$

If the fraction of the beam within (14) is chosen to be .90 (to minimize the effect of stragglers), one can show that P is equivalent to  $(.1)^{(m+2)/(m+3)}$ . In any event, the 90% contour defines an emittance in (15) which corresponds to a, c being reduced by the same factor. A further test of the index m is provided by the dependence of this emittance on the choice of P (or the 90% figure).

B. z, z' Emittance. Once the parameters b, d,  $\epsilon$ ,  $\delta$  are determined, it is possible to obtain a measure of the z, z' emittance by evaluating the area and number of particles contained within the curve

$$G(z, z') = P G(0, 0) \quad , \quad (16)$$

where G(z, z') is given in (3). To first order in  $\epsilon$  and  $\delta$ , the curve will be given by

$$\frac{z^2}{b^2} + \frac{z'^2}{d^2} = 1 - \frac{\epsilon z^3}{b^3} - P^{\frac{1}{m+2}} \left( 1 + \frac{\delta}{m+2} \frac{z}{b} \right) \quad (17)$$

The asymmetry in (17) can be exhibited by evaluating the z intercepts,  $z_{\pm}$ ,

given approximately by setting  $z \cong \pm b \left( 1 - P^{\frac{1}{m+2}} \right)^{\frac{1}{2}}$  on the right side of (17) and by making  $z' = 0$ . This leads to

$$\frac{z_{\pm}}{b} \cong \pm \left( 1 - \frac{1}{P^{m+2}} \right)^{\frac{1}{2}} - \frac{\varepsilon}{2} \left( 1 - \frac{1}{P^{m+2}} \right) \frac{\delta}{2(m+2)} P^{\frac{1}{m+2}} . \quad (18)$$

Once P is determined from the 90% condition, (18) provides further confirmation of  $\varepsilon$  and  $\delta$ , obtained earlier from (13).

## V. SUMMARY

We have suggested a parametrization of the 6-D phase space distribution which exhibits the observed asymmetry in the longitudinal direction. Procedures are developed for obtaining the values of the parameters from moments and contours of the computed particle distributions. This should eliminate the difficulty of matching an ellipse to the asymmetric distribution in the longitudinal phase space, and should enable comparisons of emittance for different asymmetries.



PROJECTIONS OF MULTIDIMENSIONAL PHASE-SPACE DISTRIBUTIONS

From a distribution in multidimensional phase space  $f(R^2)$ , where

$$R^2 = x^2 + y^2 + z^2 + x'^2 + y'^2 + z'^2 ,$$

we want to find the projected density distribution in  $x, y$ :

$$\int_{-1}^1 d \cos 2\phi \int_0^{2\pi} d\theta \int_0^{2\pi} d\alpha \int_0^\infty s^2 ds^2 f(\underbrace{r^2 + z^2 + x'^2 + y'^2 + z'^2}_{\text{go to } z = s \cos \phi \cos \theta})$$

$$\begin{aligned} x' &= s \cos \phi \sin \theta \\ y' &= s \sin \phi \cos \alpha \\ z' &= s \sin \phi \sin \alpha \end{aligned}$$

$$\rho(r^2) + \int_0^\infty dt t f(t + r^2) = \int_{r^2}^\infty dw (w - r^2) f(w) .$$

Try

$$f(w) = (1 - w)^n$$

$$\begin{aligned} \rho(r^2) &= \int_{r^2}^\infty dw (w - r^2) (1 - w)^n \\ &= \int_{r^2}^1 dw (1 - r^2 - (1 - w)) (1 - w)^n \end{aligned}$$

by completing the square. The upper limit is 1 because  $f(w)$  is to stop at 1.

$$= \left[ (1 - r^2) \frac{(1 - w)^{n+1}}{n+1} - \frac{(1 - w)^{n+2}}{n+2} \right] \Big|_{r^2}^1$$

$$\rho(r^2) = (1 - r^2)^{n+2} \frac{1}{(n+1)(n+2)} .$$


---

To get a parabolic result  $n = -1$ ; behavior is singular.

---

Suppose

$f(t + r^2) = \delta(t + r^2 - 1)$  i.e., a six-dimensional surface, then

$$= \delta(w - 1)$$

$$= \int_{r^2}^{\infty} dw (w - r^2) \delta(w - 1)$$

$$= 1 - r^2$$

so the resulting projection is parabolic.

Try  $f(w) = \sqrt{w} (1 - w)^n$

$$\int_{r^2}^1 dw (w - r^2) \sqrt{w} (1 - w)^n .$$

For  $n = 0$ :  $\frac{2}{5} [1 - r^5] - r^2 \frac{2}{3} [1 - r^3]$

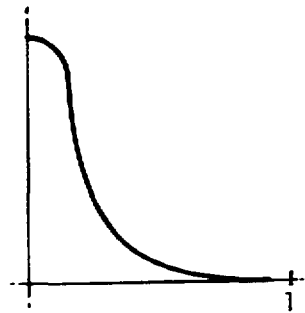
$$= \frac{2}{5} - \frac{2}{3} r^2 + \frac{2}{15} r^5 .$$



Try  $f(w) = \frac{1}{\sqrt{w}}$

$$\int_{r^2}^1 dw (w - r^2) \frac{1}{\sqrt{w}} = \frac{2}{3} (1 - r^3) - r^2 2(1 - r)$$

$$= \frac{2}{3} - 2r^2 + \frac{4}{3} r^3 \quad .$$



Try  $f(w) = \frac{1}{w^n}$  ;  $n < 1$

$$\int_{r^2}^1 dw (w - r^2) \frac{1}{w^n} = \frac{1}{2-n} [1 - r^{4-2n}] - \frac{r^2}{1-n} [1 - r^{2-2n}]$$

$$= \frac{1}{2-n} - \frac{r^2}{1-n} + \frac{r^{4-2n}}{(1-n)(2-n)} \quad .$$

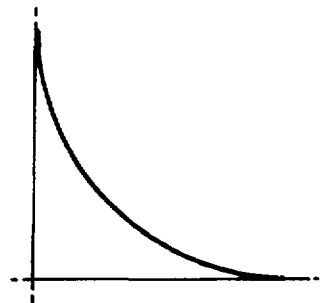
For  $n = 1$ :

$$\int_{r^2}^1 dw (w - r^2) \frac{1}{w} = 1 - r^2 - r^2 \ln \frac{1}{r^2} \quad .$$

For  $n = \frac{3}{2}$ :

$$\int_{r^2}^1 dw (w - r^2) \frac{1}{w^{3/2}} = 2(1 - r) - 2r^2 \left( \frac{1}{r} - 1 \right)$$

$$= 2 - 2r - 2r + 2r^2 = 2 - 4r + 2r^2$$



If 
$$f = \frac{1}{2} \delta(t + r^2 - 1) + \frac{1}{4(t+r^2)^{3/2}}$$

$$\int_r^{1+r^2} dw (w - r^2) \left[ \frac{\delta(w - 1)}{2} + \frac{1}{4w^{3/2}} \right]$$

$$= \frac{1 - r^2}{2} + \frac{1}{4} \left. 2w^{1/2} \right|_{r^2}^1 - \frac{r^2}{4} \left. 2w^{-1/2} \right|_1^{r^2}$$

$$= \frac{1 - r^2}{2} + \frac{1 - r}{2} - \frac{r^2}{2} \left( \frac{1}{r} - 1 \right)$$

$$= 1 - r \quad \text{Conical.}$$

Suppose  $f(w) = \frac{\delta(w - 1)}{2} + \frac{1}{4w^{3/2}}$

only near
only up to  
 $w=1$ 
 $w=1$

We can generalize:

$$\rho(t) = \int_t^{\infty} dw (w - t) f(w)$$

(a) Suppose  $f(w)$  extends to  $w = \infty$

$$\rho'(t) = - \int_t^{\infty} dw f(w)$$

$$\rho''(t) = + f(t)$$

This is the way to get  $f(t)$  from  $\rho(t)$ .

For example  $\rho = \rho_0 e^{-\alpha r^2}$

$$= \rho_0 e^{-\alpha t}$$

$$f(t) = \alpha^2 \rho_0 e^{-\alpha t}$$

(b) Suppose  $f(w)$  cuts off at  $w = 1$

$$\rho'(t) = \begin{cases} - \int_t^1 dw f(w) & t < 1 \\ 0 & t > 1 \end{cases}$$

$$\rho''(t) = \begin{cases} f(w) & t < 1 \\ 0 & t > 1 \end{cases}$$

If  $\rho'$  is not continuous, but has a discontinuity  $\Delta'$

$$f(w) = \rho''(t) + \Delta' \delta(t - 1) .$$

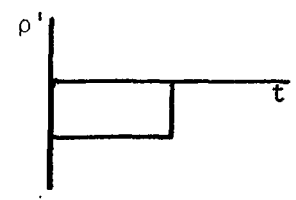
This is the case for  $1 - r^2$ ,  $1 - r$ , or any function which has a discontinuous derivative at  $r = 1$ .

For example:  $\rho = 1 - r^2 = 1 - t$

$$\rho' = -1$$

$$\rho'' = 0 + \Delta' \delta(t - 1) ; \Delta' = 1$$

$$f(w) = \delta(t - 1)$$



Or:  $\rho = 1 - r = 1 - \sqrt{t}$

$$\rho' = -\frac{1}{2\sqrt{t}} \left( = -\frac{1}{2} \text{ at } t = 1 \right)$$

$$\rho'' = \frac{1}{4t^{3/2}} + \frac{1}{2} \delta(t - 1)$$

$$f(w) = \frac{1}{4w^{3/2}} + \frac{1}{2} \delta(w - 1)$$

How does one populate the 6D phase space?

$x, x' = U, \alpha$       polar coordinates

$y, y' = V, \beta$        $R^2 = U^2 + V^2 + W^2$

$z, z' = W, \gamma$

$$dx dx' dy dy' dz dz' f(R^2) \rightarrow UVW \underbrace{dU dV dW}_{\text{spherical coord.}} d\alpha d\beta d\gamma$$

$$U = R \sin \theta \cos \phi, \quad V = R \sin \theta \sin \phi, \quad W = R \cos \theta$$

$$\rightarrow R^3 \sin^2 \theta \cos \theta \cos \phi \sin \phi R^2 dR \sin \theta d\theta d\phi d\alpha d\beta d\gamma$$

$$\rightarrow (d\alpha)(d\beta)(d\gamma)(\cos \phi \sin \phi d\phi) (\sin^3 \theta \cos \theta d\theta)$$

$$\times R^5 dR f(R^2) \text{ or } \frac{1}{2} R^4 dR^2 f(R^2)$$

where UVW is always positive,  $0 < \phi < \frac{\pi}{2}$ , and  $0 < \theta < \frac{\pi}{2}$ . The term  $(\cos \phi \sin \phi d\phi)$  is  $d(\cos 2\phi)/4$ , where  $\cos 2\phi$  is chosen between -1 and 1, and the term  $(\sin^3 \theta \cos \theta d\theta)$  is  $d(\sin^4 \theta)/4$  where  $\sin^4 \theta$  is chosen between 0 and 1.

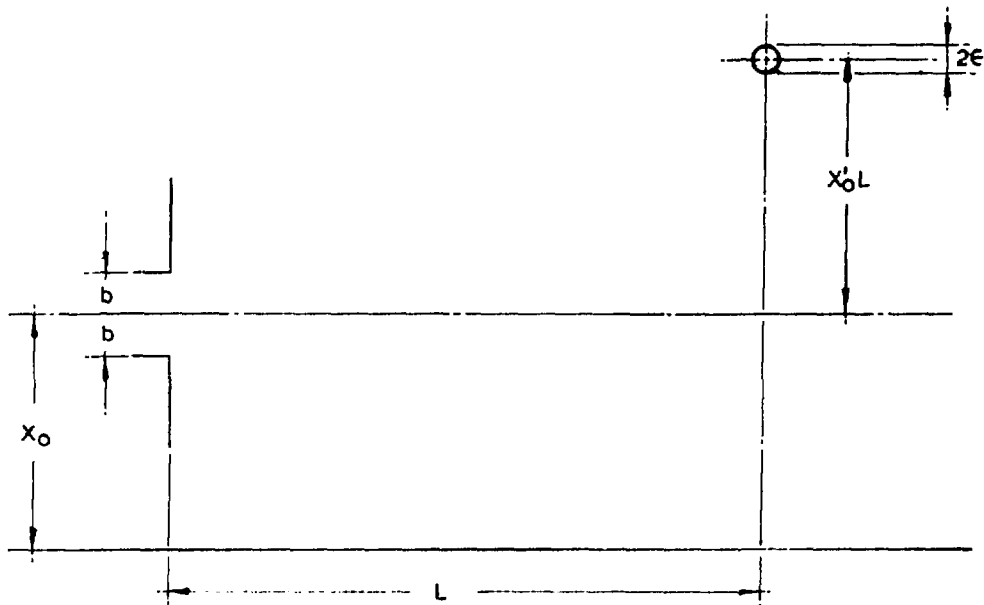
For example, if  $f(R^2) = \frac{1}{2} \delta(R^2 - 1) + \frac{1}{4R^3}$

$$R^5 dR f(R^2) \rightarrow \frac{1}{4} \delta + \frac{R^2 dR}{4} \rightarrow \frac{3\delta(R^2-1) + d(R^3)}{12}$$

This implies choosing  $R^3$  uniformly in 0 to 1 and then 3 times that many particles at  $R = 1$ .

### SLIT WIDTH EFFECT

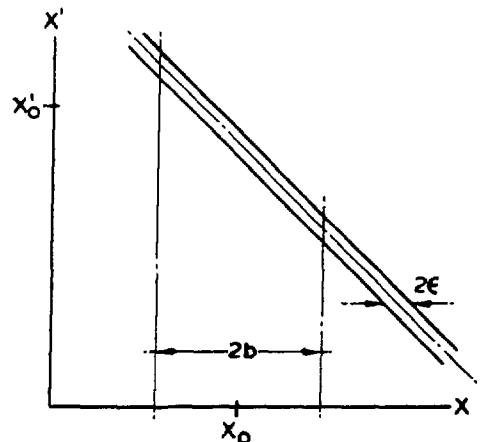
The emittance of low-intensity linac beams is commonly measured by passing a slit and collector assembly in steps through the beam. At each step, part of the beam passes through the slit and travels a distance  $L$  to the collector, where the width of the beam is measured to provide information about the angular spread of that part of the original beam. The finite slit width,  $2b$ , produces an error.



The apparent measurement at  $x_0, x'_0$  is bounded by

$$x + x'L = x'_0 L + x_0 \pm \epsilon$$

$$x - x_0 = \pm b$$



For  $\epsilon$  very small, the  $\int dx' \int dx$  integral becomes approximately

$$\hat{\rho}(x_0, x'_0) \cong \frac{L}{2b} \int_{x'_0 - \frac{b}{L}}^{x'_0 + \frac{b}{L}} dx' \rho(x_0 + x'_0 L - x' L, x')$$

Let  $x' = x'_0 + \frac{b}{L} u$

$$\hat{\rho}(x_0, x'_0) \cong \frac{1}{2} \int_{-1}^1 du \rho(x_0 - bu, x'_0 + \frac{b}{L} u)$$

Let  $\rho_{00} = \rho$

$$\rho_{01} = \frac{\partial \rho}{\partial x'}$$

$$\rho_{10} = \frac{\partial \rho}{\partial x}$$

$$\rho_{20} = \frac{\partial^2 \rho}{\partial x^2}$$

$$\rho_{02} = \frac{\partial^2 \rho}{\partial x'^2}$$

$$\rho_{11} = \frac{\partial^2 \rho}{\partial x \partial x'}$$

Now do a Taylor expansion.

$$\hat{\rho}(x_0, x'_0) = \frac{1}{2} \int_{-1}^1 du \left[ \rho_{00} - bu \rho_{10} + \frac{b^2 u^2}{2} \rho_{20} + \frac{bu}{L} \rho_{01} + \frac{b^2}{2L^2} \rho_{02} - \frac{b^2}{L} u^2 \rho_{11} \right]$$

where the arguments of  $\rho_{00}$ ,  $\rho_{01}$ , etc., are  $x_0$ ,  $x'_0$



$$\hat{\rho}(x_0, x'_0) = \rho_{00} + \frac{b^2}{6} \rho_{20} + \frac{b^2}{6L^2} \rho_{02} - \frac{b^2}{3L} \rho_{11}$$


---

Now let us calculate the apparent emittance

$$E^2 = \overline{x_0^2} \overline{x'_0{}^2} - \overline{x_0 x'_0}{}^2 \quad \text{using } \hat{\rho}(x_0, x'_0)$$

$$\overline{x_0^2} = \frac{\int dx'_0 \int dx_0 x_0^2 \hat{\rho}(x_0, x'_0)}{\int dx'_0 \int dx_0 \hat{\rho}(x_0, x'_0)}$$

Let  $\overline{x_0^2} = A$  (using  $\rho_{00}$  only)

$\overline{x'_0{}^2} = B$                    "

$\overline{x_0 x'_0} = C$                    "

Integrate by parts

$$\iint_{x_0^2} \begin{pmatrix} \rho_{20} \\ \rho_{02} \\ \rho_{00} \end{pmatrix} dx_0 dx'_0 = \begin{pmatrix} 2 \\ 0 \\ A \end{pmatrix} \mathbf{X} \left\{ \iint \rho_{00} dx_0 dx'_0 \right.$$

etc.

$$\overline{x_0^2} = A + \frac{b^2}{3}, \quad \overline{x'_0{}^2} = B + \frac{b^2}{3L^2}$$

$$\overline{x_0 x'_0} = C - \frac{b^2}{3L}$$

$$\widehat{E}^2 = \left(A + \frac{b^2}{3}\right) \left(B + \frac{b^2}{3L^2}\right) - \left(C - \frac{b^2}{3L}\right)^2$$

$$\widehat{E}^2 = \frac{AB - C^2}{E_0^2} + \frac{b^2}{3} \left(\frac{A}{L^2} + B - \frac{2C}{L}\right)$$

Try to express in terms of Courant-Snyder  $\alpha$ ,  $\beta$ ,  $\gamma$ , where  $\beta\gamma = 1 + \alpha^2$

Assume distribution  $f(W)$

$$W = \gamma x^2 + 2\alpha x x' + \beta x'^2$$

$$\iint dx dx' f(W) = 1$$

$$\text{Let } x' = -\frac{\alpha}{\beta} x + \frac{v}{\sqrt{\beta}} \quad ; \quad dx' = \frac{dv}{\sqrt{\beta}}$$

$$\int dx \int \frac{dv}{\sqrt{\beta}} f\left(\frac{x^2}{\beta} + v^2\right)$$

$$\text{Let } x = u\sqrt{\beta}$$

$$u^2 + v^2 = W = r^2$$

$$\int_{-\infty}^{\infty} du \int_{-\infty}^{\infty} dv f(u^2 + v^2) = \pi \int dW f(W)$$

$$du dv = 2\pi r dr$$

$$= \pi dW$$

$$\text{So the normalization is } \int_0^{\infty} dW f(W) = \frac{1}{\pi}$$

$$A = x^2 = \iint x^2 dx dx' f(W)$$

$$= \int dx x^2 \int \frac{dv}{\sqrt{\beta}} f\left(\frac{x^2}{\beta} + v^2\right)$$

$$\begin{aligned}
&= \beta \int du u^2 \int dv f(W) \\
&= \beta \int dW \int \frac{d\theta}{2} W \cos^2 \theta f(W) \\
&= \beta \frac{\pi}{2} \int_0^{\infty} W f(W) dW = \frac{\beta}{2} \bar{W}
\end{aligned}$$

$$\begin{aligned}
u &= \sqrt{W} \cos \theta \\
v &= \sqrt{W} \sin \theta \\
dudv &= \frac{dW}{2} d\theta \\
\bar{W} &= \frac{\int W f(W) dW}{\int f(W) dW}
\end{aligned}$$

$$B = \overline{x'^2} = \frac{\gamma}{2} \bar{W}$$

$$\begin{aligned}
C = \overline{xx'} &= \int dx x \int dv \left( \frac{v}{\sqrt{\beta}} - \frac{\alpha}{\beta} x \right) f(W) \\
&= \int du \int dv u (v - \alpha u) f(W) \\
&= -\frac{\alpha}{2} \bar{W}
\end{aligned}$$

$$\begin{aligned}
E_0^2 &= AB - C^2 \\
&= \frac{\bar{W}^2}{4}
\end{aligned}$$

$$E_0 = \frac{\bar{W}}{2}$$

$$\hat{E}^2 = E_0^2 + \frac{b^2}{3} \left( \frac{\beta}{2} \frac{\bar{W}}{L^2} + \frac{\gamma}{2} \bar{W} - \frac{\alpha \bar{W}}{2L} \right)$$

$$\hat{E}^2 = E_0^2 + 2E_0 \frac{b^2}{3} \left( \frac{\beta}{2L^2} - \frac{\alpha}{L} + \frac{\gamma}{2} \right)$$

$$\hat{E} \cong E_0 + \frac{b^2}{3} \left( \frac{\beta}{2L^2} - \frac{\alpha}{L} + \frac{\gamma}{2} \right)$$

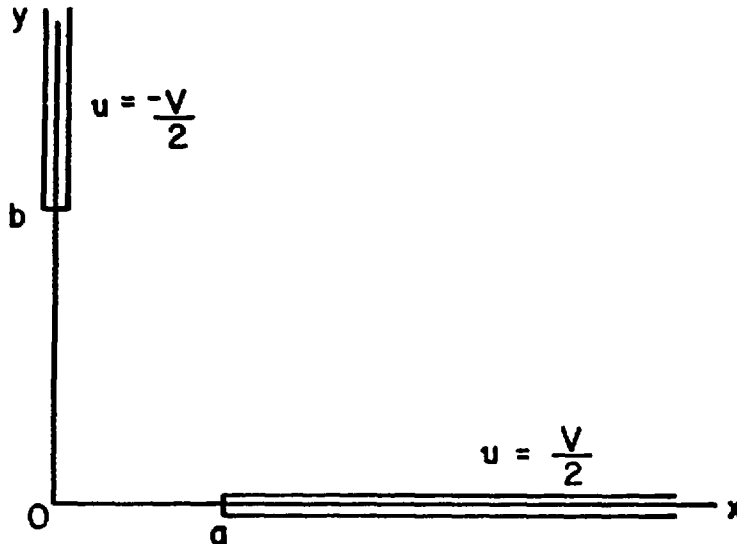
ASPECTS OF THE 4-VANE STRUCTURE

The following note contains three sections. In the first, an exact solution for Laplace's Equation near the axis of a four-vane structure is derived using a very simple Schwartz transformation.

The second section is an attempt to estimate a correction to the frequency and the "external" fields because of the central region. This section should be carefully checked before using.

Section III treats the 4-vane structure as a point-charge model. The relation of the point-charge parameters to the Kapchinsky-Teplyakov  $A$  and  $\mathcal{K}$  are derived in terms of the vane modulation parameter  $m = b/a$ .

I. We can solve the two dimensional Laplace problem in the following geometry



The solution can be obtained by the Schwartz transformation  $w = z^2$  and the problem is then standard in the  $w$ -plane. Without providing the details, I give the solution, which, since it is a function of the complex variable  $z$ , and satisfies the right boundary conditions, must be the correct one.

$$u = \frac{V}{\pi} \operatorname{Re} \sin^{-1} \left( \frac{z^2 + \frac{b^2 - a^2}{2}}{\frac{b^2 + a^2}{2}} \right) \quad (1)$$

$$u(x,y) = \frac{V}{\pi} \sin^{-1} \left[ \frac{\sqrt{(x^2 - y^2 + b^2)^2 + 4x^2 y^2} - \sqrt{(x^2 - y^2 - a^2)^2 + 4x^2 y^2}}{b^2 + a^2} \right] \quad (2)$$

As a check

$$u(x,0) = \frac{V}{\pi} \sin^{-1} \left[ \frac{x^2 + b^2 - |x^2 - a^2|}{b^2 + a^2} \right] = \left. \begin{aligned} & \frac{V}{2}, & x \geq a \\ & \frac{V}{\pi} \sin^{-1} \left( \frac{b^2 - a^2 + 2x^2}{b^2 + a^2} \right), & x \leq a \end{aligned} \right\} \quad (3)$$

$$u(0,y) = \frac{V}{\pi} \sin^{-1} \left[ \frac{|y^2 - b^2| - (y^2 + a^2)}{b^2 + a^2} \right] = \left. \begin{aligned} & -\frac{V}{2}, & y \geq b \\ & \frac{V}{\pi} \sin^{-1} \left( \frac{b^2 - a^2 - 2y^2}{b^2 + a^2} \right), & y \leq b \end{aligned} \right\} \quad (4)$$

$$u(0,0) = \frac{V}{\pi} \sin^{-1} \frac{b^2 - a^2}{b^2 + a^2} \quad (5)$$

(Our earlier guess was  $u(x,y) = \frac{V}{2} \left( \frac{b^2 - a^2 + 2x^2 - 2y^2}{b^2 + a^2} \right)$  which is not

terribly accurate at  $x = y = 0$ .)

---

It is possible to expand  $u(x,y)$  near  $x,y = 0$  as a multipole expansion. The result is

$$\frac{u(x,y)}{V} \cong \frac{1}{2} - \frac{2}{\pi} \tan^{-1} \frac{a}{b} + \frac{\overset{\text{dipole}}{n^2 \cos 2\theta}}{\pi ab} + \frac{\overset{\text{quadrupole}}{n^4 \cos 4\theta}}{4 a^3 b^3} (b^2 - a^2) (x^4 - 6x^2 y^2 + y^4) + \dots \quad (6)$$

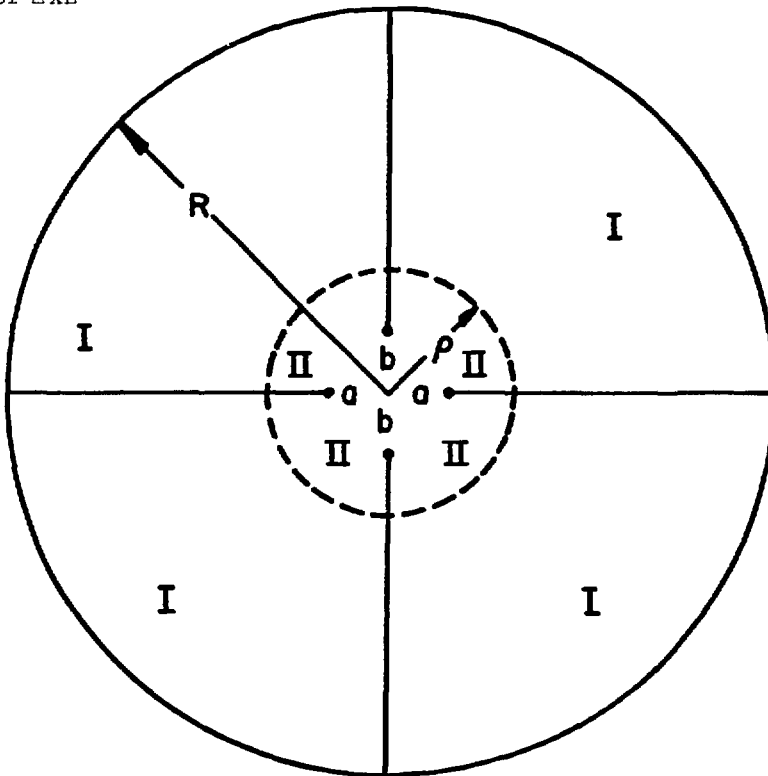
Conclusion: The Quadrupole strength will be constant if the product of  $a$  and  $b$  is constant !!!

II. Is it possible to calculate the resonant frequency approximately? The best way appears to be to use a variational statement in terms of an electric field trial function.

It is well known that

$$k^2 = \frac{\int (\nabla \times \vec{E})^2 dv}{\int E^2 dv} \quad (k = \frac{\omega}{c}) \quad (7)$$

is a variational statement for  $k^2$  in terms of trial functions  $\vec{E}$  which satisfy the proper boundary conditions and which are continuous and have continuous values of  $\Delta \times \vec{E}$



We will divide the "wave guide" into two regions (I and II) separated by  $r = \rho$ , where  $\rho$  is chosen such that

$$a, b < \rho \ll \lambda, R$$

The trial function in region I will be taken to be

$$E_{\theta}^I = E_0 (Y_1(k_1 r) - \alpha J_1(k_1 r))$$

corresponding to (8)

$$H_z^I = E_0 (Y_0(k_1 r) - \alpha J_0(k_1 r))$$

where  $\alpha = \frac{Y_1(k_1 R)}{J_1(k_1 R)}$  (9)

and  $k_1$  is chosen such that  $H_z(\rho) = 0$ , i.e.

$$\alpha = \frac{Y_0(k_1 \rho)}{J_0(k_1 \rho)}$$
 (10)

For  $k_1 \rho \ll 1$ ,  $Y_0(k_1 \rho) \cong \frac{2}{\pi} \ln \left( \frac{\mu k_1 \rho}{2} \right)$ ,  $J_0(k_1 \rho) \cong 1$ , where  $\ln \mu = \gamma = .5772$  is Euler's constant. So

$$\alpha \cong \frac{2}{\pi} \ln \left( \frac{\mu k_1 \rho}{2} \right), \text{ and } |\alpha| \gg 1.$$
 (11)

This means that  $k_1 \rho$  is near a zero of  $J_1(x)$ , In fact, if

$$k_1 R = p + \varepsilon$$

where  $J_1(p) = 0$  then

$$J_1(k_1 R) \cong \varepsilon J_1'(p) + \frac{\varepsilon^2}{2} J_1''(p)$$

$$Y_1(k_1 R) \cong Y_1(p) + \varepsilon Y_1'(p).$$

One obtains, from (9)



$$\varepsilon \frac{J_1'(p)}{Y_1(p)} \left[ \frac{1 + \frac{\varepsilon}{2} \frac{J_1''(p)}{J_1'(p)}}{1 + \varepsilon \frac{Y_1'(p)}{Y_1(p)}} \right] \cong \frac{1}{\alpha}, \quad \frac{1}{|\alpha|} \ll 1$$

$$\varepsilon \cong \frac{Y_1(p)}{\alpha J_1'(p)} \left[ 1 + \left( \frac{Y_1'(p)}{Y_1(p)} - \frac{J_1''(p)}{2J_1'(p)} \right) \frac{Y_1(p)}{\alpha J_1'(p)} \right] \quad (12)$$

$$\varepsilon \cong \frac{G}{\alpha} + \frac{H}{\alpha^2} \quad G = \frac{Y_1(p)}{J_1'(p)}, \quad H = \left( \frac{Y_1(p)}{J_1'(p)} \right)^2 \left( \frac{Y_1'(p)}{Y_1(p)} - \frac{J_1''(p)}{2J_1'(p)} \right) \quad (13)$$

-----

Let us now calculate  $k^2$

$$k^2 = \frac{\int_I (\nabla \times E)^2 dv + \int_{II} (\nabla \times E)^2 dv}{\int_I E^2 dv + \int_{II} E^2 dv} \quad (14)$$

In region I we have

$$\nabla \times E_I = k_1 E_0 (Y_0(k_1 r) - \alpha (J_0(k_1 r))) \quad (15)$$

In region II we have

$\nabla \times E_{II} = 0$ , since we will choose  $E_{II}$  to be the solution of Laplace's Equation (solution for the potential is in (2)). So we have

$$k^2 = \frac{k_1^2 \int_I dv (Y_0 - \alpha J_0)^2}{\int_I dv (Y_1 - \alpha J_1)^2 + \frac{1}{E_0^2} \int_{II} dv E^2} \quad (16)$$

$$\int_{k_1 \rho}^{k_1 R} x dx (Y_0(x) - \alpha J_0(x))^2 = \left[ \frac{x^2}{2} (Y_0(x) - \alpha J_0(x))^2 + \frac{x^2}{2} (Y_1(x) - \alpha J_1(x))^2 \right]_{k_1 \rho}^{k_1 R}$$

$$\int_{k_1 \rho}^{k_1 R} x dx (Y_1(x) - \alpha J_1(x))^2 = \left[ \frac{x^2}{2} (Y_0(x) - \alpha J_0(x))^2 + \frac{x^2}{2} (Y_1(x) - \alpha J_1(x))^2 - x(Y_1(x) - \alpha J_1(x))(Y_0(x) - \alpha J_0(x)) \right]_{k_1 \rho}^{k_1 R}$$

Using (9) and (10), one finds

$$\int_{k_1 \rho}^{k_1 R} x dx (Y_0 - \alpha J_0)^2 = \int_{k_1 \rho}^{k_1 R} x dx (Y_1 - \alpha J_1)^2$$

$$\cong \left[ \frac{k_1^2 R^2}{2} (Y_0(k_1 R) - \alpha J_0(k_1 R))^2 - \frac{k_1^2 \rho^2}{2} (Y_1(k_1 \rho) - \alpha J_1(k_1 \rho))^2 \right] \quad (17)$$

From (16) and (17), neglecting terms of order  $\rho^2/R^2$ ,

$$k^2 - k_1^2 \cong \frac{-\frac{2k_1^2}{E_0} \int_{II} r dr \int_{II} d\theta E^2}{R^2 (Y_0(k_1 R) - \alpha J_0(k_1 R))^2 2\pi} \quad (18)$$

Let us now try to evaluate  $E_{II}$ , and tie it at  $r = \rho$  to  $E_I^\theta$ . For  $r^2 = x^2 + y^2 \gg a^2, b^2$ , Eq. (2) can be written as

$$u(x, y) \cong \frac{V}{\pi} \sin^{-1} \left[ \frac{\sqrt{(x^2 + y^2)^2 + 2b^2(x^2 - y^2)} - \sqrt{(x^2 + y^2)^2 - 2a^2(x^2 - y^2)}}{b^2 + a^2} \right]$$

$$\cong \frac{V}{\pi} \sin^{-1} \left( \frac{x^2 - y^2}{x^2 + y^2} \right) = \frac{V}{\pi} \sin^{-1}(\cos 2\theta) = \frac{V}{\pi} \left( \frac{\pi}{2} - 2\theta \right)$$

so that

$$E_{\theta} \cong \frac{2V}{\pi\rho} \quad \text{in region II at } r = \rho . \quad (19)$$

From (8)

$$E_{\theta} \cong - \frac{2E_0}{\pi k_1 \rho} \quad \text{in region I at } r = \rho . \quad (20)$$

A match is therefore obtained with

$$V = \frac{E_0}{k_1} \quad (21)$$

in which case (18) can be written as

$$k^2 - k_1^2 \cong \frac{- \frac{2}{V^2} \int_{\text{II}} r dr d\theta E^2}{2\pi R^2 (Y_0(k_1 R) - \alpha J_0(k_1 R))^2} \quad (22)$$

Let us write

$$u(x,y) = \frac{V}{\pi} g(r,\theta)$$

$$E = - \frac{V}{\pi} \nabla g \quad , \quad E^2 = \frac{V^2}{\pi^2} (\nabla g)^2$$

$$\frac{2}{V^2} \int_{\text{II}} dv E^2 = \frac{2}{\pi^2} \int dv (\nabla g) \cdot (\nabla g)$$

$$= \frac{2}{\pi^2} \int ds (\vec{n} \cdot g \nabla g) - \frac{2}{\pi^2} \int dv g (\nabla^2 g) \quad (23)$$

Since  $\nabla^2 g = 0$ , the second term in (23) vanishes. Since  $\vec{\nabla} g$  is in the  $\theta$  direction at large  $r$ , the only contributions to the first integral come from the vanes. After some algebra, one finds

$$\frac{2}{v^2} \int_{II} dv E^2 \cong \frac{16}{\pi} \ell_n \frac{2\rho}{\sqrt{a^2 + b^2}} \quad (24)$$

and

$$k_{1R}^2 \cong k_1^2 R^2 - \frac{8}{\pi^2} \frac{\ell_n \frac{2\rho}{\sqrt{a^2 + b^2}}}{(Y_0(k_{1R}) - \alpha J_0(k_{1R}))^2} \quad (25)$$

We will try to keep the lowest two orders in  $1/\alpha$ , noting that, to that order

$$Y_0(k_{1R}) - \alpha J_0(k_{1R}) = Y_0(p) - \alpha J_1(p) \quad (26)$$

$$\alpha \cong \frac{2}{\pi} \ell_n \frac{\mu k_{1R} \rho}{2} \cong \frac{2}{\pi} \ell_n \left( \frac{\mu p \rho}{2R} \right)$$

and

$$\begin{aligned} \ell_n \frac{2\rho}{\sqrt{a^2 + b^2}} &= \ell_n \frac{\mu p \rho}{2R} + \ell_n \frac{4R}{\mu \sqrt{a^2 + b^2}} \cong \frac{\pi \delta}{2} \\ &= \frac{\pi \alpha}{2} + \frac{\pi \delta}{2} \end{aligned} \quad (27)$$

This leads to

$$\begin{aligned} k_{1R}^2 &= p^2 + 2p\epsilon + \epsilon^2 - \frac{\frac{4}{\pi} (\alpha + \delta)}{\alpha^2 J_0^2(p) - 2\alpha J_0(p) Y_0(p)} \\ &= p^2 + 2p \left( \frac{G}{\alpha} + \frac{H}{\alpha^2} \right) + \frac{G^2}{\alpha^2} - \frac{4}{\alpha \pi J_0^2} \left( 1 + \frac{\delta}{\alpha} + \frac{2}{\alpha} \frac{Y_0(p)}{J_0(p)} \right) \end{aligned}$$

$$= p^2 + \frac{2}{\alpha} \left( \frac{pY_1(p)}{J_1'(p)} - \frac{2}{\pi J_0^2} \right) + \frac{1}{\alpha^2} \left( 2pH + G^2 - \frac{4\delta}{\pi J_0^2} - \frac{8}{\pi} \frac{Y_0}{J_0^3} \right)$$

$$\text{But } J_1'(p) = J_0(p) - \frac{J_1(p)}{p} = J_0(p) \quad \text{and } Y_1 = -\frac{2}{\pi p J_0}$$

$$J_1'' = \frac{1}{p} J_1' - \underbrace{J_1 \left(1 - \frac{1}{p}\right)}_{=0}$$

So

$$k^2 R^2 \cong p^2 - \frac{4}{\alpha \pi J_0^2} + \frac{1}{\alpha^2} \left( 2p \frac{Y_1^2}{J_0^2} \left( \frac{Y_1'}{Y_1} + \frac{1}{2p} \right) + \frac{Y_1^2}{\pi J_0^2} - \frac{4\delta}{J_0^2} - \frac{8}{\pi} \frac{Y_0}{J_0^3} \right)$$

$$k^2 R^2 = p^2 - \frac{4}{\alpha \pi J_0^2} - \frac{4}{\alpha^2 \pi J_0^2} \left( \delta + \frac{3Y_0}{J_0} \right) \quad (28)$$

My interpretation of (28) is as follows: The choice of  $\rho$  (which to this point is only restricted by  $a, b < \rho \ll \lambda, R$ ) should be the one which minimizes Eq. (28), since the original formulation of  $k^2$  is a variational one. This implies a positive value for  $-\frac{1}{\alpha}$  which is chosen to be as small as possible. Assuming  $b \geq a$ , this suggests choosing  $\rho = b$ , since a smaller value will correspond to fields not accurately given by (19).

My guess is therefore that the frequency is given by (29):

$$\boxed{k^2 R^2 = p^2 - \frac{4}{\alpha \pi J_0^2} - \frac{4}{\alpha^2 \pi J_0^2} \left( \delta + \frac{3Y_0}{J_0} \right)} \quad (29)$$

with  $J_1(p) = 0$ ,  $p \cong 3.83$ ,  $J_0(p) \cong -.403$ ,  $Y_0(p) \cong .051$

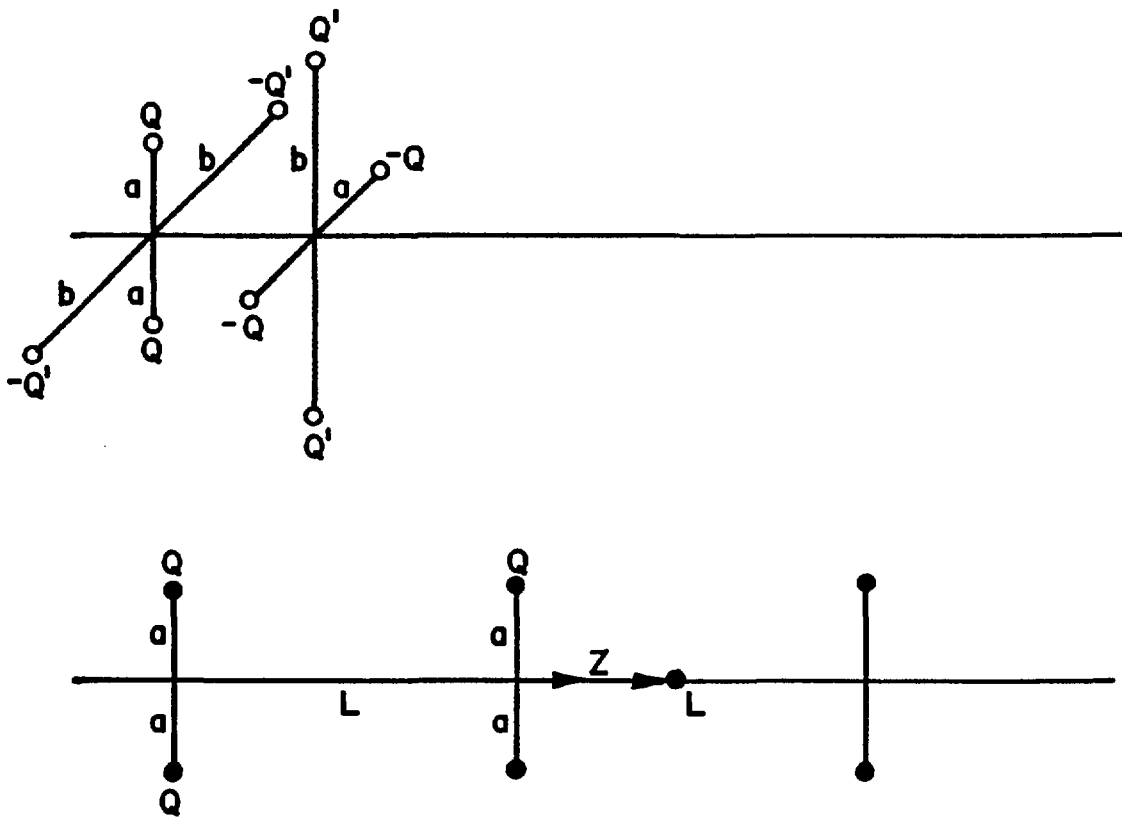
$$\frac{\pi \alpha}{2} = \ln \frac{\mu \rho \rho}{2R} \quad \rho \cong b, \quad \ln \mu = .5772$$

$$\frac{\pi \delta}{2} = \ln \frac{4R}{\mu \sqrt{a^2 + b^2}}$$

[Perhaps one should choose  $\rho = \sqrt{a^2 + b^2}$  in which case the frequency will depend only on  $\sqrt{a^2 + b^2}$ .]

It should be possible to check the accuracy of (29) by comparing with SUPERFISH calculations.

III. This is a follow up on the point charge model for the K-T, 4-line structure. It contains the relation of the point charge parameters to the K-T parameters (A and  $\mathcal{W}$ ) in terms of  $m = b/a$



Potential =

$$\sum_i \frac{Q}{\sqrt{(z - L_i)^2 + \underbrace{x^2 + (a - y)^2}_{\Delta^2}}} = \sum a_n \cos \frac{2n\pi z}{L}$$

What is the first harmonic?

$$a_1 = \frac{2}{L} \int_{-\frac{L}{2}}^{\frac{L}{2}} dz \sum_i \frac{Q \cos \frac{2\pi z}{L}}{\sqrt{(z - L_i)^2 + \Delta^2}} \quad z - L_i = s$$

$$a_1 = \frac{2Q}{L} \sum_i \int_{-\frac{L}{2} - L_i}^{\frac{L}{2} - L_i} \frac{ds \cos \frac{2\pi s}{L}}{\sqrt{s^2 + \Delta^2}} = \frac{2Q}{L} \int_{-\infty}^{\infty} \frac{ds \cos \frac{2\pi s}{L}}{\sqrt{s^2 + \Delta^2}}$$

$$= \frac{2Q}{L} \int_{-\infty}^{\infty} \frac{dt \cos\left(\frac{2\pi\Delta}{L}\right)t}{\sqrt{1 + t^2}} = \frac{4Q}{L} \int_1^{\infty} \frac{dw}{\sqrt{w^2 - 1}} e^{-\left(\frac{2\pi\Delta}{L} w\right)}$$

$$a_1 = \frac{4Q}{L} K_0(w)$$

FOR THE COMPLETE CHARGE CONFIGURATION

$$U(x,y,z) = \cos \frac{2\pi z}{L} \left[ \frac{4Q}{L} K_0 \left( \frac{2\pi}{L} \sqrt{x^2 + (a-y)^2} \right) - \frac{4Q'}{L} K_0 \left( \frac{2\pi}{L} \sqrt{x^2 + (b-y)^2} \right) \right. \\ \left. - \frac{4Q'}{L} K_0 \left( \frac{2\pi}{L} \sqrt{y^2 + (b-x)^2} \right) + \frac{4Q}{L} K_0 \left( \frac{2\pi}{L} \sqrt{y^2 + (a-x)^2} \right) \right]$$

+ [same, with  $a \rightarrow -a$ ,  $b \rightarrow -b$ ]

$$K_0 \left( \sqrt{(c-r)^2 + \delta^2} \right) = K_0 \left( c \pm \epsilon + \frac{\delta^2}{2c} \right) = K_0(c) + \left( \frac{\delta^2}{2c} \mp \epsilon \right) K_0'(c) + \frac{\epsilon^2}{2} K_0''(c)$$

$$K_0 \left( \sqrt{(c-\delta)^2 + \epsilon^2} \right) = K_0(c) + \left( \frac{\epsilon^2}{2c} \mp \delta \right) K_0'(c) + \frac{\delta^2}{2} K_0''(c)$$

$$K_0'' + \frac{1}{z} K_0' - K_0 = 0$$

$$K_0' = -K_1$$

$$K_0'' = K_0 + \frac{K_1}{z}$$

$$2K_0(c) - K_1(c) \frac{\delta^2 + \epsilon^2}{2c} + \left( K_0 + \frac{K_1}{c} \right) \frac{\delta^2 + \epsilon^2}{2} \\ = 2K_0(c) \left( 1 - \frac{r^2}{4} \left( \frac{2\pi}{L} \right)^2 \right)$$

$$U(x,y,z) = \cos \frac{2\pi z}{L} \frac{16}{L} \left( Q K_0 \left( \frac{2\pi a}{L} \right) - Q' K_0 \left( \frac{2\pi b}{L} \right) \right)$$

Longitudinal Term



Transverse Term

$$\begin{aligned}
 E_x &= 2 \sum_i \frac{Q x}{\left( (z - L_i)^2 + a^2 \right)^{3/2}} \\
 &+ 2 \sum_i \frac{Q' x}{\left( \left( z - \frac{L_i}{2} - L_i \right)^2 + b^2 \right)^{3/2}} \\
 &- 2 \sum_i \frac{Q (x \pm a)}{\left( \left( z - \frac{L_i}{2} - L_i \right)^2 + (a \pm x)^2 \right)^{3/2}} \\
 &- 2 \sum_i \frac{Q' (x \pm b)}{\left( \left( z - L_i \right)^2 + (b \pm x)^2 \right)^{3/2}}
 \end{aligned}$$

$$\frac{x - a}{\left( \Delta^2 + (a - x)^2 \right)^{3/2}} + \frac{x + a}{\left( \Delta^2 + (a + x)^2 \right)^{3/2}} =$$

$$= \frac{1}{\left( \Delta^2 + a^2 \right)^{3/2}} \left[ \underbrace{(x - a) \left( 1 + \frac{3ax}{\left( \Delta^2 + a^2 \right)} \right) + (x + a) \left( 1 - \frac{3ax}{\left( \Delta^2 + a^2 \right)} \right)}_{2x - \frac{6a^2 x}{\Delta^2 + a^2}} \right]$$



Therefore:

$$U = \frac{4}{L} (x^2 - y^2) \left( \frac{Q}{a^2} + \frac{Q'}{b^2} \right) + \cos\left(\frac{2\pi z}{L}\right) \frac{16}{L} \left( Q \kappa_o \left( \frac{2\pi a}{L} \right) - Q' \kappa_o \left( \frac{2\pi b}{L} \right) \right)$$

Therefore, in terms of K-T parameters,  $A_0, A_1$  :

$$\frac{A_1^V}{2} = \frac{16}{L} \left( \overset{(ka)}{Q \kappa_o \left( \frac{2\pi a}{L} \right)} - \overset{(mka)}{Q' \kappa_o \left( \frac{2\pi b}{L} \right)} \right)$$

$$\frac{A_0^V}{2} = \frac{4}{L} \left( \frac{Q}{a^2} + \frac{Q'}{b^2} \right)$$

$$\frac{Q}{\epsilon_1} \approx \frac{Q'}{\epsilon_2} \approx \frac{V}{2}$$

$\epsilon_1, \epsilon_2$  are radii of the "beads"

Probably should choose

$$Q' = Q \quad \epsilon_1 = \epsilon_2 = \epsilon \quad A_0 = \frac{\mathcal{H}}{a^2} \quad ; \quad m = \frac{b}{a} \quad ; \quad k = \frac{2\pi}{L}$$

$$\frac{A_1^V}{2} = \frac{8k}{\pi} \frac{V\epsilon}{2} \left( \kappa_o(ka) - \kappa_o(mka) \right)$$

$$A_1 = \frac{8k\epsilon}{\pi} \left( \kappa_o(ka) - \kappa_o(mka) \right) = 0 \text{ at } m = 1$$

$$\mathcal{H} = a^2 A_0 = a^2 \frac{8}{VL} \frac{\epsilon V}{2} \left( \frac{1}{a^2} + \frac{1}{m^2 a^2} \right)$$

Coefficients  
may not be exactly  
correct.

$$\mathcal{H} = \frac{4k\epsilon}{\pi} \frac{\left( 1 + \frac{1}{m^2} \right)}{2} = \frac{4k\epsilon}{\pi} \text{ at } m = 1$$

If we choose  $\varepsilon = \frac{\lambda}{8}$

4 BALL

$$\mathcal{H} = \frac{1}{2} \left( 1 + \frac{1}{m^2} \right)$$

vs.

K-T

$$\frac{I_0(ka) + I_0(mka)}{m^2 I_0(ka) + I_0(mka)}$$

$$A_1 = 2(K_0(ka) - K_0(mka))$$

vs.

$$\frac{m^2 - 1}{m^2 I_0(ka) + I_0(mka)}$$

---

Look similar enough to be believed

---

Might be necessary to make  $\frac{\Omega'}{Q} = \left(\frac{1}{m}\right)^j$        $j = 1 ?$

Hard to know what to choose.

At any rate, we have related the coefficients of the constant and  $\cos(kz)$  terms of the potential for the 4-ball case to those in K-T!

DISCUSSION OF BEAM DYNAMICS IN A  
"KAPCHINSKY - TEPLYAKOV" - LIKE STRUCTURE

A. Introduction

What we are doing is to group all structures which have only r-f fields with quadrupole behavior near the axis (to produce transverse focussing via alternating gradient behavior) and with an accelerating wave along the axis.

B. Longitudinal Dynamics

The result of the analysis for the longitudinal motion is the standard loaded pendulum

$$\frac{d^2\phi}{ds^2} + \frac{k_q^2}{\sin|\phi_s|} (\cos\phi - \cos\phi_s) = 0$$

$$\left[ \begin{array}{l} \text{linearized } \chi = \phi - \phi_s \\ \frac{d^2\chi}{ds^2} + k_q^2 \chi = 0 \end{array} \right]$$

where

$$\frac{k_q^2}{\sin|\phi_s|} = \frac{2\pi e}{mv^2\beta\lambda} \bar{E}$$

$\bar{E}$  is the average accelerating electric field on the axis (the amplitude of the wave component traveling with the beam).

In K-T terms

$$\bar{E} = \frac{\pi}{2\beta\lambda} A_1 V \quad \text{or} \quad \bar{E} = \frac{2V}{\beta\lambda} \textcircled{H}$$

$$k_q^2 = \frac{4\pi eV}{mv^2(\beta\lambda)^2} \textcircled{H} \sin|\phi_s|$$

### C. Transverse Dynamics

$$\frac{d^2x}{ds^2} + x \left( -\frac{k_\ell^2}{2} + K \cos\left(\frac{2\pi s}{\beta\lambda} + \psi\right) \right) = 0$$

$$K = \frac{e}{mv^2} VA_0 = \frac{eV}{mv^2 a^2} \mathcal{K}$$

The  $K$  term is the alternating gradient term and the  $-\frac{k_\ell^2}{2}$  is the standard r. f. defocussing term required by Earnshaw's Theorem.

We will convert this Mathieu equation to a matrix formalism by replacing the  $\cos\left(\frac{2\pi s}{\beta\lambda} + \psi\right)$  by  $\pm \frac{\pi}{4}$  for distances  $\frac{\beta\lambda}{2}$  to simulate the square wave's first harmonic.

$$\frac{d^2x}{ds^2} + x \left( \pm \frac{\pi K}{4} - \frac{k_\ell^2}{2} \right) = 0$$

$$b = \frac{\pi K}{4} ; \quad a = \frac{k_\ell^2}{2}$$

or 
$$\frac{d^2x}{ds^2} \pm (b + a)x = 0$$

$$\begin{aligned} b - a &= p^2 \\ b + a &= q^2 \end{aligned} \quad \ell = \frac{\beta\lambda}{2}$$

Matrix formulation

$$\begin{pmatrix} \cos(p\ell) & \frac{\sin(p\ell)}{p} \\ -p\sin(p\ell) & \cos(p\ell) \end{pmatrix} \begin{pmatrix} \cosh(q\ell) & \frac{\sinh(q\ell)}{q} \\ q\sinh(q\ell) & \cosh(q\ell) \end{pmatrix}$$

$$p^2 + q^2 = \frac{\pi K}{2}$$

$$q^2 - p^2 = k_\ell^2$$

$$\cos \mu = \cos(p\ell) \cosh(q\ell) + \frac{\sin(p\ell) \sinh(q\ell)}{2pq} (q^2 - p^2)$$

Expand for small  $\mu$ ,  $p\ell$ ,  $q\ell$ , to 4th order.

$$\begin{aligned} 1 - \frac{\mu^2}{2} + \frac{\mu^4}{24} &= \left( 1 - \frac{p^2 \ell^2}{2} + \frac{p^4 \ell^4}{24} \right) \left( 1 + \frac{q^2 \ell^2}{2} + \frac{q^4 \ell^4}{24} \right) \\ &\quad + \frac{q^2 - p^2}{2pq} \ell^2 pq \left( 1 + \frac{q^2 - p^2}{6} \ell^2 \right) \\ &= 1 + (q^2 - p^2) \ell^2 + \ell^4 \left( \frac{p^4}{24} + \frac{q^4}{24} - \frac{p^2 q^2}{4} + \frac{(q^2 - p^2)^2}{12} \right) \\ &\quad \underbrace{\frac{(q^2 - p^2)^2}{12} - \frac{(q^2 + p^2)^2}{24}} \end{aligned}$$

$$1 - \frac{\mu^2}{2} + \frac{\mu^4}{24} \approx 1 + \frac{2(q^2 - p^2) \ell^2}{2!} + \frac{[2(q^2 - p^2) \ell^2]^2}{4!} - \frac{\ell^4 (q^2 + p^2)^2}{24}$$

This can be approximated for  $\mu^2$

$$\mu^2 = -2\ell^2 (q^2 - p^2) + \frac{\ell^4 (q^2 + p^2)^2}{12}$$

The definition of transverse wave number  $k_t$  is

$$k_t = \frac{\mu}{2\ell}, \text{ so that}$$

$$k_t^2 = -\frac{q^2 - p^2}{2} + \frac{\ell^2 (q^2 + p^2)^2}{48}$$

$$k_t^2 = -\frac{k_\ell^2}{2} + \frac{\pi^2 K \ell^2}{192}$$

[The true Mathieu equation solution in lowest power of  $k_{\perp}^2$  multiplies the 2nd term by  $\frac{96}{\pi} = .99$ .]

So

$$k_t^2 = \frac{\mu^2}{\beta^2 \lambda^2} = - \frac{\pi e}{mv^2 \beta \lambda} \sin|\phi_s| \frac{2V}{\beta \lambda} \textcircled{H} + \frac{\pi^2}{192} \frac{\beta^2 \lambda^2}{4} \left( \frac{eV\mathcal{K}}{mv^2 a} \right)^2$$

K-T's equation (7) (UDC 621.384.64 1969-70)

$$\frac{1}{\beta^2 \lambda^2} \mu^2 = \frac{2\pi V}{\beta^2 E_0} \textcircled{H} \sin\phi \frac{1}{\beta^2 \lambda^2} + \frac{1}{8} \left( \frac{\mathcal{K} V \beta^2 \lambda^2}{\pi \beta^2 E_0 a^2 \beta \lambda} \right)^2$$

where  $E_0 = Mc^2$ ,  $\beta_0^2 E_0 = mv^2$

$$\begin{aligned} \text{Ratio is } & \frac{1}{8\pi^2} \cdot \frac{4 \cdot 192}{\pi^2} \\ \text{of} & \\ \text{Coefficients} & = \frac{96}{\pi^4} = .99 \end{aligned}$$

#### D. Transverse Longitudinal Coupling

The longitudinal motion is governed by the accelerating wave traveling along with the particle,  $\cos(\frac{2\pi s}{\beta \lambda}) \cos(\omega t + \phi)$ . The radial dependence of this term is controlled by the requirement that this traveling wave have a factor which permits  $E_z$  to satisfy the Laplace Equation (non-relativistic). This then leads to the standard factor

$$I_0\left(\frac{2\pi}{\beta \lambda} r\right) \approx 1 + \frac{\pi^2}{\beta \lambda^2} r^2$$

This leads to the usual coupling term in the linearized form.

$$\frac{d^2 \chi}{ds^2} + k_{\perp}^2 \chi = \frac{1}{\tan|\phi_s|} \frac{k_{\perp}^2}{2} (x^2 + y^2)$$



The corresponding term in the transverse motion comes from the dependence of the r.f. defocussing term on the phase motion, and is written directly as

$$\frac{d^2x}{ds^2} + k_t^2 x = - \frac{k_\ell^2 x}{2 \tan |\phi_s|} \cdot \chi$$

where  $k_t^2$  includes the alternating gradient effect in the "smooth" approximation.

The standard coupling analysis treats the  $2k_t - k_\ell$  "resonance" as the dominant term leading to a change in transverse amplitude of

$$\frac{\delta A}{A} \approx \frac{k_\ell^2}{8k_t |2k_t - k_\ell|} \cdot \frac{\chi_{\max}}{|\phi_s|}$$

This implies the need to keep  $\frac{\chi_{\max}}{|\phi_s|} < 1$  in order to keep the transverse motion from deteriorating. Specifically, the effect is exactly the same as in the Quad Focussed Alvarez Linac, provided  $k_t$  and  $k_\ell$  are chosen appropriately.

### E. Space Charge Effects

The space charge terms are most readily estimated by assuming a uniformly charged ellipsoid. This will lead to linear terms in the equations for  $\chi$  and  $x$  of exactly the same form as for the Quad Focussed Alvarez Linac. Specifically in the focussing terms (but not in the coupling term unless there are further couplings from the space charge distribution) one has

$$\begin{aligned} k_\ell^2 &\longrightarrow k_\ell^2 (1 - \mu_\ell) \\ k_t^2 &\longrightarrow k_t^2 (1 - \mu_t) \end{aligned}$$

where

$$\mu_{\ell} k_{\ell}^2 \equiv \frac{90 \text{ ohms } eI}{Mc^2} \frac{\lambda}{a^2 c \beta^2} f$$

$$\mu_t k_t^2 \equiv \frac{45 \text{ ohms } eI}{Mc^2} \frac{\lambda}{a^2 c \beta^2} (1 - f)$$

and  $f(\frac{c}{a}) \approx \frac{a}{3c}$ , where  $c$  is the longitudinal semi-axis, and  
 $1 - f \approx 1$   $a$  is the transverse semi-axis.

Calculational experience suggests that the beams will deteriorate if  $\mu_{\ell}$  or  $\mu_t$  get too close to 1. A crude estimate of the current limit can be obtained by choosing  $\mu \sim 3/4$ , as in conventional accelerators. This leads to two estimates (setting  $Mc^2 = 900 \times 10^6 \text{ eV}$ ).

$$I = \frac{900 \text{ MV}}{90 \text{ ohms}} (\beta k_{\ell} \lambda)^2 \frac{3ac^2}{(\beta\lambda)^3} \beta^3 \mu_{\ell}$$

$$I_{\ell} = 30 \text{ amp. } (\beta\lambda k_{\ell})^2 \frac{ac^2}{(\beta\lambda)^3} (100\beta)^3 \mu_{\ell}$$

$$I_t = 20 \text{ amp. } (\beta\lambda k_t)^2 \frac{a^2 c}{(\beta\lambda)^3} (100\beta)^3 \mu_t$$

Typical values at injection - after bunching starts

$$\frac{a}{\beta\lambda} \sim \frac{1}{4} \quad \frac{c}{\beta\lambda} \sim \frac{1}{4} \quad (180^\circ \text{ bunch})$$

$$\beta\lambda k_{\ell} = \text{phase advance per cell} \sim \frac{\pi}{2}$$

$$\beta\lambda k_t = \text{phase advance per cell} \sim \frac{\pi}{2}$$

$$\mu_{\ell} \approx \frac{1}{2} \quad \mu_t \approx \frac{3}{4}$$

$$I \cong 15 \text{ amp } \frac{\pi^2}{2} \frac{1}{64} (100\beta)^3$$

$$I \cong 0.6 \text{ amp } (100\beta)^3$$

$\beta$	W	$I_{\max}$
.005	12 KeV	75 ma
.01	50 KeV	600 ma
.02	200 KeV	5 amp.

One still must see whether it is possible to obtain  $k_{\perp} \beta \lambda \sim \frac{\pi}{2}$ ,  $k_{\parallel} \beta \lambda \sim \frac{\pi}{2}$  with realistic parameters in the K-T structure.

RELATION OF STRUCTURE TO BEAM DYNAMICS PARAMETERS  
IN A 4-VANE STRUCTURE

SUPERFISH gives the frequency and field distribution. This note suggests how to relate this information to the K-T parameters.

The general static potential has symmetry such that for  $z \rightarrow z + \frac{\beta\lambda}{2}$ ,  $\theta \rightarrow \frac{\pi}{2} + \theta$ , the sign changes (apart from the time dependence of the fields). This condition is satisfied by the form

$$U = \sum_{n=0}^{\infty} a_n r^{2+4n} \cos((2+4n)\theta)$$

$$+ \sum_{n=0}^{\infty} b_n I_{4n} \left( \frac{2\pi r}{\beta\lambda} \right) \cos 4n\theta \cos\left(\frac{2\pi z}{\beta\lambda}\right)$$

$$+ \sum_{n=0}^{\infty} c_n I_{4n+2} \left( \frac{4\pi r}{\beta\lambda} \right) \cos((4n+2)\theta) \cos\left(\frac{4\pi z}{\beta\lambda}\right)$$

$$+ \sum_{n=0}^{\infty} d_n I_{4n} \left( \frac{6\pi r}{\beta\lambda} \right) \cos 4n\theta \cos\left(\frac{6\pi z}{\beta\lambda}\right) + \dots$$

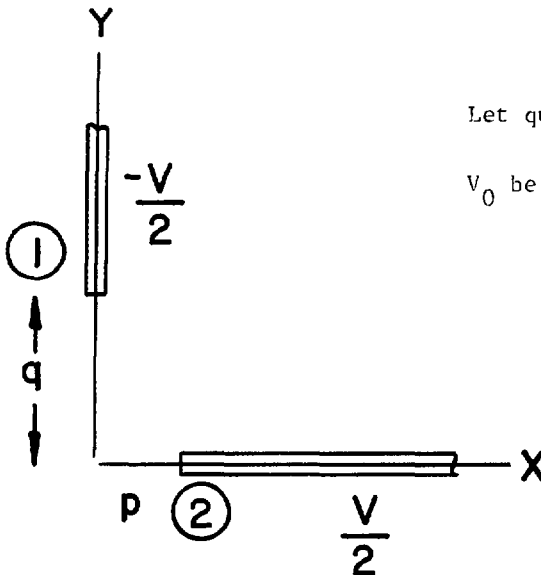
$$= \sum_{n=0}^{\infty} \sum_{m=0}^{\infty} A_{nm} I_{4n+2} \left( \frac{4m\pi r}{\beta\lambda} \right) \cos((4n+2)\theta) \cos\left(\frac{4m\pi z}{\beta\lambda}\right)$$

$$+ \sum_{n=0}^{\infty} \sum_{m=0}^{\infty} B_{nm} I_{4n} \left( \frac{4m+2}{\beta\lambda} \pi r \right) \cos(4n\theta) \cos\left(\frac{(4m+2)\pi z}{\beta\lambda}\right)$$

The accelerating term is  $B_{00}$  and the focusing term is proportional to  $A_{00}$ , with proper normalization. These can be related to the  $A_1$  and  $A_0$  or  $\textcircled{H}$  and  $\textcircled{K}$  in K-T, and thereby to the  $k_\ell^2$  and  $k_t^2$  in the Alvarez Linac.

All that remains is to extract (and presumably control!) the values of  $A_{00}$  and  $B_{00}$  from the Superfish runs.

- 1)  $A_{00}$  is the coefficient of the quadrupole field on the axis.
- 2)  $B_{00} \cos \frac{2\pi z}{\beta\lambda}$  is the potential at  $r=0$  which presumably can be calculated at each  $z$  (corresponding to a separate geometry) by finding the central potential with the two "electrodes" being at  $\pm \frac{V}{2}$ .



Let quad gradient be  $B$

$V_0$  be potential at  $r = 0$

$$v_2 = \frac{V}{2} = \frac{Bp^2}{2} + v_0$$

$$v_1 = -\frac{V}{2} = -\frac{Bq^2}{2} + v_0$$

$$V = \frac{B}{2} (p^2 + q^2)$$

$$v_0 = \frac{B}{2} (q^2 - p^2)$$

One should set  $v_0$  proportional to  $\cos(kz)$  (to obtain  $k_\ell^2$ )

and  $B$  (to obtain  $k_t^2$ )

and  $p_{\min} = a$  (for beam clearance).

This gives  $V$  and  $q_{\max}$ . Then as  $v_0$  varies as  $\cos(kz)$ , and  $B, V$  remain fixed, one finds  $p, q$  as functions of  $z$ . It may be necessary to adjust tuning.

BEAM DYNAMICS IN THE 4-VANE STRUCTURE

(with emphasis on Jacobians)

A. The fields which govern the dynamics are:

$$E_z = \frac{kAV}{2} I_0(kr) \sin kz \sin (\omega t + \alpha) \quad (1)$$

$$E_r = -\frac{\chi V}{a^2} r \cos 2\psi \sin (\omega t + \alpha) - \frac{kAV}{2} I_1(kr) \sin(\omega t + \alpha) \cos kz \quad (2)$$

$$E_\theta = \frac{\chi V}{a^2} r \sin 2\psi \sin (\omega t + \alpha) \quad (3)$$

We will define the  $t = 0$  time to correspond to  $\alpha = 0$ , and take only that wave component traveling in the  $+z$  direction. Actually  $\left\{ \begin{smallmatrix} \sin \\ \cos \end{smallmatrix} \right\} (kz)$  really need to be replaced by  $\left\{ \begin{smallmatrix} \sin \\ \cos \end{smallmatrix} \right\} \int kdz$ , where  $k = \frac{\omega}{v_s}$  will vary with position along the linac to match the acceleration of the synchronous particle. Thus

$$E_z = \frac{kAV}{4} I_0(kr) \cos (kz - \omega t) \quad (4)$$

$$E_r = -\frac{\chi V}{a^2} r \cos 2\psi \sin \omega t + \frac{kAV}{4} I_1(kr) \sin (kz - \omega t) \quad (5)$$

$$E_\theta = \frac{\chi V}{a^2} r \sin 2\psi \sin \omega t \quad (6)$$

One now changes to the independent variable  $z$  (which we will replace by  $s$  to avoid confusion) and replaces  $t$  by the phase deviation from the traveling wave, according to

$$ks \equiv \int kdz = \omega t - \phi \quad (7)$$

Thus

$$E_z = \frac{kAV}{4} I_0(kr) \cos \phi \quad (8)$$

$$E_r = -\frac{kAV}{4} I_1(kr) \sin \phi - \frac{XV}{a^2} r \cos 2\psi \sin (ks + \phi)$$

$$E_\theta = \frac{V}{a^2} r \sin 2\psi \sin (ks + \phi)$$

$$E_x = -\frac{kAV}{4} \frac{x}{r} I_1(kr) \sin \phi - \frac{XV}{a^2} x \sin (ks + \phi) \quad (9)$$

$$E_y = -\frac{kAV}{4} \frac{y}{r} I_1(kr) + \frac{XV}{a^2} y \sin (ks + \phi) \quad (10)$$

The equations of motion, taking into account the variation of  $k$ , are

$$k^3 \frac{d}{ds} \left( \frac{1}{k^3} \frac{d\phi}{ds} \right) = -\frac{e}{mv^2} \frac{k^2 AV}{4} \left[ I_0(kr) \cos \phi - \cos \phi_s \right] \quad (11)$$

$$k \frac{d}{ds} \left( \frac{1}{k} \frac{dx}{ds} \right) = -\frac{e}{mv^2} \frac{k^2 AV}{8} \times \left( \frac{I_1(kr)}{\frac{kr}{2}} \right) \sin \phi$$

$$- \frac{XV}{a^2} \frac{e}{mv^2} \times \sin (ks + \phi) \quad (12)$$

$$k \frac{d}{ds} \left( \frac{1}{k} \frac{dy}{ds} \right) = -\frac{e}{mv^2} \frac{k^2 AV}{8} y \left( \frac{I_1(kr)}{\frac{kr}{2}} \right) \sin \phi$$

$$+ \frac{XV}{a^2} \frac{e}{mv^2} y \sin (ks + \phi) \quad (13)$$

B. We can now reconstruct the Hamiltonian:

$$H = \frac{\phi'^2}{2k^3} + \frac{x'^2}{2k} + \frac{y'^2}{2k} - \frac{eAV}{4kmv^2} \left[ I_0(kr) \sin \phi - \phi \cos \phi_s \right]$$

$$+ \frac{x^2 - y^2}{2} \frac{eXV}{ka^2mv^2} \sin (ks + \phi)$$



Hamilton's equations ( $p = \frac{\partial H}{\partial \dot{q}}$ ,  $q = -\frac{\partial H}{\partial p}$ ) will duplicate (12) and (13), but the  $\phi$  dependence of the radial force in the quadrupole term must be accompanied by a radial dependence of the longitudinal force. Equation (11) must therefore be replaced by (14)

$$k^3 \frac{d}{ds} \left( \frac{1}{k^3} \frac{d\phi}{ds} \right) = - \frac{ek^2 Av}{4mv^2} \left[ I_0(kr) \cos \phi - \cos \phi_s \right] + \frac{ek^2 v}{a^2 mv^2} \frac{x^2 - y^2}{2} \cos (ks + \phi) \quad (14)$$

Equations (12), (13), and (14) should therefore be the basis of the numerical calculation, with

$$p_\phi = \frac{1}{k^3} \frac{d\phi}{ds} \text{ proportional to } \delta\omega$$

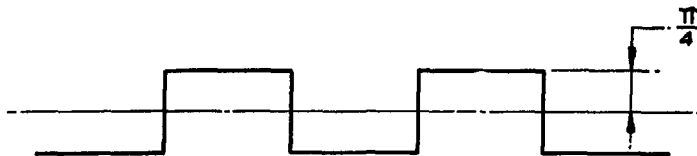
$$p_{x,y} = \frac{1}{k} \frac{d(x,y)}{ds} \text{ proportional to } \dot{x}, \dot{y}$$

C. Smoothing of the quadrupole term:

Let us write (12), neglecting the variation of  $k$ , for small transverse oscillation, as

$$x'' = + Ax + Bx \sin (ks + \phi) \quad (15)$$

This is a Mathieu equation for which one can expand the solution if desired. However, a simple approximation can be constructed by replacing  $\sin (ks + \phi)$  by a square wave having the same first harmonic.



This leads to

$x'' = \left( A \pm \frac{\pi}{4} B \right) x$  with "magnet-lengths"  $= \frac{\pi}{k}$ . Use of matrix analysis leads to the smoothed motion

$$x'' \cong -k_t^2 x$$

where

$$k_t^2 \cong \frac{\pi^4}{192} \frac{B^2}{k^2} - A$$

$$k_t^2 \cong \frac{\pi^4}{192} \frac{\chi^2 V^2}{a^4} \left( \frac{e}{mv^2} \right)^2 \frac{1}{k^2} + \frac{e}{mv^2} \frac{k^2 AV}{8} \sin \phi \quad (16)$$

If this smoothing is applied to the Hamiltonian, the last term in (12) is replaced by  $-k_t^2 x$ , the last term in (13) is replaced by  $-k_t^2 y$ , and the last term in (14) disappears.

#### D. Importance of the second term in (14):

The term oscillates, therefore leading to cancelling contributions over  $\Delta s = \frac{2\pi}{k}$ , except for the variation of  $a$ . Since

$$\int ds \cos (ks + \phi) \cong \frac{2}{k} ,$$

half cycle

the maximum effect of the second term in (14), averaged over  $\Delta s = \frac{2\pi}{k}$ , is

$$\frac{ek^2 \chi V}{2\pi m v^2 a^2} \left( 1 - \frac{a^2}{b^2} \right) \quad (17)$$

where  $2a$  is the minimum and  $2b$  the maximum vane separation. The relative size of (17) compared to  $\phi''$  in (14) can be related to the size of  $k_t$  in (16). This relative size will be of order  $x^2 k^2$ , which is proportional to the square of the ratio of the beam size to the focusing period and is therefore completely negligible.

## E. CONCLUSION

The motion is adequately represented by (12), (13) and (14). When the calculations are completed, the dependence of the quadrupole focusing contribution on  $\phi$  should be negligible, as should the contribution of the quadrupole term to the longitudinal motion. It is of course essential that whatever approximation is used in the numerical calculations correspond to a Jacobian which is exactly 1.

## APPENDIX 1

### Summary of Discussion on Jacobian

Start with Hamiltonian system

$$H(p, q)$$

$$p' = - \frac{\partial H}{\partial q} \quad q' = \frac{\partial H}{\partial p} \quad (1)$$

Convert to difference equation over interval L

$$\left. \begin{aligned} p_f &= p_i + f(p, q) & , & \quad f = -L \frac{\partial H}{\partial q} \\ q_f &= q_i + g(p, q) & , & \quad g = +L \frac{\partial H}{\partial p} \end{aligned} \right\} \quad (2)$$

---

Statements which can be proven:

(a) If  $f(p_i, q_i)$ ,  $g(p_i, q_i)$  is used on the right side of (2), then the Jacobian will not be 1 except under very unusual circumstances

---

(b) If  $f(p_i, q_f)$ ,  $g(p_i, q_f)$  is used on the right side of (2), then the Jacobian will be 1.

---

(c) Same as (b) for  $f(p_f, q_i)$ ,  $g(p_f, q_i)$

---

(d) If  $f(\bar{p}, \bar{q})$ ,  $g(\bar{p}, \bar{q})$  is used on the right side of (2), then the Jacobian will be 1.

$$\left( \bar{p} = \frac{p_f + p_i}{2}, \quad \bar{q} = \frac{q_f + q_i}{2} \right)$$

Note: The transformations can be written as

$$\bar{p} = p_i + \frac{1}{2} f(\bar{p}, \bar{q}) \quad \bar{q} = q_i + \frac{1}{2} f(\bar{p}, \bar{q})$$

$$p_f = \bar{p} + \frac{1}{2} f(\bar{p}, \bar{q}) \quad q_f = \bar{q} + \frac{1}{2} f(\bar{p}, \bar{q})$$

While

$$J_{\bar{p}, \bar{q}} \neq 1$$

$$J_{p_i, q_i} \neq 1$$

$$J_{p_i, q_i, \bar{p}, \bar{q}} \times J_{\bar{p}, \bar{q}, p_f, q_f}$$

So, if this is used for the calculation, the phase space area at  $\bar{p}, \bar{q}$  will not be the same as that at  $i$  or  $f$ .

- (e) If one does not start from an explicit Hamiltonian, but obtains  $f$  from successive physical approximations, then one starts with

$$p_f = p_i + f(p_i, q_i) \quad (3)$$

Several options are now available for proceeding:

- (1) Replace  $p_i$  by  $p_f$  directly. This will change the approximate relationship.
- (2) Solve (3) for  $p_i$  and replace  $p_i$  in  $f$  by the expression obtained. This may be impossible exactly, but it can be done by successive approximation. In this way one obtains

$$p_f = p_i + \hat{f}(p_f, q_i) \quad (4a)$$

Now integrate  $\hat{f}$  with respect to  $q_i$  to obtain  $\hat{H}$  from (2). Then take the derivative of  $\hat{H}$  with respect to  $p_f$ , as dictated by (2), to get  $\hat{g}(p_f, q_i)$

$$q_f = q_i + \hat{g}(p_f, q_i) \quad (4b)$$

The  $\hat{g}$  in (4b) is then a consistent approximation (not necessarily what was derived by the same physical approximation process used to obtain  $f(p_i, q_i)$ ), leading to a Jacobian which is exactly 1.

---

The process can be generalized to several variables by using an (i,f) combination in f and g for each variable.

APPENDIX 2

Jacobian for Longitudinal Motion

1. Easiest to start from Hamiltonian form corresponding to desired sophistication/complication

$$H(\phi, W)$$

$$\phi' = \frac{\partial H}{\partial W} = f \qquad W' = - \frac{\partial H}{\partial \phi} = g$$

$$\frac{\partial f}{\partial \phi} = - \frac{\partial g}{\partial W}$$

2. Go to difference equation

$$\phi_f - \phi_i = f(\phi, W) \qquad W_f - W_i = g(\phi, W)$$

3. Prescription to obtain  $J = 1$

Use  $\phi_i, W_f$  on both right sides (in  $f$  and  $g$ )

or  $\phi_f, W_i$  " " " "

4. Suggest  $\phi_f = \phi_i + f(\phi_i, W_f)$

$$W_f = W_i + g(\phi_i, W_f)$$

In general iteration will be required for  $W_f$ .

5. Including dependence of energy gain on energy to first order

$$\boxed{W_f = W_i + \underbrace{T(\cos \phi_i - \cos \phi_s)}_g + W_f S \sin \phi_i}$$

$$H = - T(\sin \phi - \phi \cos \phi_s) + WS \cos \phi + \underset{\substack{\uparrow \\ \text{(any function ok)}}}{h(W)}$$

$$f = \frac{\partial H}{\partial W} = S \cos \phi + h'(W)$$

$$\phi_f = \phi_i + h'(W_f) - S \cos \phi_i$$

Note:  $W_f$  can be solved for explicitly

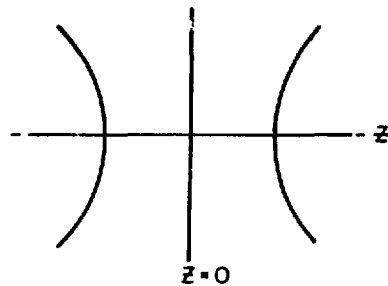
$$W_f = \frac{W_i + T(\cos \phi_i - \cos \phi_s)}{1 - S \sin \phi_i}$$

6. Discussion of longitudinal motion - test of Jacobian

$$\Delta W = \int e E_z(z) \cos(\omega t + \phi) dz$$

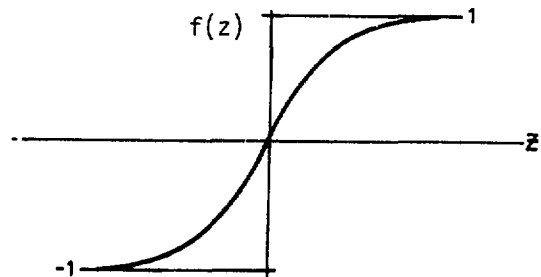
$$t = 0, z = 0$$

$$z = \int v dt$$



$$t = \int \frac{dz}{v} \quad v = v_s + \frac{\Delta W}{2} f(z)$$

$$\int \frac{dz}{v_s} \left( 1 - \frac{\Delta W}{2} f(z) \right) = \frac{z}{v_s} - \Delta W g(z)$$



$g(z)$  is even in  $z$

$$\Delta W = \int e E_z(z) \cos\left(\frac{\omega z}{v_s} + \phi - \omega W g(z)\right) dz$$

$$\cong dz \left[ \cos\left(\frac{\omega z}{v_s} + \phi\right) + \omega W g(z) \sin\left(\frac{\omega z}{v_s} + \phi\right) \right]$$



$$= \cos \phi T + \sin \phi W S$$

$$T = e \int E_Z(z) \cos \frac{\omega z}{v_s} dz \quad S = e\omega \int E_Z(z) g(z) \sin \frac{\omega z}{v_s} dz .$$

$$\Delta W = \cos \phi T + \sin \phi W S$$

$$\Delta \phi = - a \Delta W + F(\phi, W)$$

a.) Try  $\phi_f = \phi_i - a W_f + G(\phi_i, W_f)$

$$W_f = W_i + T \cos \phi_i + S W_f \sin \phi_i$$

$$\left( \frac{\partial \phi_f}{\partial \phi_i} \right)_{W_i} = 1 + \frac{\partial G}{\partial \phi_i} + \left( \frac{\partial G}{\partial W_f} - a \right) \left( \frac{\partial W_f}{\partial \phi_i} \right)_{\phi_i}$$

$$\left( \frac{\partial \phi_f}{\partial W_i} \right)_{\phi_i} = \left( \frac{\partial G}{\partial W_f} - a \right) \left( \frac{\partial W_f}{\partial W_i} \right)_{\phi_i}$$

$$J = \left( \frac{\partial W_f}{\partial W_i} \right)_{\phi_i} \left( 1 + \frac{\partial G}{\partial \phi_i} \right) = 1$$

$$W_f (1 - S \sin \phi_i) - T \cos \phi_i = W_i$$

$$1 - S \sin \phi_i = \left( \frac{\partial W_i}{\partial W_f} \right)_{\phi_i}$$

$$\frac{\partial W_f}{\partial W_i} = \left( \frac{\partial W_i}{\partial W_f} \right)^{-1}$$

$$\text{So } J = \frac{1 + \frac{\partial G}{\partial \phi_i}}{1 - S \sin \phi_i}$$

$$\text{Let } G = S \cos \phi_i$$

$$W_f = W_i + T \cos \phi_i + S W_f \sin \phi_i$$

$$\phi_f = \phi_i - a W_f + S \cos \phi_i$$

$$W_f = \frac{W_i + T \cos \phi_i}{1 - S \sin \phi_i}$$

$$\phi_f = \phi_i - a \left( \frac{W_i + T \cos \phi_i}{1 - S \sin \phi_i} \right) + S \cos \phi_i$$

b.) Try  $W_f = W_i + f(\phi_i, W_f)$

$$\phi_f = \phi_i + g(\phi_i, W_f)$$

$$\left( \frac{\partial \phi_f}{\partial \phi_i} \right)_{W_i} = 1 + \frac{\partial g}{\partial \phi_i} + \frac{\partial g}{\partial W_f} \left( \frac{\partial W_f}{\partial \phi_i} \right)_{W_i}$$

$$\left( \frac{\partial \phi_f}{\partial W_i} \right)_{\phi_i} = \frac{\partial g}{\partial W_f} \left( \frac{\partial W_f}{\partial W_i} \right)_{\phi_i}$$

$$J = \begin{vmatrix} \left(1 + \frac{\partial g}{\partial \phi_i} + \frac{\partial g}{\partial W_f} \left(\frac{\partial W_f}{\partial \phi_i}\right)_{W_i}\right) & \frac{\partial g}{\partial W_f} \left(\frac{\partial W_f}{\partial W_i}\right)_{\phi_i} \\ \left(\frac{\partial W_f}{\partial \phi_i}\right)_{W_i} & \left(\frac{\partial W_f}{\partial W_i}\right)_{\phi_i} \end{vmatrix}$$

$$= \left(1 + \frac{\partial g}{\partial \phi_i}\right) \left(\frac{\partial W_f}{\partial W_i}\right)_{\phi_i}$$

$$W_f = W_i + f(\phi_i, W_f)$$

$$W_i = W_f - f(\phi_i, W_f)$$

$$\left(\frac{\partial W_i}{\partial W_f}\right)_{\phi_i} = 1 - \frac{\partial f}{\partial W_f}$$

$$\left(\frac{\partial W_f}{\partial W_i}\right)_{\phi_i} = \frac{1}{1 - \frac{\partial f}{\partial W_f}}$$

$$J = \frac{\left(1 + \frac{\partial g}{\partial \phi_i}\right)}{1 - \frac{\partial f}{\partial W_f}} = 1$$

Requires  $\frac{\partial g}{\partial \phi_i} = - \frac{\partial f}{\partial W_f}$

In example on p. 8  $f(\phi_i, W_f) = T \cos \phi_i + S W_f \sin \phi_i$

$$g(\phi_i, W_f) = S \cos \phi_i - a W_f$$

$$\frac{\partial g}{\partial \phi_i} = -S \sin \phi_i = -\frac{\partial f}{\partial W_f}$$

### Basic Theorem

$$\text{If } W_f = W_i + f(\phi_i, W_f)$$

$$\phi_f = \phi_i + g(\phi_i, W_f)$$

This corresponds to a particular prescription to iterate the differential equations.

$$W' = \frac{1}{L} f$$

$$\phi' = \frac{1}{L} g$$

Since the system must be Hamiltonian, it must start with

$$H(q, p) = H(\phi, W)$$

$$\dot{p} = -\frac{\partial H}{\partial q} \rightarrow W' = -\frac{\partial H}{\partial \phi}$$

$$\dot{q} = \frac{\partial H}{\partial p} \rightarrow \phi' = +\frac{\partial H}{\partial W}$$

Obviously

$$\frac{\partial}{\partial W} (W') = -\frac{\partial}{\partial \phi} (\phi')$$

$$\frac{\partial}{\partial W} f = -\frac{\partial}{\partial \phi} g \quad \text{as required above.}$$

Obviously

$$W_f = W_i + F(\phi_f, W_i)$$

$$\phi_f = \phi_i + G(\phi_f, W_i)$$

will work equally well.

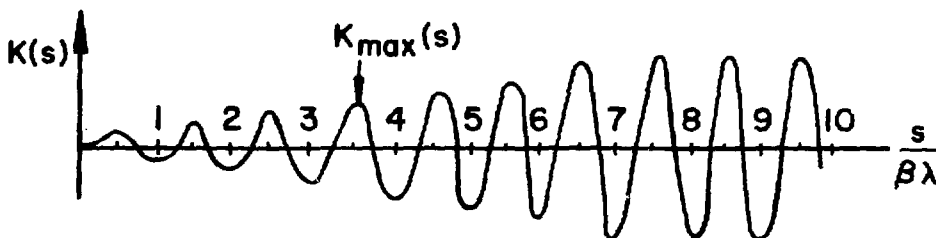
TAPERED MATCHING IN THE RADIO-FREQUENCY-QUADRUPOLE (RFQ)

I. Introduction

Since the RFQ provides transverse quadrupole focusing from electric fields which vary with the (r.f.) frequency, the transverse acceptance of the 4 vane structure will vary with the phase at which the beam enters the focussing system. In order to minimize or eliminate this variation the vane separation (bore diameter) is tapered over the first several  $\beta\lambda$  so that the quadrupole field gradient increases continuously from 0 to its final value. The purpose of this note is to show that the acceptance will indeed be approximately independent of entering phase.

II. Model

The electric quadrupole strength has the general form



A simple analysis to smooth the quadrupole focussing gives for the equivalent transverse wave number

$$k_t(s) = g\beta\lambda K_{\max}(s)$$

where  $g$  is a number of order 1. The original differential equation

$$X'' + K(s) X = 0 \tag{1}$$

(which preserves phase space area) is then approximated by

$$X'' + k_t^2(s) X = 0 \tag{2}$$

where the primary approximation is the assumption that  $K_{\max}(s)$  does not vary much in a distance  $\beta\lambda$ .

We can solve (2) in terms of known functions if  $k_t^2(s)$  is replaced by a power of  $s$ . In this case the equation (scaled in  $s$  so that the coefficient of the second term is 1) becomes

$$X'' + s^p X = 0 \quad (3)$$

which has the solution

$$X(s) = X_0 A s^{1/2} J_{\frac{-1}{p+2}} \left( \frac{2s^{\frac{p+2}{2}}}{p+2} \right) + X_0' B s^{-1/2} J_{\frac{1}{p+2}} \left( \frac{2s^{\frac{p+2}{2}}}{p+2} \right) \quad (4)$$

where

$$A = \Gamma \left( 1 - \frac{1}{p+2} \right) (p+2)^{\frac{-1}{p+2}} \quad (5)$$

$$B = \Gamma \left( 1 + \frac{1}{p+2} \right) (p+2)^{\frac{1}{p+2}}$$

are chosen so that  $X(0) = X_0$ ,  $X'(0) = X_0'$ .

The asymptotic behavior of (4) leads to

$$X(S) \rightarrow \sqrt{\frac{2+p}{\pi}} s^{\frac{-p}{4}} \left[ A X_0 \cos(\psi + \mu) + B X_0' (\psi + \mu) \right] \quad (6)$$

where

$$\psi = \frac{2s^{\frac{p+2}{2}}}{p+2} - \frac{\pi}{4}, \quad \psi' = s^{\frac{p}{2}}, \quad s^{\frac{-p}{4}} \psi' = s^{\frac{p}{4}}, \quad (7)$$

$$\mu = \frac{\pi}{2(p+2)}$$

The bracket in (6) can be written as

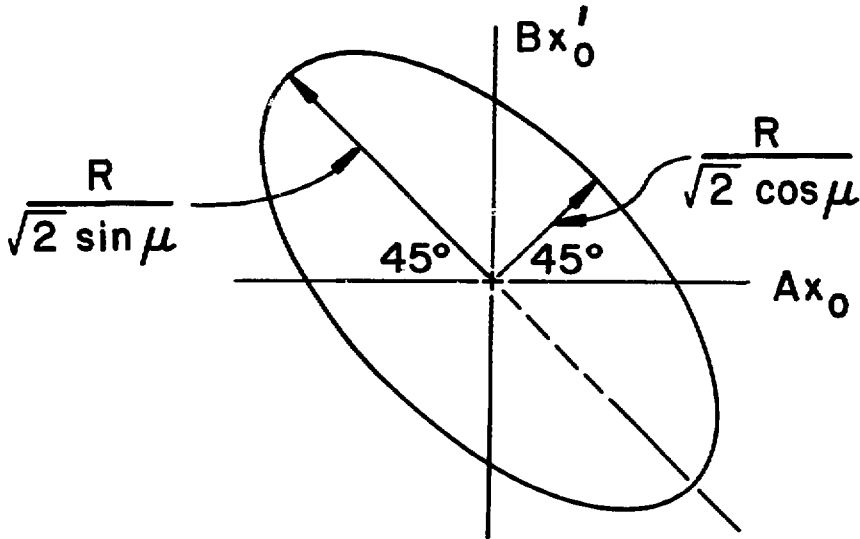
$$\left[ \right] = P \cos \psi + Q \sin \psi = \sqrt{P^2 + Q^2} \cos (\psi - \alpha) \quad (8)$$

where

$$P = (AX_0 + BX_0') \cos \mu$$

$$Q = (-AX_0 + BX_0') \sin \mu \quad (9)$$

If the initial phase space is plotted with axes  $BX_0'$  vs  $AX_0$ , it is clear that a matched final beam requires an  $X_0, X_0'$  trajectory for which  $P^2 + Q^2 = R^2$  is constant. This translates into the  $45^\circ$  ellipse



The initial phase space area occupied by the beam is

$$\text{Area} \Big|_{X_0 X_0'} = \frac{\pi R^2}{AB \sin 2\mu} \quad (10)$$



while the final phase space area is obtained from (5) as

$$\begin{aligned} \text{Area} \left\{ \begin{array}{l} \text{Final} \\ \text{Initial} \end{array} \right. &= \pi \sqrt{\frac{2+p}{\pi}} s^{\frac{-p}{4}} R \cdot \sqrt{\frac{2+p}{\pi}} s^{\frac{+p}{4}} R \\ &= \pi \left( \frac{2+p}{\pi} \right) R^2 \end{aligned} \quad (11)$$

Since

$$AB = \Gamma \left( 1 + \frac{1}{p+2} \right) \Gamma \left( 1 - \frac{1}{p+2} \right) = \frac{\pi}{p+2} \cdot \frac{1}{\sin \frac{\pi}{p+2}}$$

$$AB \sin 2u = AB \sin \frac{\pi}{p+2} = \frac{\pi}{p+2} \quad (12)$$

and the initial (10) and final (11) areas are equal, as they must be.

### III. Conclusions

Phase space areas are preserved, and a prescription for matching is given by (9):

$$(AX_o + BX_o')^2 \cos^2 \mu + (-AX_o + BX_o')^2 \sin^2 \mu = R^2 \quad (13)$$

Since the matching depends only slightly on  $p$ , the acceptance moving a distance  $\frac{\beta\lambda}{2}$  (corresponding to a  $180^\circ$  shift in entering phase) will be essentially unchanged. The rate of tapering (related to  $p$ ) will determine the orientation and eccentricity of the initially matched ellipse.

MISALIGNMENTS IN THE RFQ

I. Introduction

Concern has been expressed, because of the very small aperture, that misalignments in the RFQ may lead to unacceptable beam deflection or growth. The purpose of this note is to estimate the size and nature of such misalignments, and to project their effect on beam orbits.

II. Imperfections

A. Among those imperfections which have been considered are

1. Transverse vane location error
2. Error in vane curvature
3. Voltage perturbation on one or more vanes
4. Multipole fields other than quadrupole

B. All of the above effects have the potential to shift the center of the quadrupole, or to cause perturbations of the quadrupole gradient some place within the bore. It is not hard to see that the movement of the center will be of the form

$$\Delta X, \Delta Y \sim \frac{\Delta R}{R} a, \text{ or } \frac{\Delta V}{V} a$$

where  $a$  is the bore radius,  $R$  is a typical dimension (like the vane radius of curvature), and  $V$  is the vane voltage. Even in the case of higher order multipoles one will get effects which are largest near the bore, but which lead to forces much smaller than the quadrupole force, which clearly must dominate.

C. The critical consideration is whether any of the imperfections has a systematic variation which is synchronized with the transverse frequency. Since imperfections are most likely to vary with period  $\beta\lambda$ , and since stability requires avoiding wave lengths which are multiples of  $\beta\lambda$ , there should be no trouble.

D. Another circumstance where misalignments are important is if there are fluctuations in regions smaller than the wave length of the transverse oscillation which are uncorrelated with one another.

This is the usual misalignment situation, when alignments are made one cell at a time. Such effects seem to be absent in the present case for the method of construction currently used for the RFQ.

- E. The remaining imperfections are then ones which vary systematically and slowly over long distances.

### III. Analysis

- A. All forms of misalignment can be put into the form

$$X'' + k_t^2 X = k_t^2 \epsilon(s) \quad (1)$$

where  $\epsilon(s)$  is the effective misalignment. The solution of (1) for  $X(0) = X'(0) = 0$  is

$$X(s) = k_t \int_0^s ds' \epsilon(s') \sin k_t (s-s') \quad (2)$$

We will now handle the three special cases: sinusoidal variation of  $\epsilon$ , random fluctuation of  $\epsilon$  in short blocks, slowly varying  $\epsilon$ .

- B. If  $\epsilon(s) = \epsilon_{\max} \sin(k_\epsilon s + \alpha)$ , one can see directly from (1) that  $X$  will develop an oscillation with amplitude

$$A = \frac{k_t^2}{k_t^2 - k_\epsilon^2} \epsilon_{\max} \quad (3)$$

clearly the region  $k_\epsilon$  near  $k_t$  must be avoided. For long wave length ( $k_\epsilon \rightarrow 0$ ),  $A = \epsilon_{\max}$  and the maximum displacement will turn out to be  $2A$ . For short wave lengths ( $k_t/k_\epsilon \ll 1$ ),  $A$  will be reduced from  $\epsilon$  by a factor which is the square of the ratio of the wave length of the imperfection (like  $\beta\lambda$ ) to the wave length of the transverse oscillation.

- C. If  $\epsilon$  is random in short blocks of length  $\ell \ll 2\pi/k_t$ , one can easily show that the rms growth of  $x$  is

$$X_{\text{rms}} \approx k_t \ell \epsilon_{\text{rms}} \sqrt{\frac{N}{2}} \quad (4)$$

where  $N$  is the number of such blocks. When  $N$  is large  $X_{rms}$  can be important, unless  $\epsilon_{rms}$  is extremely small, as in the present case.

- D. If  $\epsilon(s)$  is slowly varying, one can evaluate (2) by repeated integration by parts leading to a series expansion in successively higher derivations of  $\epsilon(s)$ . The leading term is

$$X(\infty) \approx \epsilon(0) \cos k_t s \quad (5)$$

and the maximum displacement will be  $2 \epsilon(0)$  during the transient.

- E. The results for multipole effects will be similar, with added factors of the form

$$f_m \left( \frac{r}{a} \right)^m$$

where  $f_m$  is a dimensionless multipole coefficient whose value is less than 1, and where  $r/a$  is the ratio of beam size to bore radius.

#### IV. Conclusions

All systematic imperfections of wave length sufficiently different from the wave length of the transverse oscillation are unimportant. Random misalignments will only be important if there are random fluctuations in geometry on a length scale smaller than the transverse wave length. In all other cases, the fractional beam displacement (compared to the bore radius), or growth in beam size or emittance, will be proportional to the relative value of the imperfection.

BUNCHING REGION OF AN RFQ

The four vane structure is being used to accelerate and focus particles starting at very low velocities (corresponding to 100 KeV protons). Questions arise about how rapidly the accelerating field should grow with  $z$  (or  $B$ ). Here we will analyze the initial bunching of a monochromatic beam when the accelerating field grows linearly.

Let  $y$  be the deviation of  $\gamma$  from its synchronous value, and let  $\phi_s = -\frac{\pi}{2}$  during the initial period of growth of the accelerating field. The equations for the longitudinal motion are then

$$y' \equiv \frac{dy}{ds} = \frac{eET}{Mc^2} \cos\phi$$

$$\phi' \equiv \frac{d\phi}{ds} = -\frac{2\pi}{\beta^3 \lambda} y$$
(1)

leading to

$$\phi'' = -\frac{2\pi eET}{Mc^2 \beta^3 \lambda} \cos\phi$$
(2)

We will define

$$\frac{2\pi eET}{Mc^2 \beta^3 \lambda} = B$$
(3)

and assume that  $B$  varies linearly with  $s$  according to

$$B = B's \quad B' \text{ constant.}$$
(4)

Thus

$$\phi'' = -B's \cos\phi \quad (5)$$

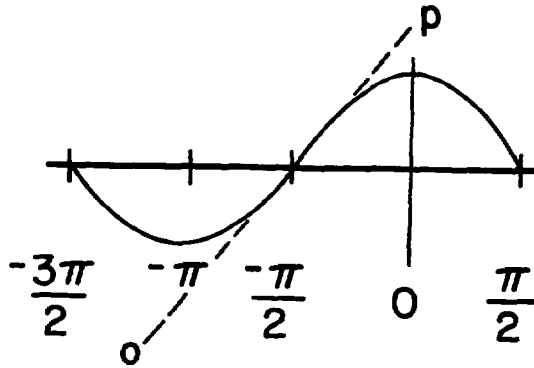
We cannot proceed further without some assumption. Let us approximate  $\cos\phi$  in the region  $-\pi < \phi < 0$  ( $\phi = -\frac{\pi}{2} + \psi$ )

by

$$\begin{aligned} \cos\phi &= \cos\left(-\frac{\pi}{2} + \psi\right) \\ &= \sin\psi \approx \psi \end{aligned}$$

leading to

$$\psi'' \approx -B's \psi. \quad (6)$$



The solutions to (6) are Airy functions of the form

$$\psi \rightarrow s^{1/2} J_{\pm 1/3} \left( \frac{2}{3} (B')^{1/2} s^{3/2} \right)$$

where

$$J_n(x) = \sum_{m=0}^{\infty} \frac{(-1)^m x^{n+2m}}{m! \Gamma(n+m+1)} \approx \sqrt{\frac{2}{\pi x}} \cos\left(x - \left(n + \frac{1}{2}\right) \frac{\pi}{2}\right)$$

Since we wish to have  $\psi(0) = \psi_0$ ,  $\psi'(0) = 0$ , we can write

$$\psi = \psi_0 A s^{1/2} J_{-1/3} \left( \frac{2}{3} (B')^{1/2} s^{3/2} \right) \quad (7)$$

where

$$A s^{1/2} \frac{\left(\frac{1}{3}(B')^{1/2} s^{3/2}\right)^{-1/3}}{\Gamma\left(\frac{2}{3}\right)} = 1$$

$$A = (B')^{1/6} \frac{\Gamma\left(\frac{2}{3}\right)}{3^{1/3}} \quad (8)$$

Asymptotically, one finds

$$\psi \approx \psi_0 (B')^{1/6} \frac{\Gamma\left(\frac{2}{3}\right)}{3^{1/3}} s^{1/2} \sqrt{\frac{2}{\pi \frac{2}{3}(B')^{1/2} s^{3/2}}} \cos\left(\frac{2}{3}(B')^{1/2} s^{3/2} - \frac{\pi}{12}\right)$$

$$\approx \psi_0 \frac{3^{1/6}}{\pi^{1/2}} \Gamma\left(\frac{2}{3}\right) \frac{(B')^{-1/12}}{s^{1/4}} \cos\left(\frac{2}{3}(B')^{1/2} s^{3/2} - \frac{\pi}{12}\right) \quad (9)$$

From (1b),

$$y \approx \frac{\beta^3 \lambda}{2\pi} \psi_0 \frac{3^{1/6}}{\pi^{1/2}} \Gamma\left(\frac{2}{3}\right) \frac{(B')^{-1/12}}{s^{1/4}} (B')^{1/2} s^{1/2} \sin\left(\frac{2}{3}(B')^{1/2} s^{3/2} - \frac{\pi}{12}\right)$$

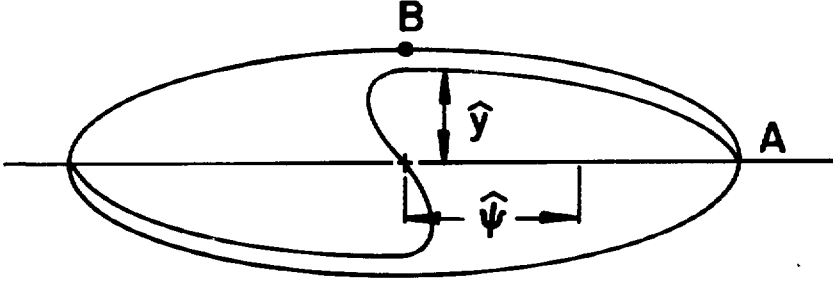
$$(10)$$

The area occupied by particles with  $-\pi < \phi < 0$  or  $-\frac{\pi}{2} < \psi_0 < \frac{\pi}{2}$  is

$$W_{\mathcal{L}} = \pi \hat{\psi} \hat{y} \approx \frac{\beta^3 \lambda}{2\pi} \frac{3^{1/3}}{\pi} \Gamma^2\left(\frac{2}{3}\right) (B')^{1/3} \psi_0^2 \left(\frac{\pi}{2}\right)^2$$

$$\approx \beta^3 \lambda \frac{\pi}{8} 3^{1/3} \Gamma^2\left(\frac{2}{3}\right) (B')^{1/3} \quad (\text{x Mc}\lambda \text{ for correct units})$$

This is the area occupied by the inner half of the bunched beam.



Actual area is perhaps twice as large because  $\psi_0$  extends to  $\pm\pi$ , but the limits on  $\hat{y}$  are controlled more by the  $\psi_0 = \pm\frac{\pi}{2}$  points.

$$W_e^{\text{actual}} \approx \beta^3 \lambda \frac{\pi}{4} 3^{1/3} \Gamma^2 \left( \frac{2}{3} \right) (B')^{1/3} (Mc\lambda) \quad (11)$$

should describe the emittance of the beam which is to be accelerated.

To complete this phase of the calculation let us calculate the area of the phase stable region. From (2) and (3) we write

$$\phi'' = -B \cos \phi \quad (12)$$

In order to calculate the phase stable area, we must assume B constant, in which case (12) may be integrated to obtain

$$\frac{\phi'^2}{2} + B \sin \phi = \text{const.} \quad (13)$$

Since  $\phi_A = \frac{\pi}{2}$ ,  $\phi_A' = 0$ ,  $\phi_B = -\frac{\pi}{2}$ , we find  $\phi_B' = 4B$ ,  $\phi'^2 + 2B \sin \phi = 2B$ .



In fact, the area is given by

$$2 \int_{-\frac{3\pi}{2}}^{\frac{\pi}{2}} y \, d\phi = \frac{\beta^3 \lambda}{\pi} \int_{-\frac{3\pi}{2}}^{\frac{\pi}{2}} |\phi'| \, d\phi = \frac{\beta^3 \lambda}{\pi} 2\sqrt{B} \int_{-\frac{3\pi}{2}}^{\frac{\pi}{2}} \sin\left(\frac{\pi}{4} - \frac{\phi}{2}\right) \, d\phi$$

$$W_e^{\text{stable}} = \frac{\beta^3 \lambda}{\sqrt{\pi}} 8\sqrt{B} \quad (\text{Mc}\lambda) \quad \text{for units} \quad (14)$$

The ratio of (11) to (14) is

$$\frac{W_e^{\text{actual}}}{W_e^{\text{stable}}} \approx \frac{\pi^{3/2}}{4} \frac{3^{1/3} \Gamma^2\left(\frac{2}{3}\right)}{8} \frac{B^{1/3}}{B^{1/2}} \quad (15)$$

From (7) it is clear that the beam starts to be bunched when  $J_{-1/3}$  starts to become oscillatory, which happens at a critical distance such that

$$B^{1/2} s_c^{3/2} \approx 1 \quad s_c \approx (B')^{1/3} .$$

This corresponds to a critical  $B_c$  given by

$$B_c = B' s_c \approx B'^{2/3} \quad \text{or} \quad B'^{1/3} \approx B_c^{1/2} .$$

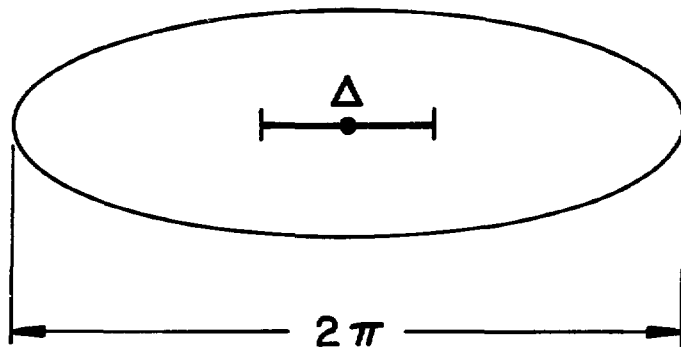
The ratio  $\frac{B'^{1/3}}{B^{1/2}}$  in (15) can therefore be written as  $\frac{B_c^{1/2}}{B^{1/2}}$ .

From this we conclude that after a few bunching oscillations, the bunch will lie comfortably within the longitudinal stability region.

5/25/79

RADIAL EFFECTS DURING INITIAL BUNCHING

Assume that we have a fraction  $\kappa$  of the particles rotating in longitudinal phase space as a rigid line of length  $\Delta$  (in phase) with frequency  $k_\parallel$ .



The transverse space charge force exerted on these particles will have the form

$$k_t^2 (1 - \mu_t) + \mu_t \frac{\kappa 2\pi}{\Delta} k_t^2 \left( \frac{1}{|\sin k_\parallel s|} - 1 \right)$$

taking into  
account average  
spreading

Since this occurs at the start of bunching we shall ignore the  $\mu_t$  in the first term and write for the transverse motion

$$x'' + k_t x = 2\pi \frac{\mu_t \kappa}{\Delta} k_t^2 \left( \frac{1}{|\sin k_\parallel s|} - 1 \right) x \quad (1)$$

where  $s=0$  corresponds to zero phase spread in the bunch of length  $\Delta$ . We shall try to estimate the perturbation on the transverse motion when the beam goes through the single "singularity" at  $s=0$ .

Using the phase - amplitude method

$$\left. \begin{aligned} x &= A \sin(\overbrace{k_t s}^{\phi_t} + \psi) \\ x' &= A k_t \cos(k_t s + \psi) \end{aligned} \right\} (2) \quad A' \sin \phi_t + A \psi' \cos \phi_t = 0$$

$$\frac{1}{k_t} (x'' + k_t^2 x) = A' \cos \phi_t - A \psi' \sin \phi_t = 2\pi \frac{\mu_t \kappa k_t}{\Delta} \left( \frac{1}{|\sin k_\rho s|} - 1 \right) A \sin \phi_t$$

leading to the relations (exact at this point in the calculations)

$$\psi' = -2\pi \frac{\mu_t \kappa k_t}{\Delta} \left( \frac{1}{|\sin k_\rho s|} - 1 \right) \sin^2(k_t s + \psi) \quad (3)$$

$$\frac{A'}{A} = \pi \frac{\mu_t \kappa k_t}{\Delta} \left( \frac{1}{|\sin k_\rho s|} - 1 \right) \sin(2k_t s + 2\psi) \quad (4)$$

We shall first approximate (3) to obtain  $\psi$  and then use the  $\psi$  in approximating (4).

Because of the singularity at  $s=0$ ,  $\sin^2 \phi_t$  will average to  $1/2$  near  $s=0$  and  $\psi'$  can be approximated by

$$\psi' \cong -\frac{\pi \mu_t \kappa k_t}{\Delta} \left( \frac{1}{|\sin k_\rho s|} - 1 \right) \quad (5)$$

In order to handle (5) analytically near  $s=0$ , we shall neglect the  $-1$  and write

$$|\sin k_\rho s| \cong k_\rho \sqrt{s^2 + \epsilon^2} \quad (6)$$

where we intend to take the limit  $\epsilon \rightarrow 0$  near the end of the calculation.

Hence

$$\psi' \approx - \frac{a}{k_\ell \sqrt{s^2 + \epsilon^2}}$$

$$a = \pi \frac{\mu_t k_t}{\Delta}$$

leading to

$$\psi = \psi_0 - \frac{a}{k_\ell} \sinh^{-1} \frac{s}{\epsilon} \quad (7)$$

$$\sinh^{-1} x = \frac{1}{2} \ln \frac{\sqrt{x^2 + 1} + x}{\sqrt{x^2 + 1} - x}$$

Substituting (7) into (4), we find, with the same assumption about the domination of the  $\frac{1}{|\sin k_\ell s|}$  term

$$\frac{A'}{A} = \frac{a}{k_\ell \sqrt{s^2 + \epsilon^2}} \sin \left( 2k_t s + 2\psi_0 - 2 \frac{a}{k_\ell} \sinh^{-1} \frac{s}{\epsilon} \right) \quad (8)$$

The integral of (8) would be infinite, except for the rapid variation of the  $\frac{2a}{k_\ell} \sinh^{-1} \frac{s}{\epsilon}$  term near  $\epsilon=0$ . For this reason, the main contribution to the integral will occur near  $s=0$ , and we can write

$$\ln \frac{A_f}{A_i} = \int \frac{ds a}{k_\ell \sqrt{s^2 + \epsilon^2}} \sin 2\psi_0 \cos \left( \frac{2a}{k_\ell} \sinh^{-1} \frac{s}{\epsilon} \right)$$

Writing  $s = \epsilon \sinh u$ , one finds

$$\ln \frac{A_f}{A_i} = \frac{a \sin 2\psi_0}{k_\ell} \int_{-u_0}^{u_0} du \cos\left(\frac{2a}{k_\ell} u\right) = \sin 2\psi_0 \sin\left(\frac{2a}{k_\ell} u_0\right) \quad (9)$$

The choice of  $u_0$  is governed by the requirement that

$$2k_t s_0 = 2k_t \epsilon \sin u_0 \ll 1.$$

Since we are to take the limit as  $\epsilon \rightarrow 0$ , this suggests that we must choose  $u_0$  to be large, in which case (9) states that the amplitude changes by its own order of magnitude when the transverse charge goes through a singularity.

Our conclusions are therefore the following:

- 1) The amplitude changes by its own order of magnitude each time a portion of the emittance line becomes vertical in the longitudinal phase space.
- 2) The corresponding change in the phase of the transverse motion is infinite - meaning random because of modulus  $2\pi$ .
- 3) Each successive change of amplitude has a phase unrelated to the previous one, and the amplitudes accumulate only in an rms sense.
- 4) The "accumulation" will stop when the length of the rigid line which is rotating  $\left(\frac{\Delta}{2\pi} \beta\lambda\right)$  becomes comparable with the transverse beam size, since the transverse space charge force is no longer that of a line charge.

5) It would probably be instructive to compare these results with numerical computations. It should be kept in mind that the behavior of the transverse motion being calculated in this note corresponds only to the singular portion of the bunched beam and will not apply to all particles.

MEASUREMENT OF AXIAL FIELD DISTRIBUTIONS  
IN A LONG TANK

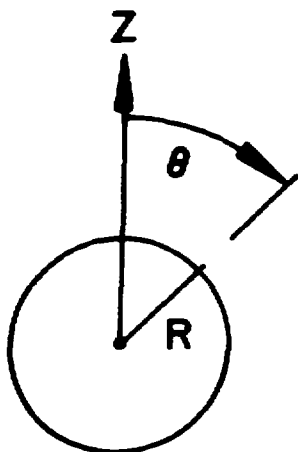
I. INTRODUCTION

Slater has shown that measurement of the frequency change caused by a small metallic or dielectric bead can be directly translated into information about the magnetic and electric field in a resonant cavity at the point where the perturbing bead is placed. The purpose of this note is to estimate the higher order terms which may contribute in a multicell cavity in which spherical metal beads are used along the axis of the cavity. The starting point is Slater's formula,

$$\frac{\delta\omega}{\omega} \cong -\frac{1}{2} \frac{\int_{\Delta V} E_{\perp}^2 dV}{\int_V E_{\perp}^2 dV}$$

where  $\Delta V$  is the (inwardly) perturbed region, and where  $E_{\perp}$  near the bead must be computed in detail.

II. UNIFORM ELECTRIC FIELD



The field near a metallic (grounded) sphere of radius R is given from the potential  $\phi$  by

$$E_r = E_0 \cos \theta \left( 1 + \frac{2R^3}{r^3} \right)$$

$$E_{\theta} = -E_0 \sin \theta \left( 1 - \frac{R^3}{r^3} \right)$$

where

$$\phi = -E_0 \left( r \cos \theta - R^3 \frac{\cos \theta}{r^2} \right) = -E_0 z + E_0 R^3 \frac{\cos \theta}{r^2}$$

At the surface of the sphere  $E_\theta = 0$ ,  $E_r = 3E_0 \cos \theta$ . The integral over a shell of radius  $R$ , thickness  $dR$  is

$$dR R^2 \int d\Omega \frac{E_r^2}{r} = R^2 dR \int 4\pi \overline{\cos^2 \theta} 9E_0^2 = 3E_0^2 \frac{4\pi R^2 dR}{dV}$$

and therefore

$$\int_{\Delta V} E_r^2 dv = 3E_0^2 V$$

Slater's first order result is therefore

$$\frac{\delta \omega}{\omega} = -\frac{1}{2} \cdot \frac{3E_0^2 \Delta V}{\int_V E^2 dV}$$

### III. More General Electric Fields

It is possible to extend the calculation in II to electric fields having gradients. For azimuthally symmetric fields, this corresponds to writing the potential as

$$\phi = -E_0 z + E_0 R^3 \frac{\cos \theta}{r^2} - \frac{E_1}{2} r^2 P_2(\cos \theta) + \frac{E_1}{2} \frac{R^3}{r^5} P_2(\cos \theta)$$

and eventually leads to replacing  $3E_0^2$  by

$$3E_0^2 \rightarrow 3E_0^2 + \frac{3}{4} E_1^2 R^2$$

where

$$E_1 = \frac{\partial E_z}{\partial z}$$



In the vicinity of shaped metal surfaces, the gradient will be controlled by the distance from these surfaces. In particular, one expects

$$\frac{E_1}{E_0} \text{ to be of order } \frac{1}{g}$$

where  $g$  is the distance from the surface. This implies a correction to  $E_0^2$  in Slater's formula of order

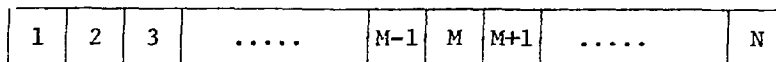
$$1 + \text{const} \frac{R^2}{g^2}$$

Similar corrections occur because of the dynamic nature of the field and are of order  $\frac{R^2}{\lambda^2}$  where  $\lambda$  is the wave length of the r.f. This term will be much smaller than the correction term  $R^2/g^2$  for cases where  $g$  corresponds roughly to a gap length at low  $\beta$ .

#### IV. FIELD TILTS

In a multicell cavity, a perturbation in a single cell causes a tilt in the electric field which may be quite large if the cavity contains many cells. It is now important to take this tilt into account to determine the local field which must be used in Slater's formula.\*

Consider the cavity to be made up of  $n$  cells, equivalent to the circuit chain shown.



The simplest form of analysis leads to the equation linking nearest neighbor cells:

---

\* This point was discussed by Owen et al., Proc. 1966 Linac Conference, p. 146.

$$\left( \frac{\omega_n^2}{\omega^2} - 1 \right) E_n = \frac{k}{2} (E_{n+1} + E_{n-1} - 2E_n) ,$$

where  $k$  is an equivalent coupling constant. The simplest version of the boundary conditions is  $E_0 = E_1$ ,  $E_N = E_{N+1}$ .

If all cells resonate at  $\omega_n = \omega_0$ , then the cavity will resonate in a flat mode. If the  $M$ th cavity has a perturbed frequency

$$\omega_M = \omega_0 (1 + \varepsilon) ,$$

the entire cavity will resonate at

$$\omega = \omega_0 (1 + \varepsilon/N)$$

and the circuit chain equation will be

$$\delta^2 E_n = \frac{-4\varepsilon}{kN} E_n \quad n = 1, \dots, M-1, M+1, \dots, N$$

and

$$\delta^2 E_M = \frac{4\varepsilon}{kN} (N-1) E_M ,$$

which has a solution

$$E_n = E_M \left[ 1 + \frac{2}{kN} \left( (M - \frac{1}{2})^2 - (n - \frac{1}{2})^2 \right) \right] \quad n = 1, \dots, M$$

$$E_n = E_M \left[ 1 + \frac{2\varepsilon}{kN} \left( (N + \frac{1}{2} - M)^2 - (N + \frac{1}{2} - n)^2 \right) \right] \quad n = M, \dots, N$$

For a relative frequency perturbation  $\varepsilon$  in the  $M$ th cell, the fields are therefore increased (relative to  $E_M$ ) in all the other cells. The denominator in the Slater formula therefore must be corrected by the sum

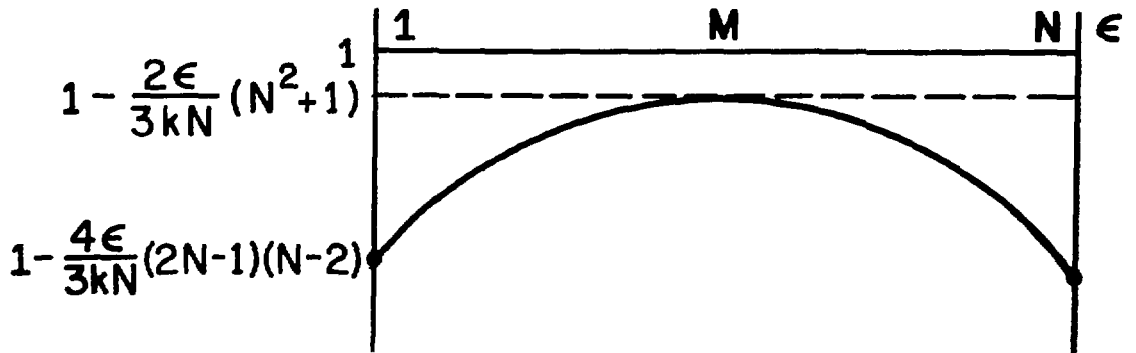
$$\begin{aligned}
& \sum_{n=1}^{M-1} \left[ 1 + \frac{2\epsilon}{kN} \left[ (M - \frac{1}{2})^2 - (n - \frac{1}{2})^2 \right] \right]^2 \\
& + 1 + \sum_{n=M+1}^N \left[ 1 + \frac{2\epsilon}{kN} \left[ (N + \frac{1}{2} - M)^2 - (M + \frac{1}{2} - n)^2 \right] \right]^2 \\
& = N \left[ 1 + \frac{2}{3} \frac{\epsilon}{kN} (N^2 + 1 + 3(N + 1 - 2M)^2) \right]
\end{aligned}$$

#### V. FINAL RESULT

The frequency shift due to a fractional field change in the Mth cell is therefore

$$\frac{\delta\omega}{\omega} \cong \frac{\epsilon}{N} \left[ 1 - \frac{2\epsilon}{kN} \left( \frac{N^2+1}{3} + (N+1-2M)^2 \right) \right]$$

The correction factor is plotted below.



If we now include the correction due to field gradients, the final result for the frequency change of the cavity is

$$\frac{\delta\omega}{\omega} \cong \frac{\epsilon}{N} \left( 1 + \text{const} \frac{R^2}{g^2} - \frac{\epsilon}{k} f(N,M) \right)$$

where

$$f(N,M) = \frac{2}{N} \left( \frac{N^2 + 1}{3} + (N + 1 - 2M)^2 \right)$$

The radius of the sphere may be related to  $\epsilon$  by approximating the integral of the square of the electric field over the cell volume as that over the gap region. In this case

$$\epsilon = \text{const} \frac{R^3}{d^2 g}$$

leading to

$$\frac{R^2}{g^2} = \text{const} \epsilon^{2/3} \left( \frac{d}{g} \right)^{4/3}$$

The frequency change expressed as a function of  $\epsilon$  is

$$\frac{\delta\omega}{\omega} \cong \frac{\epsilon}{N} \left( 1 + \text{const} \epsilon^{2/3} \left( \frac{d}{g} \right)^{4/3} - \frac{\epsilon}{k} f(N,M) \right)$$

In view of the fact that neither the constant nor  $k$  are known well, one must use an extrapolation procedure to separate the two terms, if both are important for the range of parameters used. In particular, at each location in each cell, one needs 3 bead sizes to determine  $\epsilon$  and the two constants, and a 4th bead size to check the extrapolation method. The starting point for analysis of such measurements should be a plot of

$$\frac{\delta\omega}{\omega} / R^3 \quad \text{vs} \quad R^3$$

$$\text{or} \quad \frac{\delta\omega}{\omega} / R^3 \quad \text{vs} \quad R^2 \quad .$$

COMMENTS ABOUT  $r, \dot{r}$  PHASE SPACE

Because of the fact that the transit time factor increases with  $r$ , at the threshold for particle capture, only those particles with large transverse amplitude will be accelerated. This note is an effort to predict what the appearance will be in the  $r, \dot{r}$  phase space.

Starting with the transit time factor

$$I_o \left( \frac{2\pi}{\beta\lambda} r \right) \cong 1 + \frac{\pi^2}{\beta^2 \lambda^2} (x^2 + y^2)$$

it is clear that longitudinal capture will depend on

$$\langle x^2 \rangle + \langle y^2 \rangle = \frac{x_{\max}^2 + y_{\max}^2}{2} \equiv \frac{R^2}{2}$$

Let us treat a collection of particles satisfying

$$x_{\max}^2 + y_{\max}^2 = R^2$$

$$\begin{aligned} x &= a \sin \omega t & y &= b \sin(\omega t + \phi) \\ \dot{x} &= a\omega \cos \omega t & \dot{y} &= b\omega \cos(\omega t + \phi) \end{aligned}$$

$$\begin{aligned}
 r^2 &= a^2 \sin^2 \omega t + b^2 \sin^2(\omega t + \phi) \\
 &= \frac{a^2 + b^2}{2} - \left[ \frac{a^2}{2} \cos 2\omega t + \frac{b^2}{2} \cos(2\omega t + 2\phi) \right]
 \end{aligned}$$

$$r^2 = \frac{a^2 + b^2}{2} - \frac{c^2}{2} \cos(2\omega t + 2\psi)$$

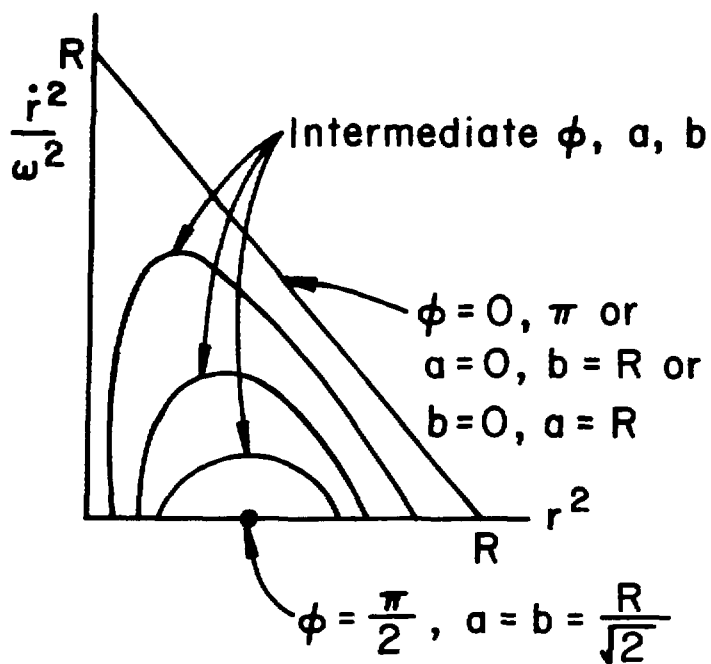
$$\begin{aligned}
 \frac{r\dot{r}}{\omega} &= a^2 \sin \omega t \cos \omega t + b^2 \sin(\omega t + \phi) \cos(\omega t + \phi) \\
 &= \frac{a^2}{2} \sin 2\omega t + \frac{b^2}{2} \sin(2\omega t + 2\phi)
 \end{aligned}$$

$$\frac{r\dot{r}}{\omega} = \frac{c^2}{2} \sin(2\omega t + 2\psi)$$

$$\begin{aligned}
 \frac{c^2}{2} &= \sqrt{\frac{a^4}{4} + \frac{b^4}{4} + \frac{a^2 b^2}{2} \cos 2\phi} && \leq \frac{a^2 + b^2}{2} \\
 &&& \geq \left| \frac{a^2 - b^2}{2} \right|
 \end{aligned}$$

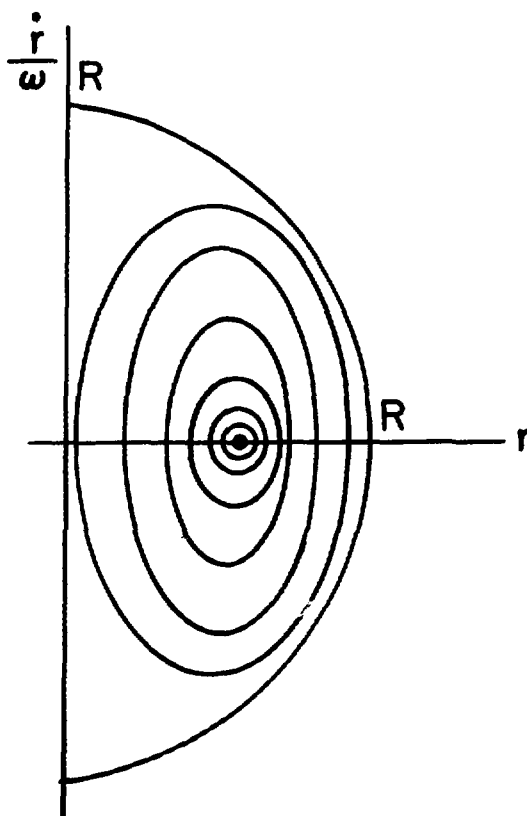
$$\left( r^2 - \frac{a^2 + b^2}{2} \right)^2 + \frac{r^2 \dot{r}^2}{\omega^2} = \frac{a^4}{4} + \frac{b^4}{4} + \frac{a^2 b^2}{2} \cos 2\phi$$

$$\frac{r^2 \dot{r}^2}{\omega^2} = r^2(a^2 + b^2) - r^4 - \frac{a^2 b^2}{2} (1 - \cos 2\phi)$$



Since all values of  $a$  and  $b$  for which  $a^2 + b^2 = R^2$  are acceptable, and as long as all values of  $\phi$  are permissible, the  $r, \dot{r}$  phase space will be totally populated.

The corresponding  $\theta, \dot{\theta}$  projection is  $[r^2 \dot{\theta}, \theta]$  since the variable canonically conjugate to  $\theta$  is  $p_\theta = r^2 \dot{\theta}$ .



DEPENDENCE OF TANK GRADIENT ON  
INCOMING BEAM ENERGY AND TANK TILT

## I Introduction

The dependence of the tank gradient on the incoming beam energy and tank tilt turns out to be a sensitive method for exploring the dynamic consequences of gap to gap field fluctuations in the first tank. This note is a crude derivation of the connection between the parameters, and serves as a means of understanding the relevant mechanisms.

In general we will assume that particles which traverse the entire first tank are captured in the longitudinal bucket. This is not completely true, since the criterion used to signify traversal is the transverse confinement. Nevertheless it is a reasonable first approximation.

In all measurements and computations to date, the tank field is tilted so that the lowest gradients are at injection. For this reason, the injection parameters are likely to govern capture. It appears that there are two more or less independent phenomena which govern.

## II Calculation of Model

### 1. Tank gradient above the threshold gradient

a) In this region, a phase stable region will exist at injection. The lowest energy particles which can be captured are those at the bottom of the fish. It can readily be shown from the energy invariant (approximate)

$$\frac{\beta^3}{2} \left( \frac{d\phi}{dz} \right)^2 + \frac{2\pi eET}{Mc^2 \lambda} \left( \frac{\phi \phi_s^2}{2} - \frac{\phi^3}{6} \right) = \text{const.}$$

that



$$W_{\min} - W_s \approx -\sqrt{\frac{2}{3\pi} mc^2 e E \lambda \beta^3} |\phi_s|^{3/2}$$

$$\approx -\sqrt{\frac{4}{3\pi} W_s \frac{\Delta W_s}{\Delta n}} |\phi_s|^{3/2}$$

Since  $\cos \phi_s \approx 1 - \frac{\phi_s^2}{2} = \frac{E_t}{E}$ , with E being the gradient at the injection end of the tank, we can write near threshold

$$\phi_s \approx \sqrt{2(x-1)} \quad \text{where } x = \frac{E}{E_t}$$

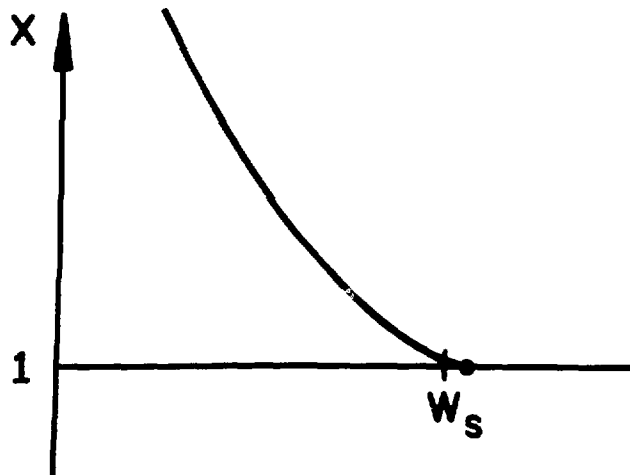
giving

$$W_{\min} = W_s - \frac{2^{7/4}}{\sqrt{3\pi}} \sqrt{W_s \frac{\Delta W_s}{\Delta n}} (x-1)^{3/4}$$

or

$$x = 1 + \frac{(W_s - W_{\min})^{4/3}}{W_s^{2/3} \left(\frac{\Delta W_s}{\Delta n}\right)^{2/3}} \frac{(3\pi)^{2/3}}{2^{7/3}}$$

For  $W_s = 750$  Kev,  $W_{\min} = 720$  Kev,  $\Delta W_s / \Delta n = 63$  Kev one finds  $x = 1.063$ , which is reasonably close to the measured values (1.03 to 1.055).



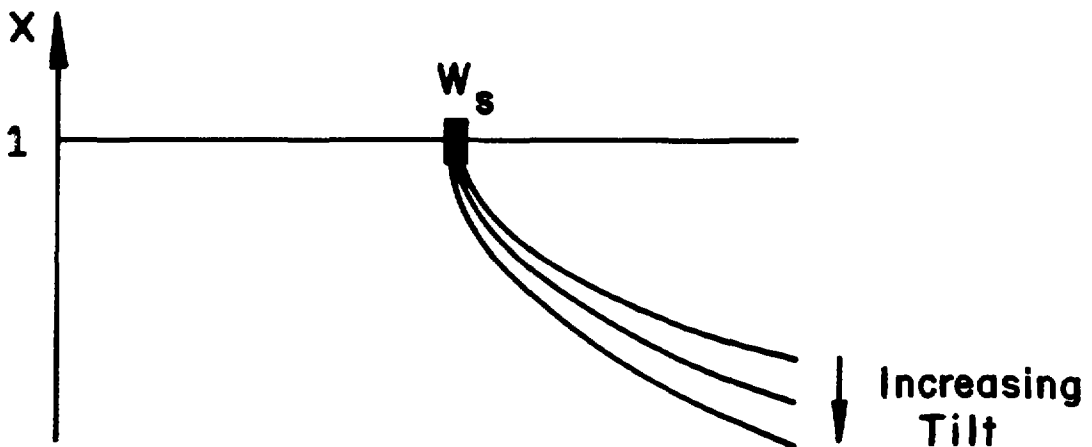
b) Dependence on tilt. If the gradient increases along the tank, the size of the phase stable region will grow and particles which at first appear to be longitudinally unstable will be captured. Thus the curve above will be shifted both to the left and downward since particles with lower energy can be captured, and capture can take place with lower initial gradient. The analytic treatment of these effects is more complicated, and not worth pursuing here.

## 2. Tank gradient below the threshold gradient

If there is a positive tilt, it is even possible to capture particles without an initial phase stable region. A crude estimate of the injection energy at which this takes place can be made by assuming that particles travel at the crest ( $\phi=0$ ) until the bucket is established, at which time they will be captured if they have the correct synchronous energy corresponding to that longitudinal position. This can be estimated to be

$$W_{\min} - W_s \cong \left( \frac{\Delta W_s}{\frac{\Delta n}{2q}} \right) (1 - x)^2$$

where  $q$  is the fractional increase in field level in the first cell. The result is shown below.



The apparent kink in the experimental data appears to be a result of the composite of the two figures.

### III Conclusion

It is important to normalize the gradients to the injection end of the tank in comparing the result for different tilts.

The general features of the dependence of  $X$  on  $W_{\min}$  are reproduced by the model. We have not included careful calculations of the effect of increasing bucket size. Moreover, in the actual tank, the field levels in the first few cells fluctuate significantly, and so one might expect some departure from the numerical calculations.

FIELD DISTRIBUTION AT LOW  $\beta$

- A. For the purpose of analysis, consider a uniform structure which will receive perturbations. One version of the field equation is

$$\frac{1}{E_z} \frac{d^2 E_z(z)}{dz^2} = \frac{8\pi^2}{\lambda^2} \frac{\delta\omega(z)}{\omega} \quad (1)$$

where  $\frac{\delta\omega(z)}{\omega}$  is the local frequency error. The circuit model has the form

$$(1 - k - \frac{\omega_n^2}{\omega^2})V_n = -\frac{k}{2} \delta^2 V_n = -\frac{k}{2} (V_{n+1} + V_{n-1} - 2V_n) \quad (2)$$

If we use the field calculation of Chasman and Gluckstern, Equation (2) can be used to interpret the result in terms of variations of cell frequency.

Note 1. There is some ambiguity as to whether  $V_n$  in (2) is the gap voltage or some normalized voltage based on energy storage (like  $E_n \sqrt{g_n} = V_n / \sqrt{g_n}$ ).

Note 2. The circuit analysis assumes that only one band is important. For this reason it should require modification if the structure is compensated.

- B. Now let us perturb one cell by changing one gap only. In reality we affect not only  $\omega_n$ , but also the coupling to the adjacent cells. However, we shall try to treat  $k$  as constant in using (2). For a more correct treatment, Jule's thesis will have to be followed.

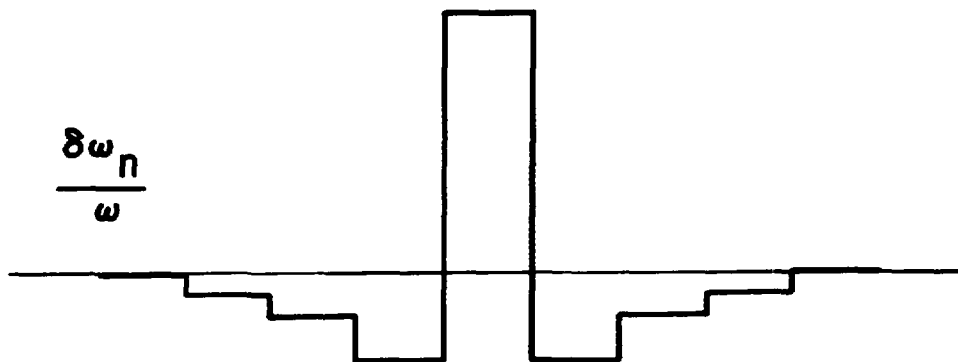
$$\text{Setting } \omega_n^2 = \omega^2(z) (1 - k)$$

$$\text{and } K = \frac{k}{1 - k}$$

Equation (2) becomes

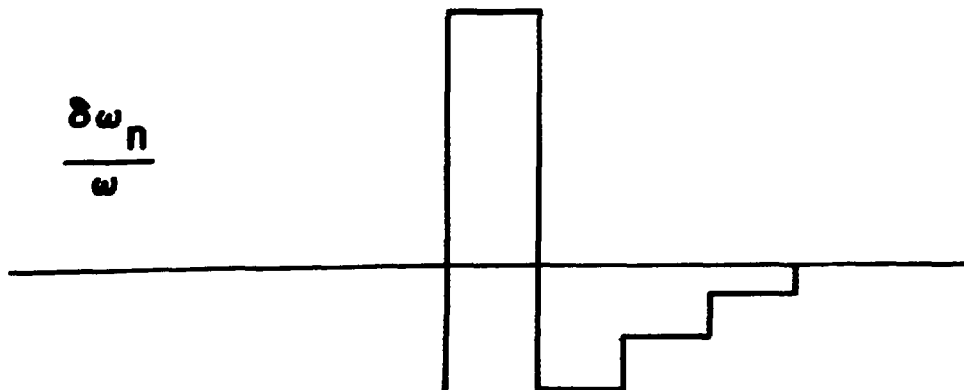
$$\delta^2 V_n \cong \frac{4}{K} V_n \frac{\delta \omega_n}{\omega} \quad (3)$$

where  $\delta \omega_n = \omega_n - \omega$ . Equation (3) can now be used to specify  $\delta \omega_n / \omega$  for a single perturbation. For low  $\beta$  this produces a pattern of  $\delta \omega_n / \omega$  like that shown below

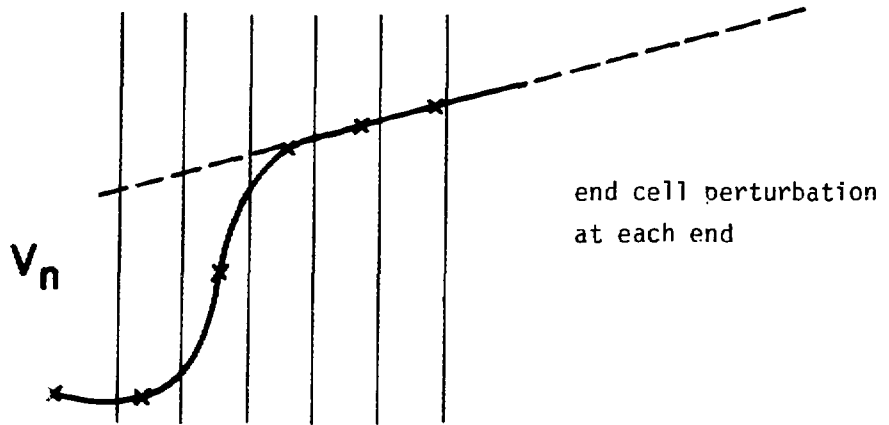


obtained by taking  $\delta^2 V_n$  and subtracting from  $\delta \omega_n / \omega$  the calculated frequency change of the overall cavity.

- C. Perturbation of the end cells requires an analysis involving the symmetry at the ends. For the  $\delta \omega_n / \omega$  shown above one needs to add the same function translated by one cell, obtaining

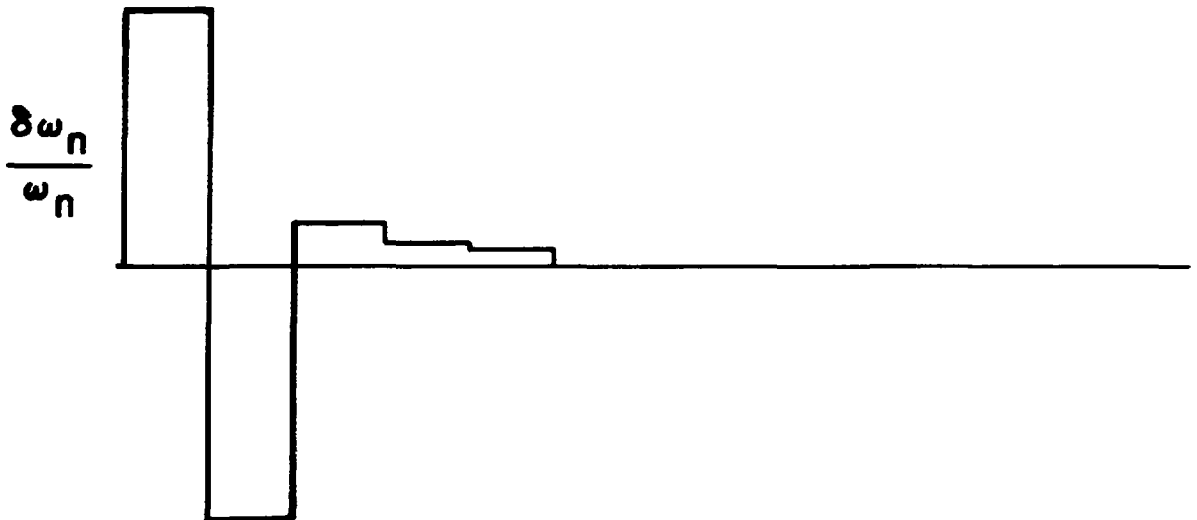


which leads to  $V_n$  of the form

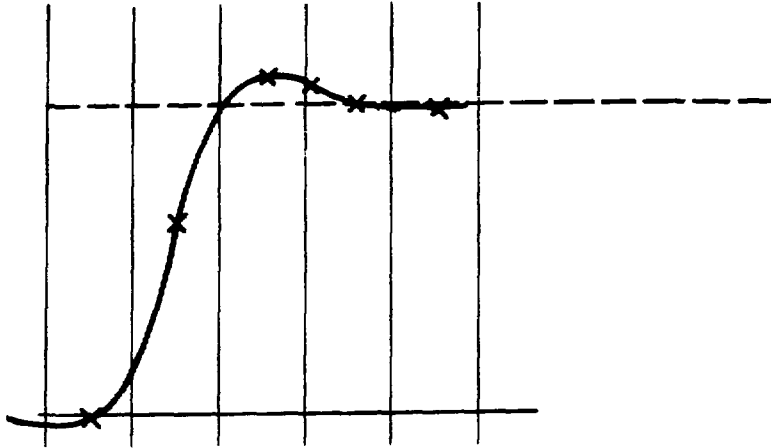


showing the deviation from the simple tilt. This effect is clearly seen in the bead pulling on Tank #1.

- D. Displacement of the first full drift tube also leads to an interesting effect. It can be obtained from the first pattern on page 2



and leads to a  $V_n$  of the form



showing the overshoot which is also observed on Tank #1. This can be corrected by moving the first and/or second drift tube suitably.

E. These calculations should be done using some sample field calculations and frequency calculations. The expectations are

- 1) That the effect of a single perturbation seems to extend over 4 or 5 cells with  $\beta = .07$ , corresponding to a distance of  $.3\lambda$  to  $.4\lambda$ . For larger  $\beta$  these effects should extend over fewer cells.
- 2) A value of  $K$  can be obtained from the calculations, which can even be performed using a structure with varying cell length corresponding to the first 5 to 7 real cells. It should then be a simple matter to correct any observed fluctuations in the field in the first few cells.
- 3) Some study will have to be made of the measured and computed results to settle the question of whether to use  $E_n$ ,  $E_n \sqrt{g_n}$ , or  $E_n g_n = V_n$  in Equation (3).
- 4) The effect on the dynamics requires also taking into account  $F_n$ . A run of PARMILA with actual voltages should be made to check that everything is OK.

BEAM COASTING THROUGH RESONANT TANKS

This note expands on a memo by D. C. Hagerman and M. Jakobson, "Energy Loss by a Proton Beam Passing Through Accelerator Cavities Without External RF Excitation," LASL Tech. Memo P-11-DCH/MJ-2, 2-19-64. In this memo, the induced voltage is apparently correctly calculated, but the phase of this voltage relative to the driving current is not taken into account. My feeling is that these are about 90° out of phase since the beam is trying to resonate the cells out of phase with one another and they won't do it. As a result the cavity acts like it is off frequency and is therefore reactive, as well as having a smaller impedance.

For example, using an equivalent circuit model operated in a zero mode:

$$-i_b^{(n)} + V^{(n)} \left( \frac{1}{i\omega L} + i\omega C + \frac{1}{R} \right) + \frac{V^{(n+1)} + V^{(n-1)}}{2} k i\omega C = 0$$

(No driving current,  $i_b^{(n)}$  is beam current,  $k$  is coupling). If there is a mismatch of beam bunch space and cell length,  $i_b^{(n)}$  will have a dependence  $Ie^{in\delta}$  where  $\delta$  is the cell-to-cell phase difference.

Zero mode resonance gives

$$\frac{i}{i\omega L} + i\omega C = -k i\omega C$$

Writing  $V^{(n)} \sim Ve^{in\delta}$ , we find

$$-Ie^{in\delta} + Ve^{in\delta} \left( \frac{1}{i\omega L} + i\omega C + \frac{1}{R} \right) + Ve^{in\delta} \underbrace{\cos \delta}_{-k i\omega C} k i\omega C = 0$$

$$-I + \frac{V}{R} - k i\omega C \underbrace{(i - \cos \delta)}_{\frac{\delta^2}{2}} V = 0$$

$$V = \frac{+IR}{1 - ik \frac{Q\delta^2}{2}}, \quad \text{where } Q = \omega CR$$



and

$$P = \text{Re} (VI^*) = \frac{(I)^2 R}{1 + \left(\frac{kQ\delta^2}{2}\right)^2}$$

$$\text{For } \frac{\delta\beta}{\beta} \sim .01 \quad \delta \sim .06 \quad Q = 15,000, \quad k \sim 1$$

$$k\frac{Q\delta^2}{2} = 27; \quad 1 + \left(k\frac{Q\delta^2}{2}\right)^2 \sim 730$$

$$\text{For } I = 20 \text{ mA}, \quad R = 30 \text{ M}\Omega/\text{m}, \quad P = \frac{12 \text{ KW/meter}}{730} \sim 16 \frac{\text{W}}{\text{m}}, \text{ very small}$$

This is an extremely crude calculation.

I looked at improvements of the following kind:

(1) Need the 1st Fourier component of the beam distribution (makes result smaller).

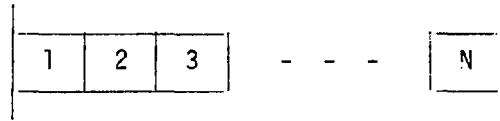
(2) Need to satisfy  $V = 0$  for  $n = 0, n = N$ . This puts a boundary condition which modifies the  $e^{in\delta}$  solution - need Green's Function to do it properly - but it does not change the result that the voltage is out of phase with the current by an amount like

$$\frac{\pi}{2} - \frac{2}{kQ\delta^2}$$

(3) Stepped or tapered phase. This introduces variations like  $e^{in^2}$  which makes the analysis even more complicated. However, the phase change is still  $\sim \pi/2$  as long as  $\delta \neq 0$ .

Conclusions:

1. Power loss much reduced over calculation in the referenced memo.
2. Might be observable for small  $\delta\beta$ , by looking for the voltage induced in a cavity (not the energy loss of the beam).
3. Not sensitive to tuning, except if  $\delta = 0$ .

EFFECT OF FREQUENCY ERRORS ON TANK FLATTENING

The basic theory is from coupled oscillator chain:

$$\left(1 - \frac{\omega_n^2}{\omega^2}\right) i_n = \frac{k}{2} (i_{n+1} + i_{n-1} - 2i_n) \quad n=1, 2, \dots, N$$

Boundary condition  $i_0 = i_1$   
 $i_{N+1} = i_N$

If all  $\omega_n = \omega_0$ , then  $\omega = \omega_0$

$$\text{and } \delta^2 i_n = 0$$

so that solution is  $i_n = I$  (constant)

If there is a frequency error, where  $\omega = \omega_0$ :

$$\omega_1 = \omega_0(1 - \epsilon) \quad 1 - \frac{\omega_1^2}{\omega^2} \cong +2\epsilon$$

$$\omega_N = \omega_0(1 + \epsilon) \quad 1 - \frac{\omega_N^2}{\omega^2} \cong -2\epsilon$$

$$+ 2\epsilon i_1 = \frac{k}{2} (i_0 + i_2 - 2i_1) = \frac{k}{2} (i_2 - i_1)$$

$$0 = i_3 + i_1 - 2i_2 \quad \text{etc.}$$

$$-2\epsilon i_N = \frac{k}{2} (i_{N+1} + i_{N-1} - 2i_N) \cong \frac{k}{2} (i_{N-1} - i_N)$$

The central region of the tank is satisfied by having

$$i_n = I + Jn \quad (NJ \ll I)$$

$$+ 2\varepsilon(I + J) = \frac{k}{2}(I + 2J - I - J) = \frac{k}{2}J$$

$$- 2\varepsilon(I + NJ) = \frac{k}{2}(I + J(N-1) - I - JN) = \frac{-k}{2}J$$

giving

$$J \approx + \frac{4I\varepsilon}{k}$$

$$T = \text{Tilt} \approx \frac{NJ}{I} \approx \frac{4\varepsilon}{k} N$$

Suppose  $\omega_1 = \omega_0(1 - \varepsilon_1)$

$$\omega_N = \omega_0(1 + \varepsilon_2)$$

$$\varepsilon_1 \neq \varepsilon_2$$

Then the frequency is no longer correct at  $\omega = \omega_0$ .

In fact, write  $1 - \frac{\omega_0^2}{\omega^2} = 2\varepsilon$

In the central region,

$$2\varepsilon i_n = \frac{k}{2}(i_n + i_{n-1} - 2i_n)$$

$$i_n = I + Jn + \underbrace{\frac{Kn^2}{2} - \frac{KnN}{2}}_{-\frac{K}{2}n(N-n)}$$

$$\underline{\underline{\delta^2 i_n = K = \frac{4\varepsilon I}{k}}}$$

$$1 - \frac{\omega_1^2}{\omega^2} = 1 - \frac{\omega_1^2}{\omega_0^2} \cdot \frac{\omega_0^2}{\omega^2} = 1 - (1 - 2\varepsilon_1)(1 - 2\varepsilon) \approx 2\varepsilon_1 + 2\varepsilon .$$

$$1 - \frac{\omega_N^2}{\omega^2} = -2\varepsilon_2 + 2\varepsilon .$$

For  $n = 1$ ,

$$(2\varepsilon_1 + 2\varepsilon)I = \frac{k}{2} \left( J - \frac{KN}{2} - \underbrace{\frac{K}{2}(4-1)}_{\frac{3K}{2} \leftarrow \text{neglect compared to } \frac{NK}{2}} \right)$$

$$2\varepsilon I = \frac{k}{2} K$$

$$(-2\varepsilon_2 + 2\varepsilon)I = \frac{k}{2} \left( -J + \frac{KN}{2} + \frac{K}{2} \underbrace{((N-1)^2 - N^2)}_{-2N+1} \right)$$

$$-J - \frac{KN}{2} + \frac{K}{2} \leftarrow \text{neglect compared to } \frac{NK}{2}$$

$$(2\varepsilon_1 + 2\varepsilon)I = \frac{k}{2} \left( J - \frac{KN}{2} \right)$$

$$(-2\varepsilon_2 + 2\varepsilon)I = \frac{k}{2} \left( -J - \frac{KN}{2} \right)$$

$$2\varepsilon I = \frac{k}{2} K$$

$$\boxed{2(\varepsilon_1 + \varepsilon_2)I = kJ}$$

$$\boxed{(2\varepsilon_1 - 2\varepsilon_2)I = -\frac{kKN}{2}}$$

$$\boxed{\varepsilon = \frac{\varepsilon_2 - \varepsilon_1}{N}}$$

This is what is expected for  $\varepsilon_1 \neq \varepsilon_2$

$$\boxed{\begin{aligned} \frac{J}{I} &= \frac{2(\varepsilon_1 + \varepsilon_2)}{k} & \varepsilon &= \frac{\varepsilon_2 - \varepsilon_1}{N} \\ \frac{KN}{I} &= -\frac{4(\varepsilon_2 - \varepsilon_1)}{k} \end{aligned}}$$

This gives the tilt and "bowing"  
of the tank fields

$$T = \frac{JN}{I} = \frac{2N(\epsilon_1 + \epsilon_2)}{k}$$

$$(B = \text{maximum bowing at } n = \frac{N}{2})$$
$$= - \frac{KN^2}{8I}$$

$$B = - \frac{N(\epsilon_2 - \epsilon_1)}{2} = - \frac{N^2\epsilon}{2}$$

The importance of B in normalization or calibration must be considered carefully. It will be important when  $\epsilon_1$  and  $\epsilon_2$  do not cancel exactly, even if tuners are used to correct the frequency, since the tuners will not duplicate the behavior of  $\epsilon_1$  and  $\epsilon_2$ .

The low power (bead pull) and high power situations can be compared by estimating "oil-can" effects via  $\epsilon_1$ ,  $\epsilon_2$ , keeping the frequency shift  $\epsilon$  in mind, etc.

DISTRIBUTED EFFECT OF LOCALIZED FREQUENCY ERRORS

The simple chain of oscillators with only nearest neighbor coupling is represented by the equation

$$\left(1 - \frac{\omega_n^2}{\omega^2}\right) i_n = \frac{k}{2} (i_{n+1} + i_{n-1} - 2i_n) \equiv \frac{k}{2} \delta^2 i_n$$

From previous analysis of Maxwell's Equations one can show that couplings also extend to next nearest neighbor cells ( $n \pm 2$ ) and beyond ( $n \pm 3$ ,  $n \pm 4$ , etc). In fact, these couplings will extend in a significant way for about 1 wave length on each side (many cells for low  $\beta$ , few cells for high  $\beta$ ).

The above equation is then extended to

$$\left(1 - \frac{\omega_n^2}{\omega^2}\right) i_n \cong -\frac{2\delta\omega_n}{\omega} i_n = \frac{k_1}{2} \delta^2 i_n + \frac{k_2}{2} \delta^4 i_n + \frac{k_3}{2} \delta^6 i_n + \dots$$

On the assumption of decreasing importance of  $k_j$  as  $\theta_j$  increases, one can solve this equation by iteration or expansion

$$\frac{k_1}{2} \delta^2 i_n + \frac{k_2}{2} \delta^4 i_n + \dots = \mu_n \equiv -\frac{2\delta\omega_n}{\omega} i_n$$

$$\delta^2 i_n = A\mu_n + B\delta^2\mu_n + C\delta^4\mu_n + \dots$$

$$\frac{k_1}{2} (A\mu_n + B\delta^2\mu_n + C\delta^4\mu_n) + \frac{k_2}{2} (A\delta^2\mu_n + B\delta^4\mu_n) + \frac{k_3}{2} (A\delta^4\mu_n) + \dots = \mu_n$$

$$\frac{k_1 A}{2} = 1 \qquad \frac{k_1 B}{2} + \frac{k_2 A}{2} = 0 \qquad \frac{k_1 C}{2} + \frac{k_2 B}{2} + \frac{k_3 A}{2} = 0$$

$$A = \frac{2}{k_1} \qquad B = -\frac{k_2 A}{k_1} \qquad C = -\frac{k_3 A}{k_1} + \frac{k_2^2 A}{k_1^2} \quad \text{etc.}$$

So

$$\frac{1}{i_n} \delta^2 i_n = \frac{2}{k_1} \left( -\frac{2\delta\omega_n}{\omega} \right) - \frac{2k_2}{k_1^2} \left( -2\delta^2 \left( \frac{\delta\omega_n}{\omega} \right) \right) \left( \frac{2k_3}{k_1^2} - \frac{2k_2^2}{k_1^3} \right) \left( -2\delta^4 \left( \frac{\delta\omega_n}{\omega} \right) \right) + \dots$$

This implies that the simple version (which requires  $\delta^2 i_n \neq 0$  only at the frequency perturbation) should be extended to adjacent cells in line with the above equation.

Let us solve this equation in steps.

Step 1 - leading term only. This is the conventional solution leading to discontinuities in slope where perturbations occur, and to curvature where the frequency is shifted

$$\langle \frac{i_n}{i_n} \rangle = 1 + S_n$$

$S_0 = S,$ $S_{NH} = S_N$ $\delta^2 S_N = -\frac{4}{k} \frac{\delta\omega_n}{\omega}$
---

Step 2 - Now add other terms following two "integrations"

$$\langle \frac{i_n}{i_n} \rangle = 1 + S_n + p_n.$$

$$p_n = \underbrace{\frac{4k_2}{k_1^2} \left( \frac{\delta\omega_n}{\omega} \right)}_{\text{isolated in cell } n} + 4 \underbrace{\left( \frac{k_3}{k_1^2} - \frac{k_2^2}{k_1^3} \right) \delta^2 \left( \frac{\delta\omega}{\omega} \right)_n}_{\text{extends to cells } n \pm 1} + \underbrace{\dots}_{\text{extends to cells } n \pm 2, \text{ etc.}}$$

Eventually a wall is reached modifying the tilt, bowing predictions. This will be important if frequency perturbations occur within a wave length of a wall, which is quite often. In fact, it is this phenomenon which accounts for the fluctuations in  $i_n$  in the first few cells, when an end cell perturbation is included.

In order to confine the influence of the  $p_n$  term to the location of the perturbation, it is possible to "soften" the frequency perturbation by spreading it to adjacent cells. For example, instead of an end-cell perturbation alone, one might consider moving the 2nd drift tube by 1/2 of the displacement of the end cell, the 3rd drift by 1/4, the 4th by 1/8, etc. In the absence of information about  $k_2, k_3$  ---, one will have to try different configurations experimentally. This should allow one to minimize the large field fluctuations near a frequency perturbation.



EFFECT OF MULTIPOLE ABERRATIONS

I. INTRODUCTION

Multipole aberrations result in coupling between the oscillations in the two transverse directions. The basic formalism was written in detail in MP-DO/2 (R. L. Gluckstern, R. R. Stevens, Jr., and P. W. Allison, MP-DO/2, 1967) and can be taken over directly.

Aberrations will generally be present for all multipole orders, but it is generally expected that they will be random for all orders except  $m = 2$  (main quadrupole term),  $m = 6$ ,  $m = 10$ , ....., where the errors can be expected to be systematic.

II. ANALYSIS

The general analysis starts with the assumption of a single multipole aberration which modifies the scalar magnetic potential as follows:

$$\text{Potential} = K \left\{ \frac{r^2}{2} \sin 2\theta + Jr^m \cos (m\theta + \phi) \right\}$$

Clearly,  $H = m J \frac{R_{\text{BORE}}^{m-2}}{R_{\text{BORE}}}$  is the pole tip field due to the aberration in units of the main quadrupole pole tip field, where  $R_{\text{BORE}}$  is the bore radius.

From (51) and (52) (in MP/DO/2, 1967), one can write:

$$\frac{\delta W_x + \delta W_y}{2\beta\gamma\delta s} = K I_m \left[ J_m (P_x \cos \phi_x + iP_y \cos \phi_y) (P_x \sin \phi_x + iP_y \sin \phi_y)^{m-1} \right]$$

with

$$\phi_x = ks + \phi_x^0$$

$$\phi_y = ks + \phi_y^0$$

$$J_m = J e^{i\phi}$$

## A. Systematic Aberration

### 1. Resonance for $k_x = k_y = k$

If the only contributions come from  $k_x = k_y = k$ , then the contribution from a systematic aberration can easily be shown to cancel. Specifically, since the bracket can be written as

$$\frac{J_m}{k} \frac{d}{ds} (P_x \sin \phi_x + i P_y \sin \phi_y)^6$$

its average must necessarily be zero. In this case there is no beam growth, other than a small amount which may originate from particular starting phases.

### 2. Resonance of the form $\mu = 2\pi/m$

In view of the systematic nature of the aberration, if the change in  $m\phi_x$  from one magnet period to the next is close to  $2\pi$ , the sums over aberration impulses can accumulate. If we write

$$\mu = \frac{2\pi + \delta}{m}$$

and extract only the  $\cos m\phi_{x,y}$  and  $\sin m\phi_{x,y}$  terms from the change in  $W$ , one finds

$$\frac{\delta W}{2\beta\gamma} = \frac{mJK\ell}{2\frac{m}{2} - 1} \sum_{n=0}^{\infty} \left[ P_x^m \sin(m\phi_x^0 + n\delta) - \frac{m(m-1)}{(1)(2)} P_x^{m-2} P_y^2 \sin((m-2)\phi_x^0 + 2\phi_y^0 + n\delta) + \dots \right]$$

where we have taken into account the reversal of the sign of  $K$  and of  $\sin(\frac{m\mu}{2} + \phi)$  for the defocusing magnets, and where each magnet is of length  $\ell$ .

The maximum value of the preceding expression occurs for

$$P_x = P_y = \frac{R_{\text{BEAM}}}{\sqrt{2}}, \quad \phi_x^0 = 0, \quad \phi_y^0 = \pi/2 \quad \text{giving}$$

$$\frac{\delta W}{2\beta\gamma} = \frac{mJK\ell}{\delta} R_{\text{BEAM}}^m, \quad W = W_x + W_y \cong \frac{\beta\gamma}{\beta_{\text{SF}}} R_{\text{BEAM}}^2$$

$$\begin{aligned} \frac{\delta W}{2W} &= \frac{mJK\ell}{\delta} \beta_{\text{SF}} R_{\text{BEAM}}^{m-2} \\ &= \frac{\kappa\ell\beta_{\text{SF}}}{\delta} \left( \frac{R_{\text{BEAM}}}{R_{\text{BORE}}} \right)^{m-2} H \end{aligned}$$

For a (+ - + -) focusing system with  $\ell = \beta\lambda/2$ , one can estimate the beam growth in the smooth approximation to be

$$\frac{\delta R_{\text{BEAM}}}{R_{\text{BEAM}}} = \frac{\delta W}{2W} = \frac{\sqrt{3}}{\delta} \left( \frac{R_{\text{BEAM}}}{R_{\text{BORE}}} \right)^{m-2} H.$$

To illustrate the order of magnitude, for  $H = .05$ ,  $m = 6$ ,  $R_{\text{BEAM}} = \frac{2}{3} R_{\text{BORE}}$ ,  
 $\delta = .1 \cong 6^0$ ,

$$\frac{\delta R}{R} \sim \frac{1}{6},$$

that is, a 17% increase in beam radius if  $\mu$  stays within  $1^0$  (of  $60^0$ ) over approximately 100 magnets. In actual fact,  $\mu$  will probably not sit on  $m\mu = 2\pi$  or any other resonance with  $1^0$  accuracy for very long, so the result for  $\frac{\delta R}{R}$  will likely be much smaller.

## B. Random Aberrations

In this case

$$\frac{\delta W_{\text{rms}}}{2\beta\gamma} = Km\ell J_{\text{rms}} \sqrt{N} \left[ \text{Re} (P_x \cos\phi_x + iP_y \cos\phi_y)(P_x \sin\phi_x + iP_y \sin\phi_y)^{m-1} \right]_{\text{rms}}$$

It may be possible to evaluate the last rms bracket for general  $m$  by averaging over  $\phi_x$  and  $\phi_y$ , but it will probably be easier to just square and multiply the terms out and average over  $\phi_x$  and  $\phi_y$  explicitly. In any case, the form of the final result, using the same assumptions as before, will be

$$\frac{\Delta R}{R} \sim \text{const} \left( \frac{R_{\text{BEAM}}}{R_{\text{BORE}}} \right)^{m-2} H_{\text{rms}} \sqrt{N} .$$

EFFECT OF MAGNETIC MULTIPOLE

- A. The most likely pattern of multipoles for a quadrupole is a systematic series in the magnetic potential of the form

$$\begin{aligned} \phi = & \phi_2 r^2 \sin 2\theta + \phi_6 r^6 \sin 6\theta + \phi_{10} r^{10} \sin 10\theta \\ & + \phi_{14} r^{14} \sin 14\theta + \dots \end{aligned} \quad (1)$$

where the  $\phi_2$  term is the dominant quadrupole term. In addition, one might expect random terms of all orders in the form

$$\phi_{\text{random}} = \sum_{n=1}^{\infty} (p_n r^n \cos n\theta + q_n r^n \sin n\theta) \quad (2)$$

due to misalignments of individual pole tips and/or coils. It is possible however that some of the terms in (2) may be systematic due to special coil return configurations. These questions should be able to be settled from magnetic field distribution measurements.

- B. Systematic multipole effects by themselves will lead to a distortion of the transverse phase space but should not lead to the development of tails in the transverse phase space unless there are also present misalignments or errors in the steering or significant transverse - longitudinal coupling. The higher the order of the multipole, the more extended will be the tail.
- C. Random multipole effects can lead to the formation of tails even in the

absence of misalignments or steering errors. However the effect will be enhanced if there is coherent transverse motion also present.

D. In the calculations which have recently been performed, it is important to identify the primary terms which lead to the generation of tails. For this reason the calculation should be repeated with one multipole at a time, taking into account whether the multipole magnitude and phase is systematic or random from magnet to magnet.

E. Fringing fields in the quadrupole also lead to systematic multipole terms of order 4, 6, 8, - - - . It should be sufficient to use the results in Eq (8) and (9) of MP-D0/2(1967) (See also 1966 Linac Conf. p.250) which gives the net effect of a full quadrupole, taking into account the fringing field at both ends. The results should be comparable with those in Section B.

PERMANENT MAGNET CALCULATION

A. If magnet material satisfies the following equations

$$B_x = M_0 + H_x \quad (1)$$

$$B_y = H_y$$

inside the material and

$$B_x = H_x \quad (2)$$

(3)

$$B_y = H_y$$

outside, then, one has the equations

$$\vec{\nabla} \times \vec{H} = 0 \quad (4)$$

$$\vec{\nabla} \cdot \vec{B} = 0 \quad (5)$$

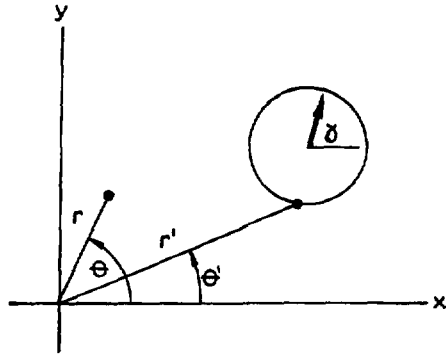
The second of these can be rewritten as

$$\vec{\nabla} \cdot \vec{H} = -\vec{\nabla} \cdot \vec{M}_0 = \vec{n} \cdot \vec{M}_0 \delta(\text{boundary}) \quad (6)$$

Equations (4) and (6) therefore correspond to a "magnetic" surface charge density whose strength is  $(\vec{n} \cdot \vec{M}_0)$ , where  $\vec{n}$  is the outward normal to the material. It is therefore easy to use scalar potential theory to solve for the fields due to regularly arranged sections of these permanent magnets.

We will treat the two-dimensional problem only at this time.

Note: This work was triggered by Ron Holsinger's verbal explanation of Klaus Halbach's invention, given to RLG on Dec. 21, 1978.



Setting  $\vec{H} = -\nabla\phi$ , one finds for the potential at  $r, \theta$  due to a "magnetic line charge" of strength  $\tau$  located at  $r', \theta'$

$$\begin{aligned}
 \phi(\vec{r}) &= -\frac{\tau}{4\pi} \ln(r'^2 - 2rr' \cos(\theta - \theta') + r^2) \\
 &= -\frac{2\tau}{4\pi} \operatorname{Re} \left\{ \ln(r' - r e^{i(\theta - \theta')}) \right\} \\
 &= -\frac{2\tau}{4\pi} \ln r' + \frac{2\tau}{4\pi} \operatorname{Re} \sum_{n=1}^{\infty} \frac{1}{n} \left( \frac{r e^{i\theta}}{r' e^{i\theta'}} \right)^n \\
 &= -\frac{\tau}{4\pi} \ln r'^2 + \frac{2\tau}{4\pi} \operatorname{Re} \sum_{n=1}^{\infty} \frac{1}{n} \frac{(x+iy)^n}{(x'+iy')^n} \tag{7}
 \end{aligned}$$

If we orient axes  $x'', y''$  along  $\vec{M}_0$

$$\begin{aligned}
 x'' &= x' \cos \gamma + y' \sin \gamma \\
 y'' &= -x' \sin \gamma + y' \cos \gamma \\
 x'' + iy'' &= e^{-i\gamma} (x' + iy') \\
 r'' &= r' \\
 \theta'' &= \theta' - \gamma \tag{8}
 \end{aligned}$$

We now can integrate around the magnetic periphery, replaced  $\tau$  by  $\vec{n} \cdot \vec{M}_0 = M_0 dy''$ , obtaining

$$\phi(r, \theta) = \frac{M_0}{4\pi} \int dy'' \left[ -\ln(x''^2 + y''^2) + 2 \operatorname{Re} \sum_{n=1}^{\infty} \frac{1}{n} \frac{r^n e^{in\theta}}{r''^n e^{in\theta'' + in\gamma}} \right]$$



$$= \frac{M_0}{4\pi} \int dy'' \left[ -2n(x'' + y'') + 2\text{Re} \sum_{n=1}^{\infty} \frac{e^{-iny} (x+iy)^n}{(x''+iy'')^n} \right]$$

But  $\int dy'' F(x'', y'')$  can be converted to an area integral by writing

$$\iint dx'' dy'' \frac{\partial F}{\partial x''}$$

Therefore

$$\begin{aligned} \phi(r, \theta) &= \frac{2M_0}{4\pi} \iint dx'' dy'' \left[ \frac{-x''}{x''^2 + y''^2} \text{Re} \sum_{n=1}^{\infty} \frac{e^{-iny} (x+iy)^n}{(x''+iy'')^{n+1}} \right] \\ &= -\frac{2M_0}{4\pi} \text{Re} \iint dx'' dy'' \left[ \sum_{n=0}^{\infty} \frac{e^{-in} (x+iy)^n}{(x''+iy'')^{n+1}} \right] \end{aligned}$$

We can now rotate the axes back to  $x', y'$ , obtaining

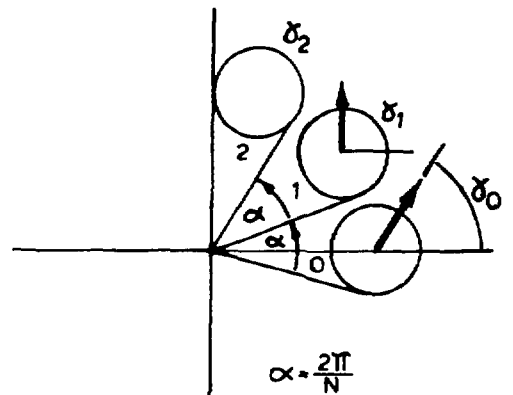
$$\begin{aligned} \phi(r, \theta) &= -\frac{2M_0}{4\pi} \text{Re} \iint dx' dy' \sum_{n=0}^{\infty} \frac{e^{iy} (x+iy)^n}{(x'+iy')^{n+1}} \\ &= -\frac{2M_0}{4\pi} \text{Re} \sum_{n=0}^{\infty} (x+iy)^n e^{iy} \iint \frac{dx' dy'}{(x'+iy')^{n+1}} \end{aligned} \quad (9)$$

This is the basic relationship from which the potential can be calculated for a set of magnet pieces regularly arranged in an azimuthal pattern.

B.  $N$  regularly arranged magnets:

Let us now calculate the potential from  $N$  such magnets arranged in a circular pattern as shown. Clearly, for the  $j$ th magnet

$$x'_j + iy'_j = (x'_0 + iy'_0) e^{ij\alpha}$$



The potential due to the magnets  $j = 0, 1, \dots, N - 1$  is therefore

$$\phi(r, \theta) = \frac{2M_0}{4\pi} \operatorname{Re} \sum_{n=0}^{\infty} (x + iy)^n I_0 \left[ e^{i\gamma_0} + e^{i(\gamma_1 - (n+1)\alpha)} + e^{i(\gamma_2 - (n+1)2\alpha)} + \dots \right] \quad (10)$$

where

$$I_0 = \iint_{\text{Oth magnet}} \frac{dx' dy'}{(x' + iy')^{n+1}}$$

Let  $\gamma_j = \gamma_0 + 3j\alpha$ . Then the bracket [ ] is

$$\left[ e^{i\gamma_0} \sum_{j=0}^{N-1} e^{i\alpha(2-n)j} \right], \text{ where } \alpha = \frac{2\pi}{N}$$

The sum will vanish unless  $n = 2 + \ell N$  where  $\ell = 0, 1, 2, \dots$ , in which case it becomes

$$N e^{i\gamma_0}$$

Therefore

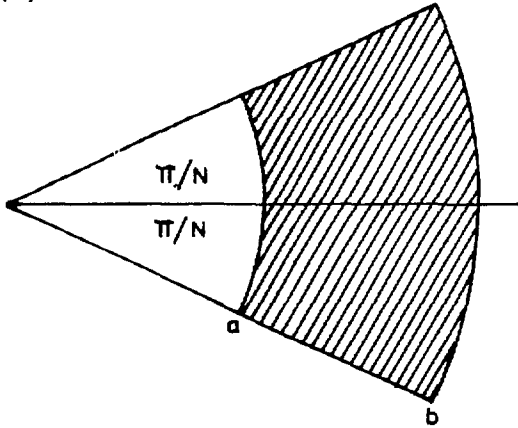
$$\phi(r, \theta) = \frac{2NM_0}{4\pi} \operatorname{Re} \sum_{\substack{n=2+N\ell \\ \ell=0,1,2}}^{\infty} (x+iy)^n I_0 e^{i\gamma_0} \quad (11)$$

For the lowest term ( $\ell=0, n=2$ ; next lowest is  $2+N=n$ ). The maximum pole tip field at  $r=a$  is

$$H_{r=a}^{\text{quad}} = \frac{4N}{4\pi} M_0 a |I_0| \quad (12)$$

C. Calculation of  $I_0$  for specific shapes:

(1) Sector



$$I_0 = \iint \frac{dx' dy'}{(x' + iy')^3}$$

$$\begin{aligned} \rho^2 &= x'^2 + y'^2 \\ \rho \sin \phi &= y' \\ \rho \cos \phi &= x' \end{aligned}$$

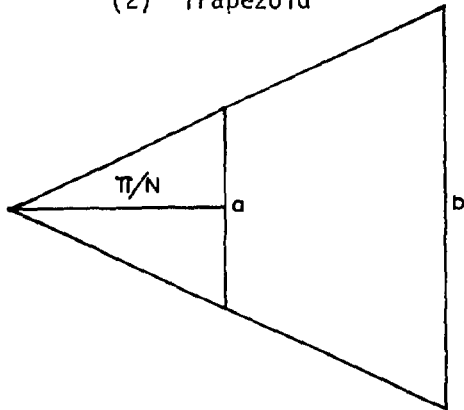
$$= \int_a^b \frac{\rho d\rho}{\rho^3} \int_{-\frac{\pi}{N}}^{\frac{\pi}{N}} d\phi e^{-3i\phi}$$

$$= \left( \frac{1}{a} - \frac{1}{b} \right) \frac{2\pi}{N} \frac{\sin \frac{3\pi}{N}}{\frac{3\pi}{N}}$$

$$\left. \begin{array}{l} \text{quad} \\ H \\ r=a \\ \text{max} \end{array} \right| = 2 M_0 \left( 1 - \frac{a}{b} \right) \frac{\sin \frac{3\pi}{N}}{\frac{3\pi}{N}}$$

(13)

(2) Trapezoid

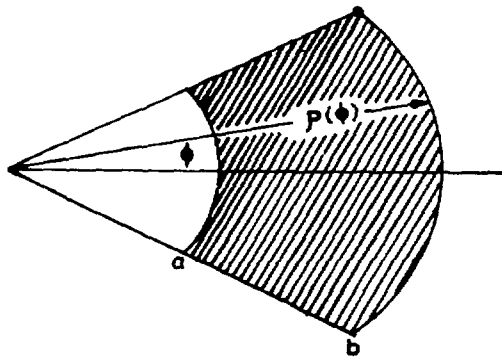


$$\iint \frac{dx' dy'}{(x' + iy')^3} = \frac{i}{2} \int \frac{dx'}{(x' + iy')^2}$$

$$= \frac{i}{2} \cos^2 \frac{\pi}{N} \left( e^{-2i\frac{\pi}{N}} - \text{c.c.} \right) \int_a^b \frac{dx'}{x'^2}$$

$$I_0 = \sin \frac{2\pi}{N} \cos^2 \frac{\pi}{N} \left( \frac{1}{a} - \frac{1}{b} \right)$$

(3) Sector (r=a inside)



It can be shown, for fixed inner radius, that the shape of the outer surface which gives the largest quadrupole strength for fixed area of magnetic material, is not a circle, but is

$$\rho(\phi) - \text{const} [\cos 3\phi]^{1/3}$$

PHASE ROCKING

This note was written to investigate simultaneous transverse and longitudinal stability limits for a finite-sized bunch when longitudinal oscillations are present. The motivation was partly for alternating-phase-focused structures. (Ed.)

A. Smooth longitudinal approximation

Take phases to be  $-\phi_1 + \psi$  and  $+\phi_2 + \psi$  ( $\phi_1$  and  $\phi_2$  taken to be positive) with  $\psi$  the amplitude of the phase oscillation. For each cell - assume all cells same length - take an average for one cell.

$$\delta\gamma = \frac{eET\beta\gamma}{Mc^2} \cos \frac{\phi_2 + \phi_1}{2} \left[ \cos \left( \frac{\phi_2 - \phi_1}{2} + \psi \right) - \cos \left( \frac{\phi_2 - \phi_1}{2} \right) \right] \quad (1)$$

$$\phi_s = \frac{\phi_2 - \phi_1}{2} \text{ is equivalent synchronous phase}$$

- also governs the size of the fish

$$\delta\psi = -\frac{2\pi\delta\gamma}{\beta^2} \quad \gamma \approx 1 \quad (2)$$

B. Transverse oscillation - average  $\mu_T$  per cell

$$\cos 2\mu = 1 - \frac{\Delta}{2} (\sin \phi_2 - \sin \phi_1) - \frac{\Delta^2}{8} \sin \phi_2 \sin \phi_1 \quad (3a)$$

$$\text{for } \psi^2 = 0$$

$$\cos 2\mu_T = 1 - \frac{\Delta}{2} (\sin(\phi_2 + \psi) - \sin(\phi_1 - \psi)) - \frac{\Delta^2}{8} \sin(\phi_2 + \psi) \sin(\phi_1 - \psi)$$

$$\text{for } \psi \neq 0 \quad (3b)$$

$$\text{where } \Delta = \frac{2\pi eE\gamma}{Mc^2\beta} \quad (3c)$$

Problem: Want transverse stability for all permissible values of  $\psi$ .

$$\frac{\phi_2 - \phi_1}{2} < \psi < \phi_1 - \phi_2 \quad (4)$$

This was tried and found to require

$$\phi_2 \approx 4|\phi_s|$$

$$\phi_1 \approx 6|\phi_s|$$

$$\Delta \sim 4$$

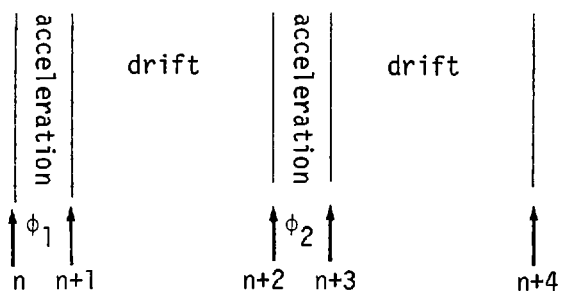
in order to have stability throughout the phase oscillation. This leads to a poor acceleration factor  $\cos 5|\phi_s| \cos |\phi_s|$ , requiring  $|\phi_s|$  to be  $10^\circ$  or less, which is probably too small.

C. We have clearly neglected the alternating gradient in the longitudinal oscillation and should not. Taking this into account for the linearized motion, one finds

$$\cos 2\mu_L = 1 + \Delta(\sin \phi_2 - \sin \phi_1) - \frac{\Delta^2}{4} \sin \phi_2 \sin \phi_1 \quad (5)$$

There is clearly no trouble in simultaneously getting longitudinal and transverse stability for small oscillations ( $\phi_2 = \phi_1$  is probably best) but is not at all clear how large  $\psi$  can be, since we need a non-linear analysis of the longitudinal motion for this purpose.

D. Non-linear analysis of longitudinal motion.



Let  $X = \delta\gamma \left( \frac{Mc^2}{eET\delta\lambda} \right)$  and expand to 2nd order in  $\psi$

$$X_{n+2} = X_n + \sin \phi_1 \psi_n - \frac{\cos \phi_1}{2} \psi_n^2 \quad (6a)$$

$$\psi_{n+2} = \psi_n - \Delta X_{n+2} \quad (6b)$$

(The form chosen has a unit Jacobian and is easily converted to a differential equation.)

Now iterate to  $n + 4$ . After much work

$$X_{n+4} - X_n = \psi_n \left( \frac{\sin \phi_1 - \sin \phi_2 + \Delta \sin \phi_1 \sin \phi_2}{1 + \Delta \sin \phi_2} \right) + \frac{\Delta \sin \phi_2}{1 + \Delta \sin \phi_2} X_{n+4} \\ - \frac{\cos \phi_1}{2} \psi_n^2 - \frac{\cos \phi_2}{2} \frac{(\psi_n - \Delta X_{n+4})^2}{(1 + \Delta \sin \phi_2)^3} \quad (7a)$$

$$\psi_{n+4} - \psi_n = - \frac{\Delta X_{n+4} (2 + \Delta \sin \phi_2)}{1 + \Delta \sin \phi_2} - \frac{\Delta \sin \phi_2}{1 + \Delta \sin \phi_2} \psi_n \\ - \frac{\Delta \cos \phi_2 (\psi_n - \Delta X_{n+4})^2}{2(1 + \Delta \sin \phi_2)^3} \quad (7b)$$

Writing  $X' = X_{n+4} - X_n$ ,  $\psi' = \psi_{n+4} - \psi_n$  one finds a Hamiltonian from which these two equations can be derived

$$X' = \frac{\partial H}{\partial \psi} \quad \psi' = - \frac{\partial H}{\partial X}$$

$$H(X, \psi) = \frac{S_1 - S_2 + \Delta S_1 S_2}{1 + \Delta S_2} \frac{\psi^2}{2} + \frac{\Delta S_2}{1 + \Delta S_2} \psi X + \frac{\Delta (2 + \Delta S_2)}{1 + \Delta S_2} \frac{X^2}{2} \\ - \frac{C_1}{6} \psi^3 - \frac{C_2}{6} \frac{(\psi - \delta X)^3}{(1 + \Delta S_2)^3} \quad (8)$$

This should lead to fish shaped contours ( $H = \text{constant}$ ) which control the limits of stability. Unfortunately, the results for these limits cannot be put in simple form (I don't think).

A partial solution would be to obtain the location of the unstable fixed point and to infer the size of the phase stable region from the distance between the stable fixed point ( $X = \psi = 0$ ) and the unstable fixed point. The unstable fixed point turns out to be the solution of (7a) and (7b) being simultaneously set = 0. However, this leads to a cubic equation for  $\psi_n$  or  $X_{n+4}$  which is not readily solved.

#### E. Conclusions and comments

(1) Numerical calculations needed to get stability limit, although it may be adequate to use Eq. (7a), (7b) rather than a full dynamics program.

(2) We have assumed equal cell length. It probably can be extended without difficulty to unequal cell lengths, but then one has to watch for unequal strength in the "lenses." An adjustment may be necessary like  $-\phi_1, -\phi_1, \phi_2, -\phi_1, -\phi_1, \phi_2$ . Swenson and Crandall have suggested  $-\phi, 0, \phi, 0, -\phi, 0$ ... or simple variations thereof.

(3) Any solution will probably require  $\Delta$  to stay constant (roughly). This implies field gradients proportional to  $\beta$ , which is inefficient at very low  $\beta$ , but may be OK for the low  $\beta$  part alone.

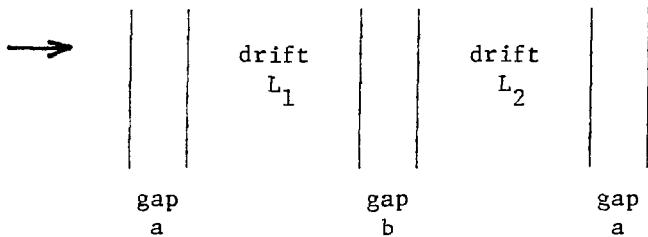
(4) Probably should be used in some combination with magnets - perhaps permanent magnets.

(5) If  $-90^\circ, 0^\circ, 90^\circ, 0^\circ$ , --- structure is used, the analysis will require terms in the next order of  $\delta\gamma$  (or  $X$ ) since there will be symmetry around  $\psi = 0$ .

(6) The cubic difficulties are really troublesome, since for  $\phi_2 = -\phi_1$ , one should be able to get a simpler solution (the two cells are identical). The trouble appears to be the method of going to a differential equation ( $X_n, \psi_{n+4}$ ), but this is essential to get preservation of phase area. On the other hand, I am convinced that the result in Eq. (8) is correct. It gives the expected limits for small oscillations, as well as for small angles, and for small  $\Delta$ .

(7) The idea is worth further exploration - probably numerically for a while.



ALTERNATING PHASE FOCUSING (APF)A. Analysis of Longitudinal Motion

Using the above geometry one can write a series of difference equations representing the changes in energy and phase in one repeat length. The small oscillation approximation leads to a longitudinal motion phase advance per repeat period,  $\mu_\ell$ , given by

$$\cos \mu_\ell = 1 + \frac{\ell_1 + \ell_2}{2} (\epsilon_a \sin \phi_a + \epsilon_b \sin \phi_b) + \frac{\ell_1 \ell_2}{2} \epsilon_a \epsilon_b \sin \phi_a \sin \phi_b \quad (1)$$

where

$$\epsilon_a = \frac{E_a T_a g_a}{Mc^2} \text{ etc.}, \quad \ell_1 = \frac{2\pi}{\lambda} \frac{1}{\beta^3 \gamma^3} L_1 \text{ etc.}$$

on the assumption of an average of  $2\pi$  r-f phase advance per gap. Longitudinal stability clearly requires at least one negative rf phase. We expect no significant effect of the transverse motion on the longitudinal motion.

## B. Transverse Motion

Here we expect the longitudinal phase to play an important role in the motion. The analysis is linear in  $x, x'$ , and leads to a phase advance per repeat period  $\mu_t$ , given by

$$\begin{aligned} \cos \mu_t = 1 - \frac{\ell_1 + \ell_2}{4} \left( \varepsilon_a \sin(\phi_a + \psi) + \varepsilon_b \sin(\phi_b + \psi) \right) \\ + \frac{\ell_1 \ell_2}{8} \varepsilon_a \varepsilon_b \sin(\phi_a + \psi) \sin(\phi_b + \psi) \end{aligned} \quad (2)$$

where  $\psi$  (assumed constant in the period) is the deviation of the longitudinal phase from its "synchronous" value.

The first approximation is to set  $\psi = 0$  in (2) and observe that the linear term in (2) is 1/2 the size and opposite in sign to the linear term in (1). (This is precisely the Earnshaw Theorem about the impossibility of simultaneous longitudinal and transverse focusing in linear approximation.) Setting this term = 0, one finds simultaneous  $\ell$  and  $t$  stability as long as

$$\sqrt{\ell_1 \ell_2} \left( \varepsilon \sin \phi \right) < 2 \quad (3)$$

where  $\varepsilon_a \sin \phi_a = -\varepsilon_b \sin \phi_b \equiv \varepsilon \sin \phi$ .

If the fields are too strong, the longitudinal motion becomes unstable first.

### C. Longitudinal Stability Limit

This is the most difficult quantity to calculate, but is needed in order to guide us as to realistic values to use for  $\psi$  in (2). This requires a non-linear analysis of the longitudinal motion which has been carried out only in powers of  $\epsilon_a \sin\phi_a$  and  $\epsilon_b \sin\phi_b$ , assuming approximate cancellation of the sum of these two terms. The result for the location of the unstable fixed point is

$$\begin{aligned} \psi_{\text{UFP}} &= \frac{2}{\epsilon_a \cos\phi_a + \epsilon_b \cos\phi_b} \left[ -\frac{l_1 l_2}{l_1 + l_2} \epsilon_a \epsilon_b \sin\phi_a \sin\phi_b - \epsilon_a \sin\phi_a - \epsilon_b \sin\phi_b \right] \\ &\approx \frac{4}{(l_1 + l_2)(\epsilon_a \cos\phi_a + \epsilon_b \cos\phi_b)} (1 - \cos \mu_\ell) \\ &\approx \frac{2}{(l_1 + l_2)(\epsilon_a \cos\phi_a + \epsilon_b \cos\phi_b)} \sin^2 \mu_\ell \end{aligned} \quad (4)$$

where the last form has been chosen to reflect the disappearance of phase stable region when the motion starts to become unstable.

### D. Choice of Parameters

An attractive choice of parameters is one with large  $|\phi_a|$  and  $|\phi_b|$ , but not so large as to inhibit acceleration. A first try is  $-60^\circ, +60^\circ$ , with  $\epsilon l_{1,2}$  adjusted so as to maximize acceptances. A primitive use of (4) in (2) suggests that coupling effects can be reduced by going to a somewhat

unequal pair like  $-65^\circ$ ,  $+55^\circ$ , or  $-70^\circ$ ,  $50^\circ$  or even  $-75^\circ$ ,  $+45^\circ$ . Numerical calculations should explore these pairs.

Although this analysis is only for phase alternation of period 2 gaps, other variations may prove to be at least as attractive (like  $[-90^\circ, 30^\circ, 30^\circ]$  or  $[-90^\circ, 0^\circ, 90^\circ, 0^\circ]$  etc.) These can be approximated in the present analysis by suitable choice of  $\epsilon_a$ ,  $\epsilon_b$ ,  $\ell_1$ ,  $\ell_2$ , etc., to reflect the equivalent single impulse.

#### E. Longitudinal Transverse Coupling

A number of observations should be made with regard to the  $\ell$ - $t$  coupling.

1) The equation of transverse motion will have roughly the same structure as that with a quadrupole magnet focusing system. This implies effects on the transverse phase space of the order

$$\frac{\delta A}{A} \sim \frac{k_\ell^2}{8k_t(2k_t - k_\ell)} \frac{\psi}{|\phi_{a,b}|} \quad (5)$$

where the wave numbers  $k_{\ell,t}$  are proportional to the phase advances  $\mu_{\ell,t}$ . (1966 Linac Conference, RLG, P. 207).

2) In the absence of the linear terms in (1) and (2), one finds  $\mu_\ell \approx 2\mu_t$ . Equation (5) makes it clear that resonant effects may be important, and should be explored numerically in some detail.

3) The traditional method of allowing for the  $\ell$ - $t$  sampling is to choose parameters such that (2) leads to stability for all choices of (4)

consistent with stable longitudinal motion. (One should check this numerically because of the very crude approximations used in deriving (4).) It is likely that this method will yield satisfactory results, although transverse growths like those in (5) will be significant.

4) A possible method of interpreting numerical calculations of the coupled motion is presented in the following: The radius of the bore tube will define an ellipse in the initial transverse space representing the acceptance. This ellipse is characterized by the area  $\pi W$  and by the Courant Snyder orientation and shape parameters  $\beta, \alpha, \gamma$ . The values of  $W, \beta, \alpha, \gamma$ , will depend on the starting phase of the longitudinal motion. Clearly the permissible starting transverse phase space (uncorrelated to the starting point in longitudinal phase space) will be the overlapping area of the collected of  $(x, x')$  acceptance ellipses.

The overlap of two ellipses can be approximated by an analytic treatment of Gaussian phase space distributions of the form

$$\rho(x, x') = \frac{1}{\pi W} \left( e^{-\frac{\gamma x^2 + 2\alpha x x' + \beta x'^2}{W}} \right) \quad (6)$$

This leads to an overlap area of the form

$$\frac{1}{W_{ov}} = \sqrt{\frac{1}{W_1^2} + \frac{1}{W_2^2} + \frac{1}{W_1 W_2} (\beta_1 \gamma_2 + \gamma_1 \beta_2 - 2\alpha_1 \alpha_2)} \quad (7)$$

which goes to the correct limit for  $W_1 \rightarrow \infty$  for  $W_1$  and  $W_2$  close to one another (this corrects for the case of uniform phase space density within elliptical borders).

Equation (7) can easily be generalized to several ellipses

$$\frac{1}{W_{ov}} \approx \frac{1}{n} \sqrt{\frac{1}{W_1^2} + \frac{1}{W_2^2} + \frac{1}{W_3^2} + \dots + \sum_{\text{pairs}} \frac{1}{W_i W_j} \left( \beta_i \gamma_j + \gamma_i \beta_j - 2\alpha_i \alpha_j \right)}$$

which can be written as

$$\frac{1}{W_{ov}} \approx \sqrt{\left( \frac{\bar{\beta}}{W} \right) \left( \frac{\bar{\gamma}}{W} \right) - \left( \frac{\bar{\alpha}}{W} \right)^2} \quad (8)$$

Equation (8) permits taking a collection of starting points in longitudinal phase space and determining the overlapping admittance in  $(x, x')$  space.

For a restricted region in longitudinal phase space the overlap area should be quite large. For a large region in longitudinal phase space the overlap area will be quite small. The optimum will very likely be a solution which maximizes the product of the areas in the  $(\delta W, \phi)$  and  $(x, x')$  phase spaces, and should be readily obtained numerically.

#### F. General Observations

1) Coupling effects will be quite important and should be investigated numerically.

2) Tolerances on transverse alignments should be comparable with those for quadrupole focused linacs.

3) Tolerances on longitudinal drift tube alignments and lengths will have to be investigated with care. They may be comparable with transverse tolerances.

4) The additional use of permanent quadrupoles or solenoids should be considered.

5) An alternating phase focused linac will have the r-f features of a biperiodic structure. This should be borne in mind when trying to achieve r-f compensation.

ESTIMATE OF X-Z COUPLING IN APF

The differential equation for  $\phi$  in an accelerator which has a varying  $\phi_s$  is easily derived, and turns out to be

$$\frac{d^2\phi}{ds^2} - \frac{d^2\phi_s}{ds^2} = - \frac{2\pi e E_o T}{\beta^3 M c^2 \lambda} \left( \left(1 + \frac{\pi^2 r^2}{\beta^2 \lambda^2}\right) \cos\phi - \cos\phi_s \right) \quad (1)$$

Here we have neglected damping effects, but have taken into account the dependence of the transit time factor on transverse displacement.

Conventional Linac

In the case of a conventional accelerator with constant  $\phi_s$ , one has

$$\frac{k_\ell^2}{\sin|\phi_s|} = \frac{2\pi e E_o T}{\lambda M c^2 \beta^3} \equiv q \quad (2)$$

and

$$\frac{d^2\chi}{ds^2} + k_\ell^2 \chi = - \frac{k_\ell^2}{\sin|\phi_s|} \cos\phi_s \frac{\pi^2 r^2}{\beta^2 \lambda^2} \quad (3)$$

with  $\chi = \phi - \phi_s$ .



### Alternating Phase Focusing

The analysis starts from the same point, namely

$$\frac{d^2\chi}{ds^2} - q \sin\phi_s \chi = q \cos\phi_s \frac{\pi^2 r^2}{\beta^2 \lambda^2} \quad (4)$$

In this case  $\phi_s$  will have a strong focusing character. Note that the coupling term will not fluctuate in sign when  $\phi_s$  does.

It is possible to go to the smooth variables  $u$  and  $z$  which are given by

$$\begin{aligned} \chi &= u \sqrt{\beta_{SF}} \\ ds &= \beta_{SF} dz \end{aligned} \quad (5)$$

and  $\beta_{SF}$  is the usual strong focusing (envelope) parameter, leading to

$$\frac{d^2u}{dz^2} + u = \beta_{SF}^{3/2} q \cos\phi_s \frac{\pi^2 r^2}{\beta^2 \lambda^2} \quad (6)$$

For an accurate calculation of the effect of the coupling term, one needs the average of the right hand side. However, it is clear that the effect can be approximated by

$$\frac{d^2\chi}{ds^2} + k^2 \chi \cong q \langle \cos\phi_s \rangle \frac{\pi^2}{\beta^2 \lambda^2} \langle r^2 \rangle \quad (7)$$

where  $k\mathcal{L} = \mu$  is the phase advance in a period of length  $\mathcal{L}$ .

If one assumes  $\sin\phi_s$  to fluctuate between equal + and - values with period  $\mathcal{L}$ , an approximate form for k is given by

$$\begin{aligned} \cos\mu &= 1 - \frac{|q \sin\phi_s|^2 \mathcal{L}^4}{6 \cdot 16} \left( = 1 - \frac{\theta^4}{6} \right) \\ \mu &\approx \frac{|q \sin\phi_s| \mathcal{L}^2}{4\sqrt{3}} = k \mathcal{L} \\ k &\approx \frac{|q \sin\phi_s| \mathcal{L}}{4\sqrt{3}} \end{aligned} \quad (8)$$

in which case the coefficient of the right hand side of equation (7) is

$$\begin{aligned} q |\cos\phi_s| &= \cot|\phi_s| 4\sqrt{3} \frac{k}{\mathcal{L}} \quad \text{APF} \\ &= \cot|\phi_s| \frac{4\sqrt{3}}{\mu} k^2 \quad \text{APF} \end{aligned} \quad (9)$$

This is to be compared with the same coefficient in the conventional case (Equations 2-3).

$$\cot|\phi_s| k_\ell^2 \quad \text{Conventional}$$

Using  $|\phi_s| = 30^\circ$  - conventional.

$$\phi_s = \pm 60^\circ, \mu \approx 60^\circ - \text{APF}$$

and  $k^2 = k_\ell^2$  for the same equivalent focusing (q will have to be much larger for the APF), the ratio of the coupling coefficients will be

$$\frac{\text{APF}}{\text{Conventional}} = \frac{\cot 60^\circ}{\cot 30^\circ} \frac{4\sqrt{3}}{60^\circ} \approx 2.2 \quad (10)$$

For smaller  $\mu$ , the ratio will be larger.

### Conclusion

x - z and y - z coupling effects are probably larger in the APF than in the conventional linac. Detailed coupled orbit calculations are needed to determine the relative importance of the coupling term more precisely.